EFFECTS OF WASTE GLASS AND POLYMER ADDITION ON THE PERFORMANCE OF CONCRETE MASONRY BLOCKS

EFFECTS

OF

WASTE GLASS AND POLYMER ADDITION

ON THE PERFORMANCE OF

CONCRETE MASONRY BLOCKS

By

SYLVIA NICOLE MIHALJEVIC, B. ENG.

A Thesis

Submitted to the School of Graduate Studies

in Partial Fulfillment of the Requirements

for the Degree

Master of Applied Science

McMaster University

MASTER OF APPLIED SCIENCE (2009) McMaster University

(Civil Engineering) Hamilton, Ontario

TITLE: Effects of Waste Glass and Polymer Addition on the Performance of Concrete Masonry Blocks

AUTHOR: Sylvia Nicole Mihaljevic, B. Eng. (McMaster University, 2007)

SUPERVISOR: Professor Samir E. Chidiac, Ph.D., P.Eng

NUMBER OF PAGES: xii, 122

ABSTRACT

Concrete masonry blocks are widely used in North America and the world; however, production poses some environmental implications, specifically the depletion of natural resources and contribution to the release of carbon dioxide into the atmosphere. Accordingly, methods to improve the sustainability of the industry need to be developed. The replacement of cement with post-consumer waste glass powder and/or the replacement of fine aggregate with post-consumer waste polymer in the production of concrete blocks are proposed as potential options to reduce the environmental impact of block production while maintaining adequate block performance.

The effect of using glass powder and polymers on the block and prism properties has been analyzed to determine the most effective implementation of these post-consumer waste materials. Physical properties, mechanical properties and alkali-silica reaction of the blocks and the mechanical properties of the prisms were tested. From the experimental program, it was determined that replacing Portland cement with waste glass powder up to 25% had no detrimental effect on the block and prism properties. Replacing the sand with polymer aggregate was found to have a detrimental impact on the strength of the block. The effect of adding up to 6% polymer aggregate as sand replacement on the prism mechanical properties was found to be minimal. The reduction in block compressive strength when polymer aggregates are used is attributed to the increase in the material's porosity.

ACKNOWLEDGEMENTS

I would like to thank and acknowledge all the help and support I have received while working on this thesis. I wish to thank my supervisor, Dr Samir Chidiac, whose guidance and support were vital in the successful completion of this thesis. Thank you to the technicians of the McMaster Applied Dynamics Laboratory, Dave Perrett, Kent Wheeler, Rhys Westmoreland and Peter Koudys for assisting me with testing the blocks and prisms. Thank you to Atlas Block for the use of their facilities and materials, especially to Patt Wainhouse, Rob Page, Don Schmidt, Mike Peaker, John Neal and Don Gordon for their assistance in producing the blocks. Thank you to the Canadian Masonry Design Centre for providing a mason to construct my prisms. I would also like to thank the faculty, staff and students of the McMaster Civil Engineering department for their support and encouragement. And a very special thank you to Omar Daoud, without his help the completion of the experimental program would have been impossible. Thank you to my family and friends for their support and encouragement. Also thank you to the Ontario Graduate Scholarship, the Natural Sciences and Engineering Research Council of Canada and the Department of Civil Engineering for their financial support.

Sylvia Mihaljevic

TABLE OF CONTENTS

LIST OF TABLES

LIST OF FIGURES

CHAPTER 1 INTRODUCTION

1.1 Objective of Thesis

Concrete is one of the most widely used construction materials; however, there are environmental issues associated with its use that need to be addressed. Concrete production uses large quantities of natural resources in the form of aggregates and contributes to the release of carbon dioxide during the production of cement. One ton of carbon dioxide is released into the atmosphere when one ton of cement is produced, which is approximately 7% of the world's total yearly production of CO_2 (Meyer, 2004). Concrete masonry blocks are a common construction material in Canada and their production causes the same environmental concerns as that of regular concrete.

In recent years, there has been an increasing incentive to minimize the environmental effect of the construction industry through programs such as the Leadership in Energy and Environmental Design (LEED) Green Building Rating System, which awards points for sustainable construction practices (CaGBC, 2009). Greater sustainability of the construction industry can be achieved if a portion of the virgin aggregate or cement is replaced with waste materials.

Significant experimental work has been performed on the use of recycled concrete aggregate to replace virgin aggregate and on the use of pozzolanic materials, such as fly ash, silica fume and ground granulated blast furnace slag, to replace a portion of cement. Due to the successful implementation of these waste materials into regular concrete there is increased desire to find new post-consumer materials to use in a similar way. The experimental work presented in this thesis looks at the use of glass, as a pozzolanic material to replace cement, and polymers, as aggregates to replace sand in the production of concrete masonry blocks.

1.2 Outline of Thesis

This thesis is broken down into 7 chapters, including the introduction. Chapter Two is a comprehensive analysis of the literature into the use of glass and polymers in concrete. The uses of glass as an aggregate and as a supplementary cementing material and the use of polymers as an aggregate are discussed in detail.

Chapter Three outlines the experimental procedure and test setup used to determine the effect of waste addition on the properties of concrete blocks. The determination of the mix design, the production of the concrete blocks and the testing procedure for the blocks and assemblages is discussed in this chapter. The testing procedure employed was based on Canadian Standards Association (CSA) and American Society for Testing and Materials (ASTM) standards.

The results of the experimental program are given in Chapter Four. The data presented was analyzed using statistical methods to determine the significance of the results and the effect of waste type and content on the tested properties in comparison to the control specimens.

Chapter Five summarizes the regression analysis performed to determine the relationships between the waste material content and type of waste material on the tested properties. A discussion of the results and a comparison to previous studies is included in this chapter.

A model for the effect of polymers on compressive strength when they are used in concrete blocks is presented in Chapter Six. The model is based on the assumption that the polymers have no compressive strength and, therefore, cannot carry any load.

The final chapter summarizes the results found through the experimental program and the analysis of the data. Recommendations for the use of waste material within concrete masonry blocks are provided and some suggestions are given for further research in this area.

CHAPTER 2 LITERATURE REVIEW

2.1 Introduction

Glass can be recycled many times without significantly altering its physical and chemical properties (Shayan & Xu, 2004); however large quantities of glass are not recycled because it is broken, the colours are mixed or it is too expensive to recycle (Terro, 2006). Waste glass (WG) could be put to a beneficial use in concrete to replace a portion of the aggregate since it is a hard material with almost negligible water absorption. However, when glass is used as an aggregate in concrete, there is a concern that an alkali-silica reaction (ASR) may occur, which would be detrimental to the durability of the concrete (Shi & Zheng, 2007). Another beneficial use for the WG is to use it as cement replacement. When glass is ground to a fine powder, it demonstrates pozzolanic properties. Replacing cement with waste glass powder (WGP) is the most effective option since cement is the most expensive component of concrete as well as the one with the most negative effect on the environment.

Its low cost, low weight and ability to be shaped into any form has led to an ever increasing use of plastic. It is estimated that plastic makes up 7 to 8% of Ontario household residual waste (Enviros RIS, 2001). There are two categories of plastics: thermoplastics and thermosetting plastics. Thermoplastics can be recycled easily by melting. When they are heated thermoplastics soften, which allows them to be molded into other shapes and the process may be repeated many times without degradation of the plastic quality. Some examples include polyethylene, polypropylene and polyethylene terephthalate (PET). Thermosetting plastics cannot be recycled by melting since they contain cross-links, which form a firmly bonded mesh. While this does not allow thermosetting plastics to be recycled by melting, it allows them to maintain their strength and shape for high temperature applications. Examples of these are polyurethane and melamine (Panyakapo & Panyakapo, 2008). Although there are many plastics that can be recycled, there is a significant portion that still ends up in landfills. Since most plastics are non-biodegradable, their disposal has significant environmental repercussions. This is why alternative uses for waste plastic need to be developed. One option is to use plastic in concrete or mortar to replace a portion of the aggregate, thereby reducing the need for virgin material in concrete production. Because plastics have a lower density than regular aggregate, there is great potential for them to be used in concrete as lightweight aggregate, as long as their adverse effects on the mechanical properties of the concrete can be mitigated (Panyakapo & Panyakapo, 2008).

This chapter looks at the available literature on the research into the use of WG and waste plastics to produce concrete and concrete blocks. Since the focus of this thesis is concrete blocks, only the properties important to masonry will be discussed in this chapter. It highlights findings about the effects of using waste material in concrete, a part of which has already been presented in Mihaljevic and Chidiac (2009).

2.2 Waste Glass as Aggregate Replacement

Glass is made from a molten mixture of materials, which commonly include silica, soda ash and calcium carbonate ($CaCO_3$) depending on the type of glass. The mixture is then cooled so that it solidifies without crystallizing (Park, Lee, & Kim, 2004). The most common type of glass is soda-lime glass, which is used to make containers and bottles. It makes up approximately 80% of the WG collected (Shi & Zheng, 2007). Of the WG collected, 63% is flint (clear), 25% is amber and 10% is green and all other colours make up only 2% (Siddique, 2008).

Comparing the physical propertied of WG and sand, the density of glass is very similar to that of sand. WG has only a 1% lower density, which is not significant. However, as can be seen in Table 2.1, the absorption of WG is far lower than that of sand. WG absorbs 14% less water than sand, which suggests that concrete made with glass aggregate would have a lower water absorption than concrete made with sand. Also, glass shows some pozzolanicity while sand does not (Ismail & Al-Hashmi, 2009).

Table 2.1 Physical properties of sand and WG (Ismail & Al-Hashmi, 2009)

Physical properties	Sand	WG
Specific gravity	2.57	2.19
Density (kg/m^3)	1688	1672
Fineness modulus	2.37	2.36
Absorption (%)	2.71	0.39
Pozzolanic index (%)	-	80

The chemical composition of the three most common bottle glass colours is given in Table 2.2. The main constituent of the glass, SiO_2, makes up 71% to 73%, which is only slightly lower than the silica content of sand, which is approximately 78%. Although the high silica content of glass is similar to that of sand, it is also a concern when glass is used as an aggregate in concrete since, unlike sand, the structure of silica in glass is amorphous so it is likely to undergo a potentially detrimental alkali-silica reaction. It should be noted that the chemical composition of the three glass colours is very similar for the main constituents, but varies for the components that make up only a small portion of the composition. This is apparent in the higher concentration of chromium oxide (Cr_2O_3) in the emerald green glass. The Cr_2O_3 gives green glass its colour and studies have shown that glass with greater than 1% Cr_2O_3 has the potential to significantly reduce ASR expansion when it is used in concrete (Jin, Meyer, & Baxter, 2000).

Table 2.2 Chemical Composition of WG separated by colour (Park et al., 2004)

	Chemical Composition (%)		
Type	**Flint**	**Emerald green**	**Amber**
SiO_2	73.04	71.3	72.1
Al_2SO_4	1.81	2.18	1.74
$Na_2O + K_2O$	13.94	13.07	14.11
$CaO + MgO$	10.75	12.18	11.52
SO_3	0.22	0.053	0.13
Fe_2O_3	0.04	0.596	0.31
Cr_2O_3	-	0.44	0.01

2.2.1 Compressive Strength

Compressive strength is one of the most important characteristics of concrete and concrete blocks and in the literature it is often used as the main indicator of whether waste materials can be incorporated into concrete. In general, glass aggregate results in a reduction of compressive strength due to its angular shape, which causes poor workability and compaction of the concrete. Also, the bond between glass and the cement paste and friability of the glass may contribute to this lower strength. This section summarizes some of the effects of WG aggregate on the compressive strength of concrete.

Topçu and Canbaz used green waste soda glass to replace 15%, 30%, 45% and 60% of the coarse aggregate. The glass size was between 4 and 16 mm. Increasing the replacement of natural aggregate with WG resulted in a linear decrease in the compressive strength, as shown in Figure 2.1. At 30% replacement, the compressive strength was reduced by 15%. The poor geometry of the coarse WG aggregate had the most influence in reducing the compressive strength. Also, crushing of the glass weakened the concrete because it produced cracks within the glass aggregate particles. (Topçu & Canbaz, 2004).

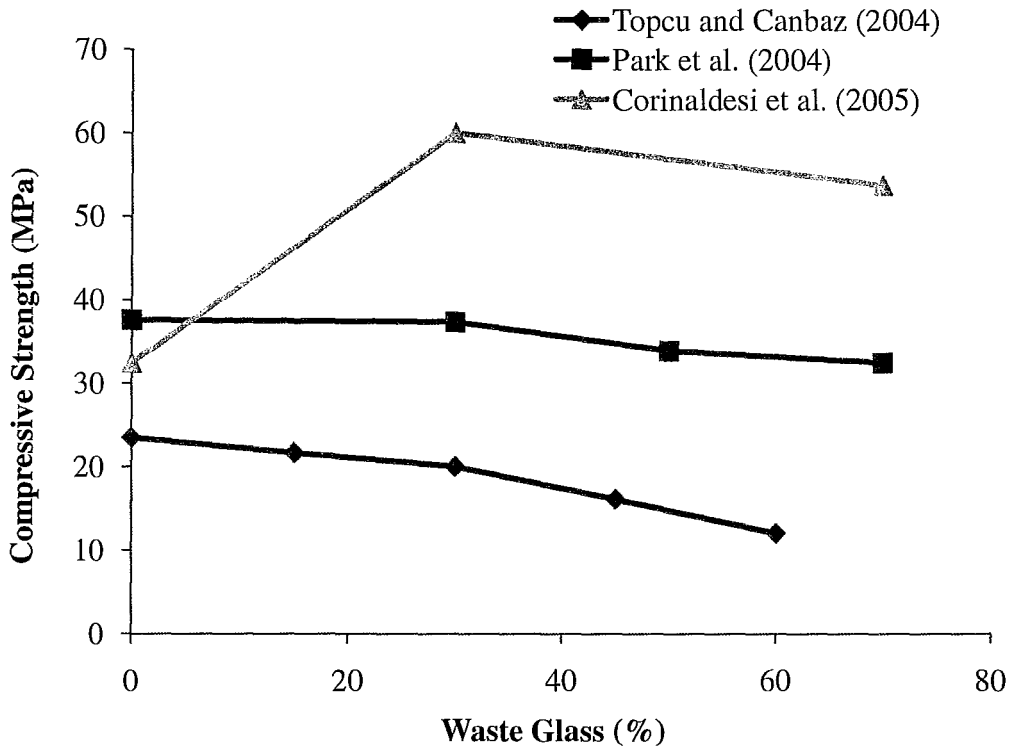

Figure 2.1 Compressive strength of concrete with WG aggregate (Mihaljevic & Chidiac, 2009)

Park et al. tested the compressive strength of concrete made with WG aggregate separated by colour and crushed finer than 5 mm. The fine aggregate was replaced by 30, 50% and 70% WG. Figure 2.1 shows the compressive strength of the emerald green glass at 28 days. No difference was determined based on colour. When 30% of the fine aggregate was replaced by WG, the strength was only about 1% lower than that of the control, which is a promising result. Even at higher replacement levels, the strength was not significantly affected by WG. The authors suggest that the lower strength was due to lower adhesion between cement and glass than between sand and cement, which is probably due to the lower absorption of glass compared to sand (Park et al., 2004).

Corinaldesi et al. replaced the fine aggregate used to make mortar with WG. They replaced either 30% or 70% of the sand with one of three glass particle sizes, less than 36 μm, greater than 36 μm and less than 50 μm, and greater than 50 μm and less than 100 μm. The 180 day compressive strength is shown in Figure 2.1 for the mortar with glass particles less than 36 μm. They found an improvement in strength with the addition of WG (Corinaldesi, Gnappi, Moriconi, & Montero, 2005). The WG particles used in this study were fine enough to undergo a pozzolanic reaction (Shayan & Xu, 2004; Shao, Lefort, Moras, & Rodriguez, 2000), which would result in a higher compressive strength at 180

days than that of the control and the denser micorstructure observed in this study (Mihaljevic & Chidiac, 2009).

The work of Jin et al. is one of the few studies which looked at the effect of replacing fine aggregate with WG for concrete masonry blocks. They replaced either 10% of the aggregate, 10% of the cement or both 10% of the cement and 10% of the sand with WG. They produced good quality blocks with adequate strength in all cases (Jin et al., 2000).

Lam et al. used crushed, mixed colour WG to replace fine aggregate in precast concrete paving blocks. The fine aggregate was 100% replaced with waste materials, consisting of WG and recycled fine aggregate (RFA) obtained by crushing concrete from demolition sites. Pulverized fly ash (PFA) was used to prevent ASR. In all cases where PFA was used, the paving blocks had higher strength than the control when WG content was increased. 50% RFA and 50% WG aggregate blocks, with 10% by weight of cement PFA, were found to produce the best quality blocks (Lam, Poon, & Chan, 2007). Precast concrete paving blocks are made using a dry mix and, since structural concrete masonry blocks are also made using a dry mix, concrete blocks may also benefit from WG aggregate (Mihaljevic & Chidiac, 2009).

Chen, Huang, Wu and Yang (2006) and Sangha, Alani, & Walden (2004) found an improvement in strength when WG replaced the virgin aggregate. Chen et al. (2006) used E-glass waste, which is cylindrical in shape so that it acts to prevent crack propagation. Sangha et al. (2004) crushed WG using a process which ensures no sharp, angular pieces. This suggests that alternative type of glass waste and different processes for crushing can be used to improve the strength of concrete with WG aggregate.

2.2.2 Tensile Strength and Flexural Strength

The tensile and flexural strength are adversely affected by the addition on WG to replace the virgin aggregate. This was shown by the work of Park et al. (2004) and Topçu and Canbaz (2004). At a replacement level of 30% for the fine aggregate, the tensile strength decreased by 3%, in comparison to the control (Park et al., 2004).

2.2.3 Alkali-Silica Reaction

ASR is a reaction that occurs between silica and alkalis to form a gel, which expands when it absorbs water. The silica comes from the aggregate and its reactivity depends on its structure, concentration and particle size (Fournier & Berube, 2000). The particle size has been shown to have a pessimum effect, meaning that the maximum expansion occurs at intermediate size (Fournier & Berube, 2000). Research carried out by Jin et al. (2000) has determined that glass of particle size 1.18 to 2.36 mm produced the highest expansion whereas low expansion was observed at larger and smaller particle sizes. The hypothesis suggested to explain this phenomenon is that gel formation causes pressure; however, the gel also permeates into the concrete, thereby relieving some of the

pressure, so the pessimum value occurs when the transportation of ASR gel is slowest and the gel formation is highest (Jin et al., 2000). The alkalis are released from the cement and the paste must have a sufficient concentration of alkali hydroxides (Na^+, K^+, OH^-) (Fournier & Berube, 2000) to produce a pore solution with pH ranging between 12.5 and 13.5, otherwise dissolution of silica will not occur (Kurtis & Monteiro, 2003). Alkalis may also be released from the aggregates, which is a concern with glass because of its Na_2O content. The third factor in ASR expansion is water which plays a significant role. ASR gel expands and causes damage by absorbing water. For gel expansion to occur, a relative humidity of 80% to 85% is needed within the concrete (Fournier & Berube, 2000). A discussion of the mechanisms of ASR can be found in Federico and Chidiac (2009).

ASR damage is caused by the hydrostatic pressure generated by the expansion of the ASR gel when it is confined within a cement matrix. Since cement paste is porous, ASR gel, which is viscous in nature, can permeate into the surrounding paste. This reduces some of the pressure, but as more and more gel is formed, internal pressure increases until it exceeds the tensile strength of the matrix leading to cracks in the concrete. The extent of damage depends on the permeability of the concrete, the elastic modulus of matrix and aggregate, the viscosity of the ASR gel and the content and size of the reactive aggregate (Jin et al., 2000).

Although ASR will always be a concern when glass is used within concrete, there are methods to prevent damage from occurring. Some common methods to reduce deterioration associated with ASR are to use low alkali cement (Fournier & Berube, 2000), use supplementary cementing materials (Fournier & Berube, 2000), treat the aggregates with admixtures (Fournier & Berube, 2000; Topçu & Canbaz, 2008), use emerald green glass (Jin et al., 2000) or prevent water from entering the concrete (Fournier & Berube, 2000).

A fly ash content of 20%, of total binder content, greatly reduces the ASR expansion of WG aggregate concrete (Polley, Cramer, & de la Cruz, 1998). 10% PFA was used by Lam et al. (2007) to prevent ASR damage for paving blocks. Shayan and Xu (2004) found that both silica fume (10%) and WGP (>20%) used for cement replacement where able to ensure that no negative ASR expansion occurs in mortar bars.

2.2.4 Water Absorption

Taha and Nounu (2007) looked at the water absorption of concrete with waste glass replacing sand or glass powder replacing cement. It was found that, since glass is an impermeable material, the water absorption of the concrete was greatly reduced when glass was used as an aggregate, which could potentially improve the durability of concrete. Lower water absorption was also observed by Lam et al. (2007) for the paving blocks made with WG aggregate.

2.3 Waste Glass as Pozzolan

The high silica content, high surface area and amorphous structure of WGP suggests that it would perform well as a supplementary cementing material (SCM) and, therefore, could be used to replace a portion of the cement in concrete. Table 2.3 compares the chemical composition of WGP with ordinary Portland cement (OPC) and two common pozzolans, silica fume (SF) and fly ash (FA). Silica fume has only slightly higher silica content than WGP, however it is significantly finer. Silica fume particles are less than 1 μm, with an average size of 0.1 μm (Kosmatka, Kerkhoff, Panarese, MacLeod, &McGrath, 2002), while WGP is usually not crushed finer than 38-45 μm. Because of its high silica content and fine particle size, silica fume is a very good pozzolan. Fly ash has less silica but is also finer than glass powder with particle size of approximately 20 μm (Kosmatka et al., 2002). Based on the silica content of glass and its fineness, if it is adequately crushed, WGP is expected to perform well as a SCM. WGP should perform better than fly ash, however it cannot be expected to perform as well as silica fume. A concern with using glass as an SCM is the potential that the glass itself will release enough alkalis to induce ASR (Schwarz, & Neithalath, 2008). The Na_2O and K_2O in glass could potentially be released, in the form of sodium and potassium ions, into the cement paste and increase the pH of the paste. WGP has a larger amount of alkalis than other pozzolans, such as FA and SF, which do not undergo ASR, so glass might prove to be a weaker pozzolan or even induce ASR in reactive aggregates.

Table 2.3 Comparison of WGP with cement and other pozzolans

	Chemical Composition (%)			
Type	**WGP[1]**	**OPC[2]**	**SF[1]**	**FA[2]**
SiO_2	72.61	20.33	89.75	47.8
Al_2O_3	1.38	4.65	0.14	23.4
Na_2O	12.85	0.24	0.19	0.72
K_2O	0.43	0.59	0.34	1.70
CaO	11.42	61.78	0.38	3.36
MgO	0.79	3.29	0.05	0.81
SO_3	0.09	3.63	0.04	1.33
Fe_2O_3	0.48	3.04	0.03	15.1

[1] (Shayan & Xu, 2004); [2] (Shi & Zheng, 2005)

2.3.1 Compressive Strength and Pozzolanic Activity

Shao et al. tested the pozzolanic activity and strength of concrete made with finely ground WGP. Thirty percent of the cement was replaced with ground WG, silica fume or fly ash. The glass sizes used were 150 μm, 75 μm and 38 μm. As can be seen in Figure 2.2, only the mix with 30% silica fume performed better than the control at 28 days; however, at 90 days the concrete with the 38 μm glass replacing cement produced concrete that is 8% higher in strength in comparison to

the control. The concrete with finer glass particles achieved higher strength than the concrete with coarser glass particles since finer glass is more reactive. According to ASTM C 618 (2008), a strength activity index of 75% is needed for a pozzolan to be beneficial to concrete. The 75 μm and 38 μm WG satisfied this requirement and their corresponding mixes achieved results similar to fly ash (Shao et al., 2000).

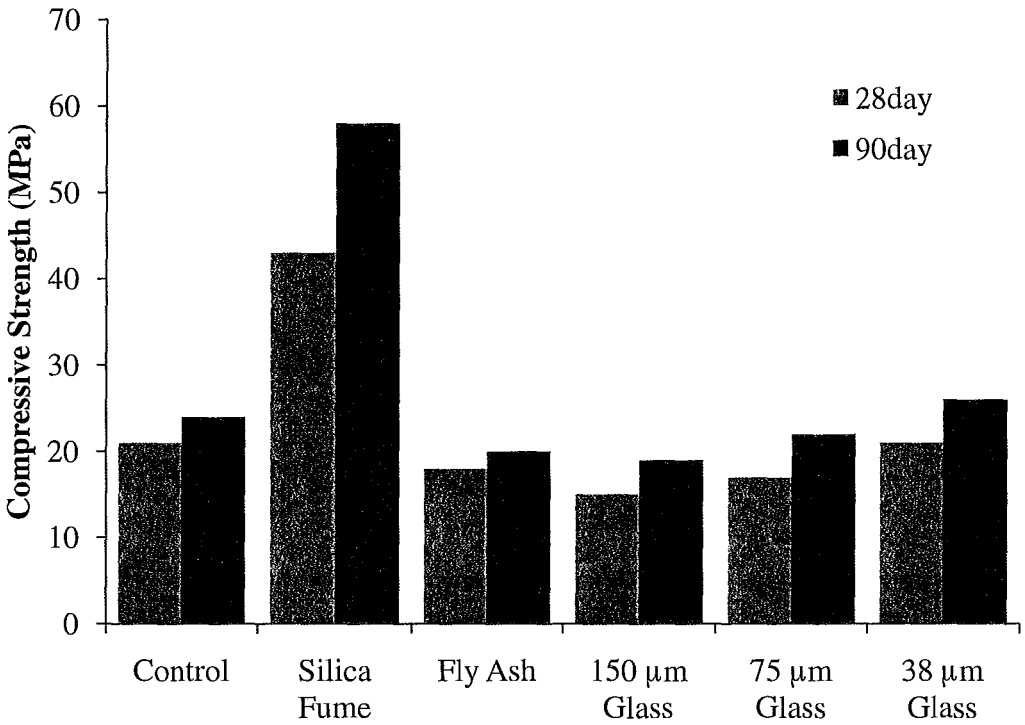

Figure 2.2 Compressive strength of concrete with 30% of cement replaced (Shao et al., 2000)

Shayan and Xu used WGP with particle size small than 10 μm to replace 10%, 20% and 30% of the cement. In all cases, the 28 day compressive strength was lower for the mixes with WGP compared to the control. However, as can be seen in Figure 2.3, the 90 day strength of the concrete was higher or approximately the same as that of the control for all the mixes with WGP. This is attributed to the pozzolanic reaction of the WGP which is slower than the hydration of Portland cement (Shayan & Xu, 2004).

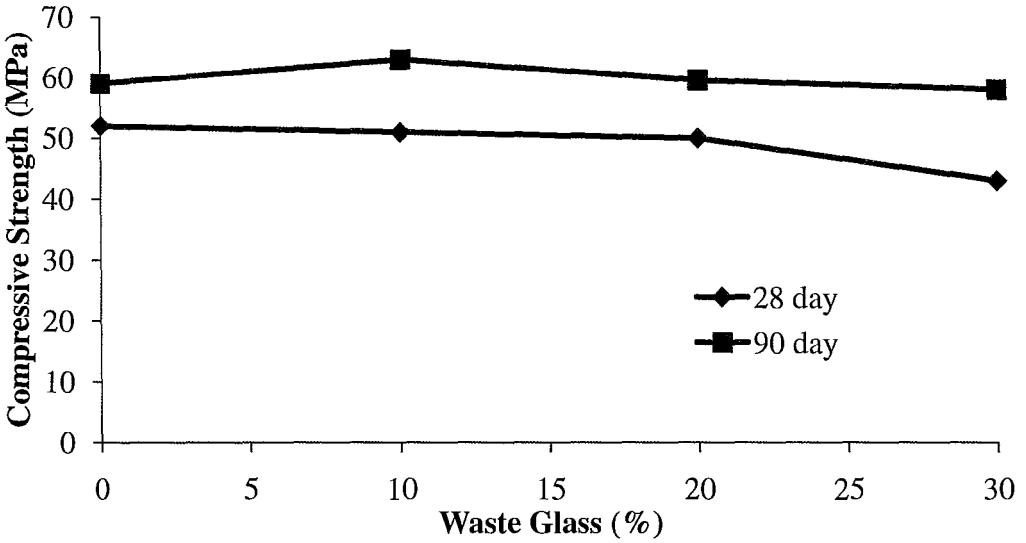

Figure 2.3 Compressive strength of concrete with WGP (Shayan & Xu, 2004)

According to the work of Schwarz et al., it was optimum to replace 10% of cement with WGP, when 72% of the particles were smaller than 45 μm. However, the optimum replacement of cement with fly ash was 20%. The concrete paste having 10% replacement of cement with glass had a higher compressive strength than the concrete modified with fly ash at 28 days, however, at 90 days, the fly ash mix had higher strength. This was attributed to the greater pozzolanic activity of fly ash (Schwarz, Cam, & Neithalath, 2008).

2.3.2 Tensile Strength

In addition to looking at the effect of only replacing sand with glass, Taha and Nounu investigated the effect of substituting 20% of the cement with glass powder on the tensile strength of the concrete. They showed that splitting tensile strength was adversely affected when both crushed glass and glass powder were used but there was no difference in the flexural strength (Taha & Nounu, 2007).

2.3.3 Alkali-Silica Reaction

No damaging effects due to ASR were observed with WGP, with particle size less than 40 μm used to replace up to 30% of the cement, in the work presented in the literature. In fact, the mortar bars with WGP showed lower expansion than the control concrete. This includes the work by Shao et al. (2000), Shayan and Xu (2004), Shayan and Xu (2006), and Schwarz et al. (2008).

2.3.4 Water Absorption

The water absorption increased when 20% WGP replaced the cement in the study by Taha and Nounu (2007). The authors suggest that this is due to a

change in the hydration products and the microstructure of the concrete when glass powder is used as a pozzolanic material.

2.4 Plastics as Aggregate Replacement

2.4.1 Compressive Strength

Babu and Babu used two commercially available expanded polystyrene (EPS) beads with nominal diameters of 6.3 mm (type A) and 4.75 mm (type B). The addition of EPS resulted in a decrease in compressive strength, though mixes with the smaller polymer beads had higher strength than the mixes with the same volume of type A beads. The failure of the specimens with EPS was more ductile than that of regular concrete (Babu & Babu, 2003; Babu, Babu, & Wee, 2005). Further study looked at the difference between using unexpanded polystyrene (UEPS) and EPS as aggregates in concrete. The Concrete with UEPS achieved higher strength than that with EPS, but was more brittle (Babu, Babu, & Tiong-Huan, 2006).

Plastic aggregate was used to replace coarse aggregate by 5, 10, and 15% to make concrete at 3 different w/c ratios in the work by Ghaly and Gill (2004). The plastic aggregate used was chopped up from post-consumer materials and was poorly graded. A fairly linear decrease in strength was noted with increasing quantities of plastic aggregate. Even at the 5% replacement level, the compressive strength decreased significantly. It was between 6 and 15% lower than the control. The compressive strength corresponding to w/c of 0.42 is presented in Figure 2.4. The authors observed larger displacements and a more ductile failure mechanism for the concrete with plastic. The low strength of the polymer aggregate and its poor gradation were given as reasons for a reduction in compressive strength (Ghaly & Gill, 2004).

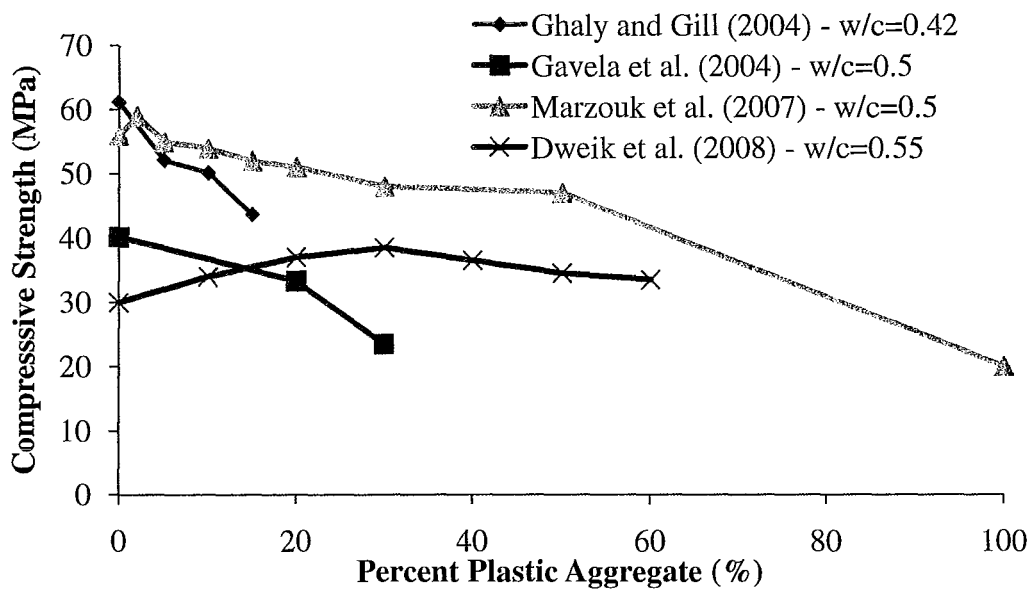

Figure 2.4 Compressive strength of concrete with polymers

Gavela et al. (2004) used either polypropylene (PP) or PET waste plastic to replace either 20% or 30% of the total aggregate in concrete. The compressive strength is given in Table 2.4 and Figure 2.4. The findings of this study follow the same trend as other works and show that the compressive strength of the concrete decreases with the addition of waste plastics (Gavela et al., 2004).

Table 2.4 Compressive strength of concrete with polymer aggregate (Gavela et al., 2004; Mihaljevic & Chidiac, 2009)

Mix Constituents	Strength (MPa)
Control mix, w/c=0.5	40
Control mix, w/c=0.5	41
20% PP, w/c=0.5	33
20% PP, w/c=0.6	24
30% PP, w/c=0.5	26
20% PET, w/c=0.5	35
30% PET, w/c=0.6	24

For the mortar mixtures, Marzouk et al. (2007) used PET waste from plastic bottles to replace 2 to 100% by volume of the sand. The plastic aggregate was separated into three categories based on maximum aggregate size. Type A had a maximum size of 0.5 cm, type C had a maximum size of 0.2 cm, and type D had a maximum size of 0.1 cm. Water was added to the mortar to achieve workability rather than to maintain constant w/c. The strength decrease was not very large up to 50% replacement; however, the strength decreased dramatically beyond 50% replacement of the sand. The type A aggregate, for which results are given in Figure 2.4, achieved the highest strength of the three plastic sizes. While this study showed that it would be feasible to use PET plastic as a fine aggregate below 50% sand replacement for mortar, it failed to account for the varying w/c, which significantly affects compressive strength (Marzouk, Dheilly, & Queneudec, 2007).

Ismail and Al-Hashmi used plastics, which consisted of 80% polyethylene and 20% polystyrene. Sand was replaced by plastics at the following replacement ratios: 10%, 15% and 20% at a w/c of 0.53. The compressive strength decreased with the addition of plastic which is consistent with the results of other studies. The reasons presented to explain the loss of strength include a poor bond between the plastic and cement paste, elongated shape of the plastic aggregate and hydrophobic nature of the plastic, which prevents water from distributing throughout the concrete mix resulting in low hydration of cement (Ismail & Al-Hashmi, 2008).

Unlike the studies already presented which looked at using thermoplastics in concrete, the study by Dweik et al. used a thermosetting plastic, melamine-formaldehyde (MF), to replace a portion of the sand from 0% to 60%. They looked at the effect on the strength of both mortar and concrete. The strength of one of the concrete mixes is presented in Figure 2.4. For the concrete and mortar,

the compressive strength increased with the addition of MF, up to 30% sand replacement, and then decreased as the MF content was increased beyond 30%. The good gradation of the MF, its smooth and semi-angular shape where considered to be the reasons for improved strength when MF is used to replace the sand. Furthermore, it was suggested that a chemical bond may form between MF and cement (Dweik, Ziara, & Hadidoun, 2008).

2.4.2 Tensile Strength and Flexural Strength

Gavela et al. (2004) tested the flexural strength of concrete made with either PP or PET plastic replacing 20% or 30% of the natural aggregate. The flexural strength is significantly affected when 30% of the aggregate was replaced by either polymers, but the strength decrease was not as significant for the 20% replacement level (Gavela et al., 2004).

Marzouk et al. found that the flexural strength was affected more significantly than compressive strength when PET was used to replace sand in mortar. The trends were the same as those for compressive strength. Type A aggregate achieved the highest flexural strength (Marzouk et al., 2007).

Using the direct tension test on mortar specimens, Dweik et al. determined the tensile strength of mortar made with MF aggregate. The tensile strength was the greatest when 20% of the sand was replaced with MF and was 16% greater than that of the control. When more that 30% MF was used, the tensile strength decreased (Dweik et al., 2008).

2.4.3 Modulus of Elasticity

The effect of mixed plastic waste aggregate on the elastic modulus of concrete was studied by Ghaly and Gill when the coarse aggregate is replaced by 5%, 10%, and 15%. The results are given in Figure 2.5. In all cases, the addition of plastic resulted in a decrease in stiffness, except for the mix with w/c equal to 0.42. The concrete with a w/c of 0.54 had the highest modulus; this is however, inconsistent with other results where the modulus of elasticity decreased with an increase in w/c. At the 15% replacement level and w/c of 0.54, the elastic modulus was 15% less than that of the control (Ghaly & Gill, 2004).

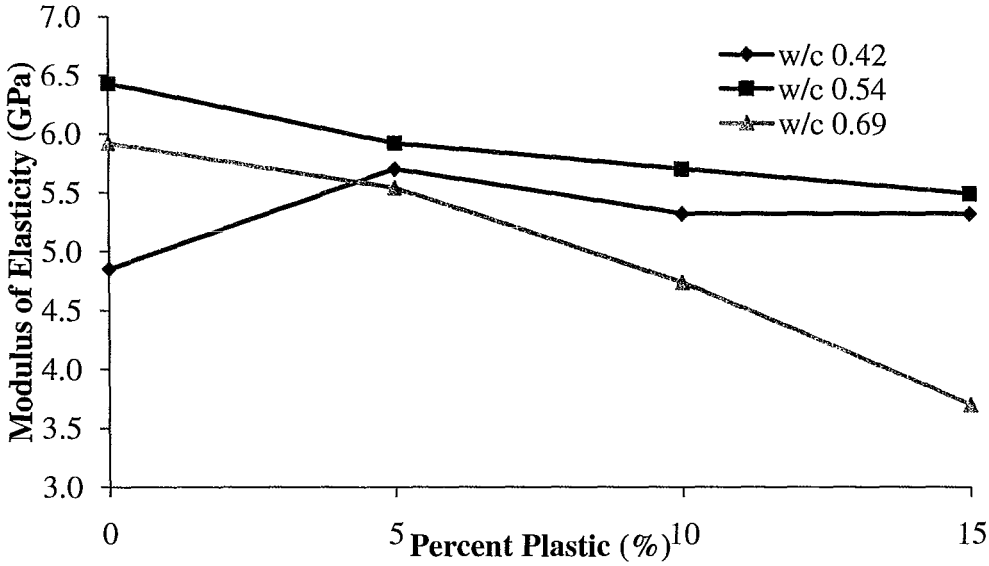

Figure 2.5 Elastic modulus of concrete with plastic aggregate (Ghaly & Gill, 2004; Mihaljevic & Chidiac, 2009)

2.4.4 Density

In the work of Marzouk et al., the density of the mortar decreased with the replacement of the sand with PET aggregate. There was no significant difference in the density when up to 30% of the sand is replaced by PET aggregate. However, above 30% PET, the density decreased dramatically. The mortar with the largest PET aggregate had a slightly higher density than the other mortars (Marzouk et al., 2007).

Ismail and Al-Hashmi attempted to make lightweight concrete by replacing sand with waste polyethylene and polystyrene aggregate. At 28-days, all the concrete mixes had densities higher than the maximum for concrete to be classified as lightweight even though the plastic used had a density 67% lower than the sand. At 20% replacement of sand, the density was 2224 kg/m^3 compared to 2400 kg/m^3 for the control concrete (Ismail & Al-Hashmi, 2008).

Dweik et al. (2008) showed that using MF as a fine aggregate reduces the density of mortar and concrete. When 60% MF was used, the mortar density decreased by 21% compared to plain concrete. The concrete had a 8.5% decrease in density when MF replaced 60% of the sand (Dweik et al., 2008).

2.4.5 Water Absorption

Babu and Babu (2003) found that concrete made with large quantities of EPS aggregate had lower water absorption than the concrete with low amounts of EPS. All the concrete tested had low water absorption.

Marzouk et al. used sorptivity as an indicator of durability of mortar made with waste PET aggregate. They showed that as the amount of PET increased, the coefficient of sorptivity decreased for substitutions up to 50%. The lower rate of

sorptivity is attributed to the negligible water absorption of the PET aggregate. Therefore, the water must travel around the PET aggregate to penetrate the mortar. The results suggest that the mortar with PET would be durable (Marzouk et al., 2007).

2.5 Summary

The review presented in this chapter gives an overview of studies into the use of glass and plastic waste to produce concrete. From the work presented, there is indication that both glass and polymer waste can be used in a concrete mix. Up to 30% replacement of sand with WG aggregate allows for large quantities of glass to be incorporated, without significantly affecting compressive strength, as long as the issue of ASR is addressed. Glass particles finer than 40 μm exhibit pozzolanic properties. The literature review has shown that WGP as a cement replacement yields concrete with good strength without adversely affecting other properties. When WGP is used in concrete, ASR should be evaluated, even though the literature does not give any indication of negative ASR expansion.

The review has revealed that thermoplastics were mostly used to replace natural fine aggregate. The results also showed that there is a large decrease in compressive strength even at low substitution levels. The addition of thermosetting plastics as sand replacement has, however, shown minimal effect on strength. The use of 20% or more plastic does not appear to be feasible, although the weight of the concrete above this level is greatly reduced.

The major issues with using WG as either an aggregate or a pozzolanic material are the possibility of ASR damage, the cost of crushing, sorting and cleaning the glass and finding a consistent, reliable source for the glass. For glass to be implemented as a SCM, the cost of the WGP will need to be lower than that of other pozzolanic materials. Research shows that it is possible to use glass as both an aggregate and a pozzolanic material; however it appears to be more economically viable to use glass as cement replacement since it is the most expensive component of the concrete and also the biggest polluter. Also, by using WGP, the risk of a detrimental ASR reaction is much lower.

Challenges facing the use of plastics as aggregates in concrete include the low strength of the polymer aggregate and the adverse interaction of polymers and water in the cement paste. Further research is needed to determine how plastics interact with cement paste and its long term effects on the properties.

2.6 Problem Statement

WGP and polymer aggregate have the ability to be used within concrete to reduce the detrimental environmental effect of concrete production while providing a useful alternative for these waste materials. Since the constituents of concrete masonry blocks are similar to that of regular concrete, it follows that WGP and polymers can be used to replace cement and fine aggregates, respectively, within concrete blocks.

CHAPTER 3 EXPERIMENTAL PROGRAM

3.1 Introduction

A comprehensive experimental program was developed to evaluate the feasibility of using post-consumer waste glass or polymers in concrete masonry blocks. The blocks were made by replacing a portion of the sand with varying amounts of polymer or by substituting some of the Portland cement with waste glass powder (WGP). The testing program was established to evaluate properties of concrete blocks and masonry assemblages and to test the effect of the materials added on these properties. The block properties tested include compressive strength, elastic modulus, density and absorption. For the prism assemblages, the compressive strength, elastic modulus and bond strength were tested. Also, the wetting angle of the polymers and the reactivity of the glass in an alkali solution were analyzed. The testing program was organized so that all the results could be analyzed statistically. Specimens were tested according to the Canadian Standards Association (CSA) and/or the American Society for Testing and Materials (ASTM) standards. The following sections outline the methodology used to determine the physical, mechanical and chemical properties of concrete masonry blocks and assemblages.

3.2 Materials

3.2.1 Coarse Aggregate

The coarse aggregate used for the production of concrete blocks was crushed limestone mined in Ontario. The maximum nominal size of the aggregate was 5 mm. The gradation of the coarse aggregate is shown in Figure 3.1 with the specification limits of the plant where the blocks were produced.

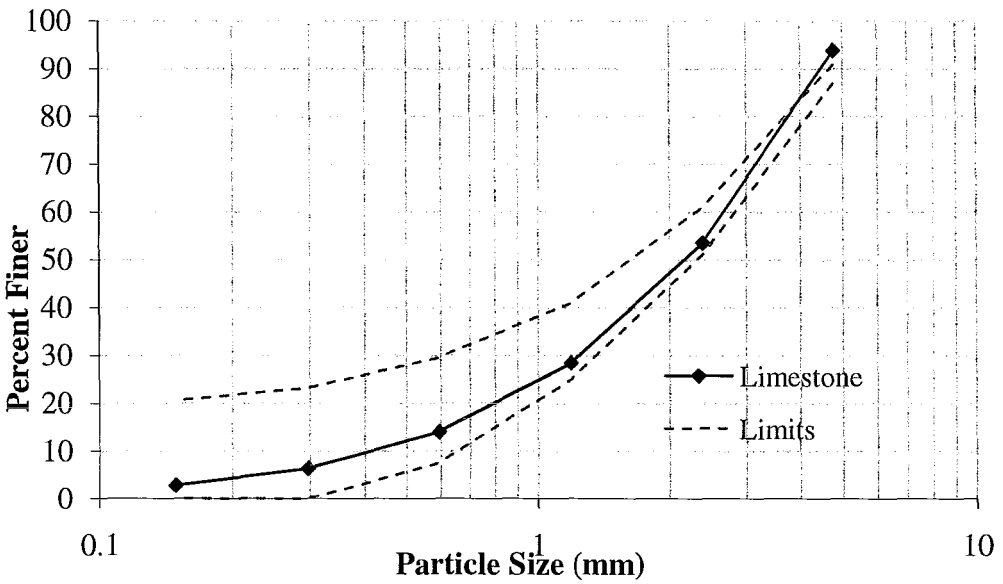

Figure 3.1 Gradation of coarse aggregate

3.2.2 Fine Aggregate

The fine aggregate used to produce the blocks was siliceous sand. The gradation of the sand is presented in Figure 3.2. The sand falls within the gradation limits used by the block manufacturer. The fineness modulus (FM) of the sand was 3.2. The density of the sand was 1600 kg/m^3.

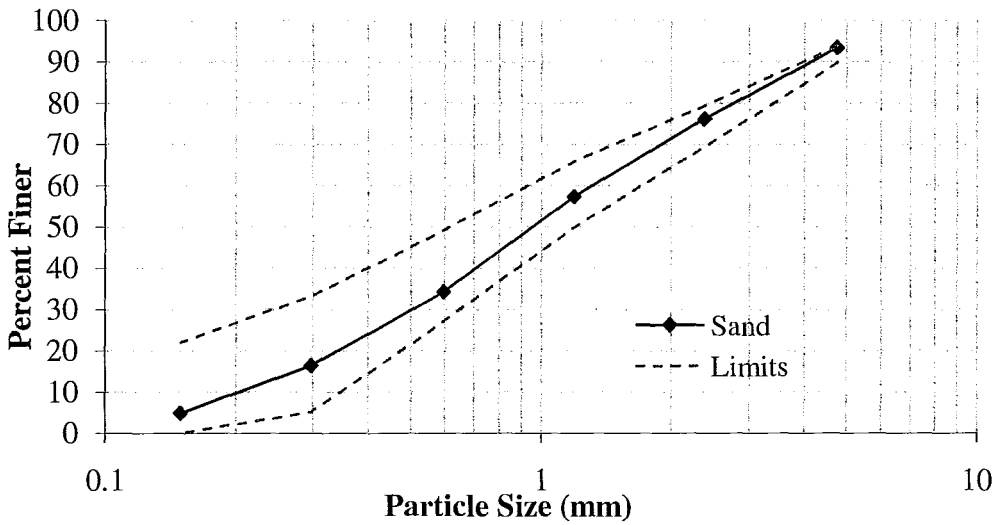

Figure 3.2 Gradation of sand

3.2.3 Cement

The cement used in the production of concrete block was Holcim Type 30 cement. The general specifications of the cement are given in Table 3.1. For the mortar used to construct the masonry prisms, Lafarge Type 10 cement was used.

Table 3.1 General specifications for Type 30 cement

Chemical Properties	
Loss of Ignition (%)	1.3
Insoluble residue (%)	0.2
$C_3A > 8.0\%$ (%)	4.4
$C_3A < 8.0\%$ (%)	~0
Magnesium oxide (%)	2.5

Physical Properties	
Fineness (%) (> 45 μm)	2
Expansion (%)	0.06
Setting time (min)	105
Compressive strength - 1 day (Mpa)	30
Compressive strength - 3 day (Mpa)	38
Compressive strength - 7 day (Mpa)	42
Compressive strength - 28 day (Mpa)	50

3.2.4 Glass

The WGP was obtained from a waste source consisting of soda lime glass and was not treated prior to use. A sample of WGP is shown in Figure 3.3. Characterization of the glass is given in Table 3.3. Results show that the particles are less than 36 μm, this suggests that WGP will undergo some pozzolanic reaction (Shao et al., 2000).

Figure 3.3 WGP sample

Table 3.2 Characterization of WGP

Properties	Values
Particle size > 36 μm	8 % Max.
Moisture	0.1 % Max.
Silica	69 – 73 %
Sodium and Potassium Oxide	13 – 15 %
Aluminum Oxide	1 – 3 %
Remainder	1 – 3 %

3.2.5 Polymers

Polymers were obtained from Ingenia Polymers of Brantford Ontario and they were virgin material. Virgin material was used in this trial to focus solely on the effect of polymers. Figure 3.4 shows the appearance of a typical polyethylene, polymer aggregate sample. The polymers used were low density polyethylene (LDPE), high density polyethylene (HDPE) and grafted high density polyethylene. Polyethylene was chosen since it is a common polymer and large quantities can be found in the waste stream. All the polymers were in the shape of pellets. The density of the polymers was approximately 1000 kg/m^3.

Figure 3.4 Polymer sample

The results of the sieve analyses for the polymers are summarized in Figure 3.5, Figure 3.6 and Figure 3.7. The results show that the particle gradation of the polymer aggregate is slightly coarser than the sand used in the production of the concrete blocks and all the gradations fall outside the limits for sand used by the block manufacturing plant. The grafted HDPE complied most closely with the limits. The FM for the LDPE, HDPE and grafted HDPE was 3.9, 4.1 and 3.6, respectively. This is slightly coarser than the sand which it replaced, but considered suitable for use as the fine aggregate in the blocks.

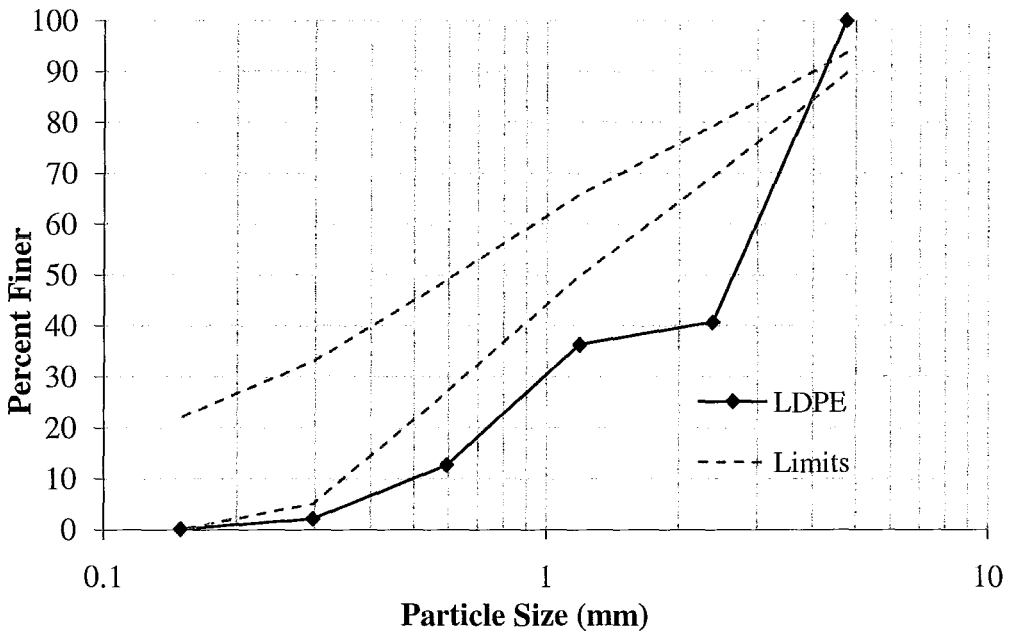

Figure 3.5 Gradation of LDPE polymer aggregate

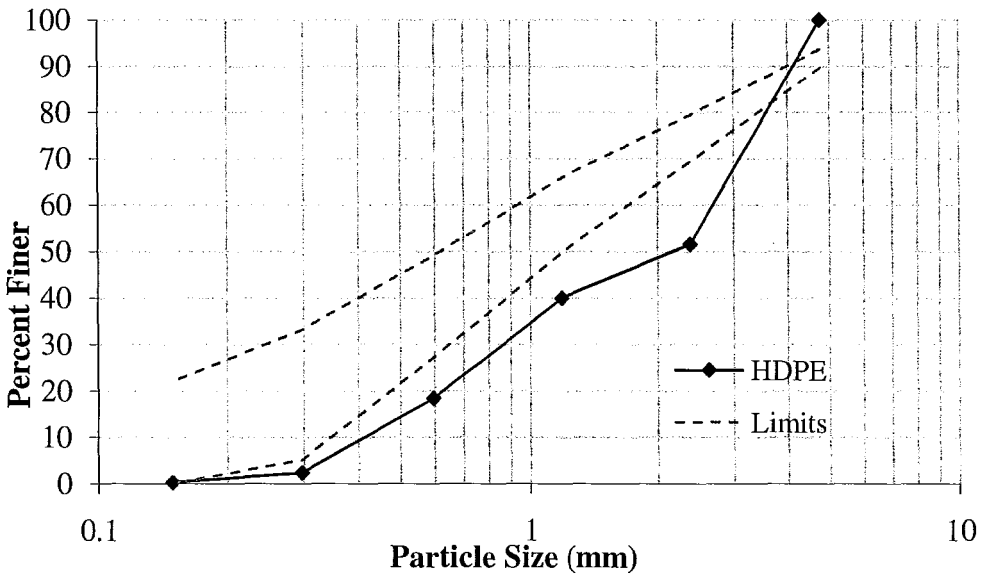

Figure 3.6 Gradation of HDPE polymer aggregate

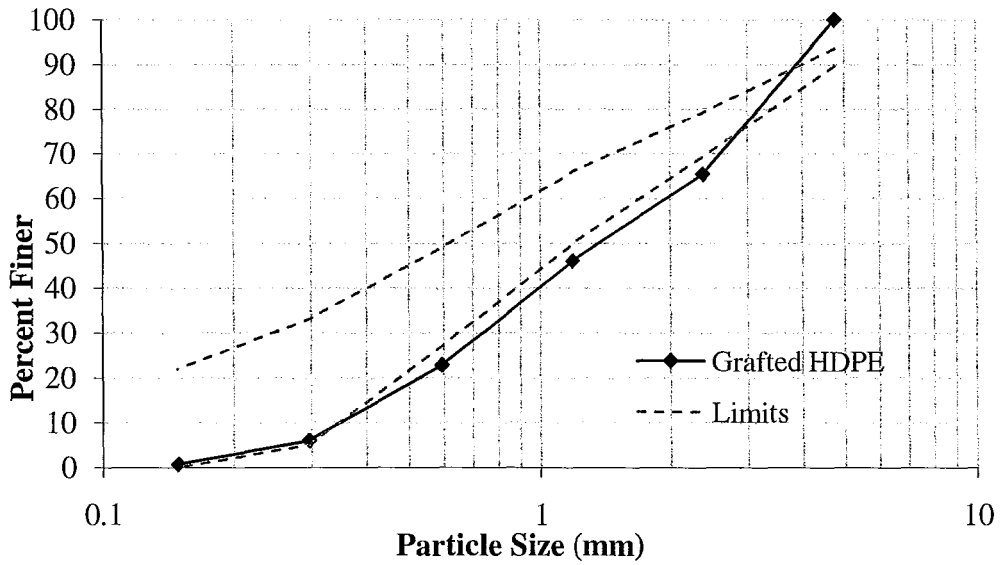

Figure 3.7 Gradation of grafted polymer aggregate

3.2.5.1 Contact angle of polymers

Polyethylene is a hydrophobic material. Since the production of concrete blocks requires water, the extent of the hydrophobic nature of the polymer needs to be determined. This may be determined by using the contact angle of the polymer as evaluated by following the procedure in ASTM D 5946 (2009).

The contact angle, θ, is a measure of the wettability for a particular solid and liquid (Berg, 1993). Figure 3.8 shows the location at which the contact angle is measured for a resting drop of liquid on a flat, smooth, solid surface. The

contact angle may range from 0^{o} to 180^{o}. Small contact angles indicate a high attraction between the surface and the liquid and large values of θ indicate a low attraction (Berg, 1993).

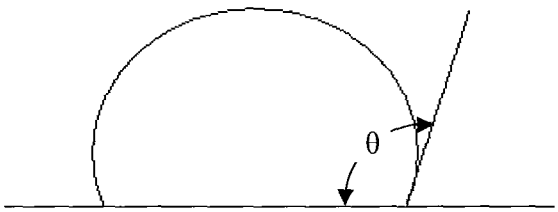

Figure 3.8 Measurement of contact angle, θ (ASTM D 5946, 2009)

The grafted polymer was selected to determine whether it could improve the bonding characteristics of plastics to increase the strength of concrete with polymers. Grafting is a process where "functional" groups of molecules are attached to a polymer backbone to modify the behaviour of the polymer (Frechet, 1994).

Before the contact angle could be determined, the polymer aggregate needed to be prepared by molding it into flat, smooth sheets. The apparatus used was the hand press shown in Figure 3.9. To prepare a sample, the polymer pellets were placed between the hot plates of the press. The temperature was set to $185.0^{o}C \pm 0.5^{o}C$ so that the polymer would become soft and malleable. The top crank was tightened until the top plate touched the specimen and allowed to sit for approximately 2 minutes. Then, the crank was tightened all the way. The specimen was allowed to compress for approximately 30 s before the press was loosened and the specimen removed. Figure 3.10 shows an image of the prepared sample.

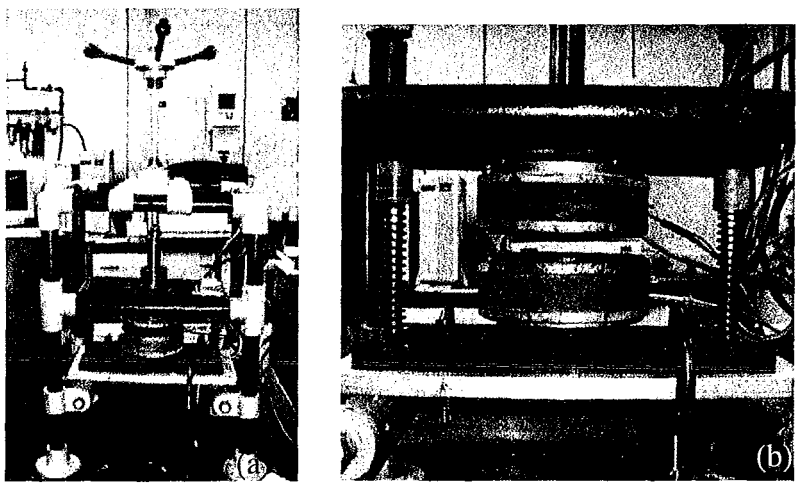

Figure 3.9 (a) Hand-press apparatus (b) close-up view of hot plates

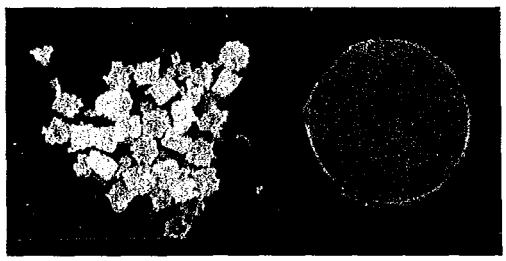

Figure 3.10 Polymer specimen for contact angle measurement

The contact angle for the LDPE, HDPE and grafted HDPE following ASTM D 5946 (2009), which is used to test the water contact angles of polymer films, and ASTM D 5725 (2008), which outlines the use of an Automated Contact Angle Tester. The sample was placed in the sample holder below a syringe filled with distilled water. A 5 to 8 μm water droplet was suspended from the end of the syringe and the surface of the sample was raised to touch the surface of the droplet. The sample was then lowered to transfer the droplet to the polymer sheet. A light source was used to illuminate the sample so that a video camera could capture the image of the water droplet on the surface of the polymer. Image analysis software was then used to trace the outline of the water droplet and the surface of polymer so that the software could calculate the average contact angle. Figure 3.11 shows the test setup. The contact angle was measured three times for each polymer type. A material with a contact angle with water greater than 90° is classified as hydrophobic.

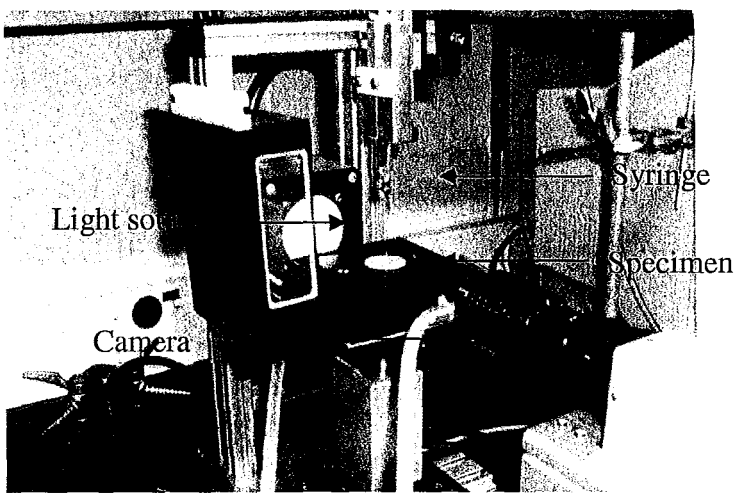

Figure 3.11 Automated contact angle tester

3.3 Concrete Mixture Design

3.3.1 Block

The design of the concrete mixture for the control blocks was the standard mix of the manufacturing plant. The mix was modified by either using WGP to replace a portion of the cement or by using the polymers to replace a portion of

the sand, for a total of 12 different mixes. The determination of the mixture proportions was based on the size of the minimum batch the plant could produce, the availability of the replacement materials, and the effect of the replacement on the concrete blocks after the first replacement attempt with polymers. The small quantity of available grafted material permitted only one batch to be made with it and only 3% of the sand could be replaced. Also, due to the detrimental effects the plastic produced on the blocks, the volume of sand replaced was lowered compared to what was initially planned. It was decided that the sand would be replaced by 3%, 6%, 9% and 15% with either LDPE or HDPE or by 3% with grafted HDPE aggregate. The sand was replaced by volume with the polymers. The cement was replaced by either 10% or 25% of WGP. The cement was replaced by weight with WGP. Table 3.3 shows the mix design for the 12 mixes. The coarse aggregate was 522 kg for all 12 mixes. The water to cementing material ratio (w/c) was maintained at 0.40 for all the mixes.

Table 3.3 Mix design

Mix	Mix Designation	Cement (kg)	Sand (kg)	LDPE (kg)	HDPE (kg)	Grafted (kg)	WGP (kg)
Control	C	118	841	0	0	0	0
3% LDPE	LP3	118	816	16	0	0	0
6% LDPE	LP6	118	790	31.5	0	0	0
9% LDPE	LP9	118	765	47	0	0	0
15% LDPE	LP15	118	715	79	0	0	0
3% HDPE	HP3	118	816	0	16	0	0
6% HDPE	HP6	118	790	0	31.5	0	0
9% HDPE	HP9	118	765	0	47	0	0
15% HDPE	HP15	118	715	0	79	0	0
3% grafted	GP3	118	816	0	0	16	0
10% WGP	G10	106	841	0	0	0	12
25% WGP	G25	88	841	0	0	0	29

3.3.2 Mortar

Structural type S mortar was chosen for the construction of the prisms. The mortar mix consisted of Portland cement, hydrated lime, fine mortar sand and water. The mortar mix used was the typical mix developed at McMaster University and conformed to the CSA A179 (2004) requirements for type S mortar. The proportion of the mortar mix used was 1:0.46:4.16 cement:lime:sand, by volume. The volume of water was chosen to ensure good flow of the mortar. The mass of water used was 6.7 kg and the batch size was chosen so that the mortar could be used up within one hour. Table 3.4 gives the mix used.

Table 3.4 Mortar mix for one batch of mortar

	Cement	Hydrated Lime	Sand
Mass (kg)	7.6	1.5	27
Density (kg/m^3)*	1505	640	1280
Proportions (by volume cement)	1	0.46	4.16

*The density is based on the values given by CSA 179 (2004) Table 2

3.4 Sample Preparation

3.4.1 Block Production

All the concrete blocks tested were produced in an industrial block making plant. The control batch was made first, followed by the mixes with polymers replacing aggregate and then the mixes with glass. This section will outline the mixing procedure followed in the plant and some production challenges.

First, the fine and coarse aggregate were added to the mixer and mixed for 20 sec. To add the polymer aggregate or WGP, the mixer was stopped and the back hatch opened so that the pre-weighed materials could be placed directly into the mixer. Then, the cement was added and mixed for approximately 20 sec. Then, the water was added to ensure a consistent mix and a w/c of 0.4. Depending on the moisture of the aggregate, the time of mixing was adjusted. The water added to each mix is given in Table 3.5. Figure 3.12 shows the addition of polymer and WGP.

Table 3.5 Water added and total batch mixing time

Mix	Water added (L)	Mix time (s)
C	32	135
LP3	30	126
LP6	30	110
LP9	30	110
LP15	40	110
HP3	30	126
HP6	30	110
HP9	30	105
HP15	29	105
GP3	27	125
G10	32	130
G25	32	130

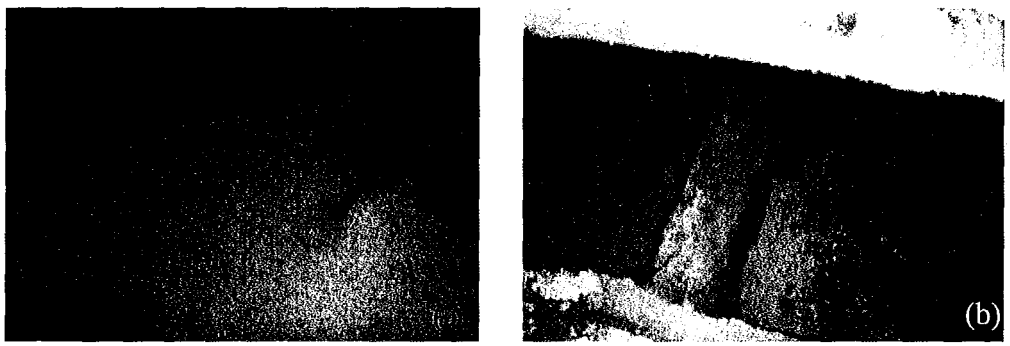

Figure 3.12 (a) Polymer being added to the mixer (b) WGP added to mixer

The mixture was then removed from the mixer and the consistency of the mix was checked. No segregation of polymer aggregates was observed and all the mixes appeared to be acceptable based on visual inspection. Subsequently, the mixture was placed into the molds and compacted. The blocks were marked so that the mixes could be easily identified. The blocks were steam cured for about 12 hrs, after which they were sealed in plastic and stored outdoors, following the standard practice of the plant. One month after production, the blocks were shipped to the McMaster Applied Dynamics Laboratory.

Visual inspection of the blocks, after they were de-molded, indicated no observable flaws for most of the blocks produced from the various mixes. However, some of the batches with higher polymer contents showed cracks in the wet blocks. This was more pronounced for both the 15% LDPE and 15% HDPE mixes. Some cracks were also observed with the mixes having 9% of the sand replaced with polymers. The cracks in the webs of the 15% LDPE blocks, after compaction, can be seen in Figure 3.13. Due to these cracks, it was decided to limit sand replacement, with polymers, to 15%. It is believed that the cracks formed due to the repulsive forces generated between the wet material and the hydrophobic polymers during compaction, which caused expansion when the molds were removed. No observable defects were detected in the mixes with the glass powder or those with low quantities of polymer.

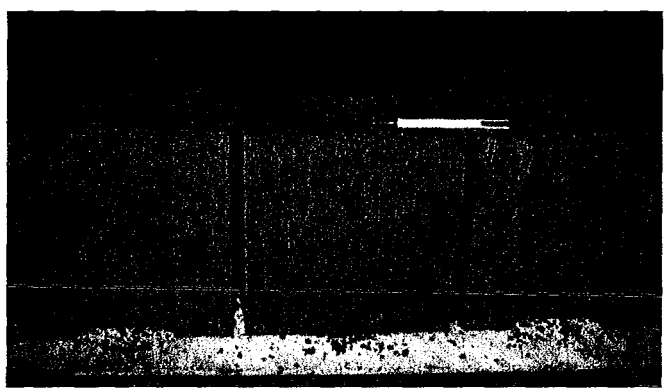

Figure 3.13 Cracks in webs of wet 15% LDPE blocks

3.4.2 Mortar Preparation

The mortar was mixed in a wheelbarrow with a shovel. First the dry components, the sand, cement and lime, were mixed thoroughly. Then half of the water was added. Once that was blended, the rest of the water was added and the mortar was mixed again, as shown in Figure 3.14. No additional water was added and the mortar was used up within an hour, so the mortar remained workable. Once the mortar was mixed, the flow was tested and mortar cubes were molded. In total, 16 batches of mortar were made.

Figure 3.14 Batch of mortar

3.4.3 Prism Construction

The prisms for compressive strength testing were constructed 4 units high and 1 unit wide in a running bond pattern. Four unit high prisms were used to minimize end confinement and slenderness effects, so that the compressive strength correlation factor is 1.00 according to CSA S304.1 (2004) Annex D Table D.1. Blocks were cut with a large diamond saw using a wet blade to form a running bond to simulate construction practice. The mortar joints were 10 mm high and face shell mortar bedding was employed. Type S structural mortar was used and the joints were tooled to form a concave profile. The prisms were not grouted. The prisms for the bond wrench test were constructed 4 blocks high, but stacked instead of using a running bond, following the procedures outlined in CSA S304.1 (2004) Annex E and ASTM C1072 (2006). The joints were also 10 mm, face shell bedded and concave. Typical prisms for compressive testing and for bond wrench testing are shown in Figure 3.15. Five prisms were constructed for compression testing for each of the concrete block mixes for a total of 60 prisms with running bonds. For the bond wrench test, 2 prisms were constructed for each mix for a total of 24 stack pattern prisms.

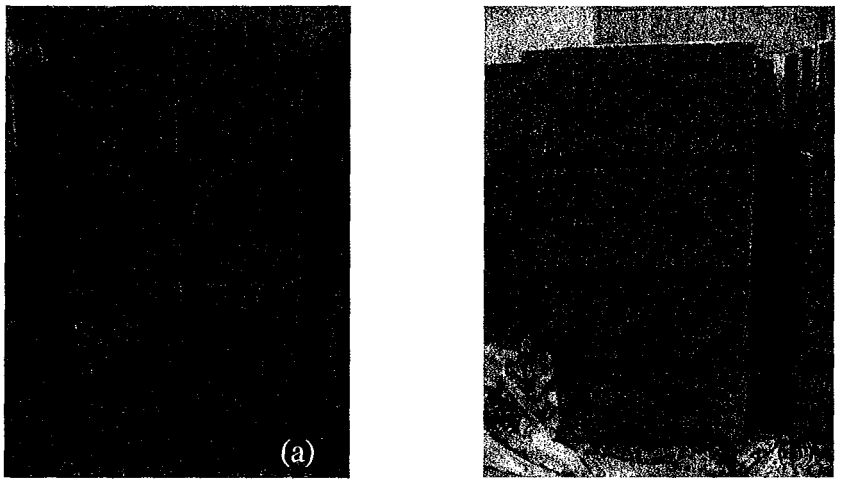

Figure 3.15 (a) Prism for compressive test, (b) prism for bond wrench test

The prisms were constructed by a certified mason from the Canadian Masonry Design Centre and were constructed in the basement of the McMaster University Applied Dynamics Laboratory over four days. To ease construction, the mason placed 10 first course blocks and built up; course by course, so that the constructed prism consisted of more than one mortar batch. After each set of 10 prisms, he tooled the mortar to produce concave joints on both sides of the prisms. Figure 3.16 shows the prism construction.

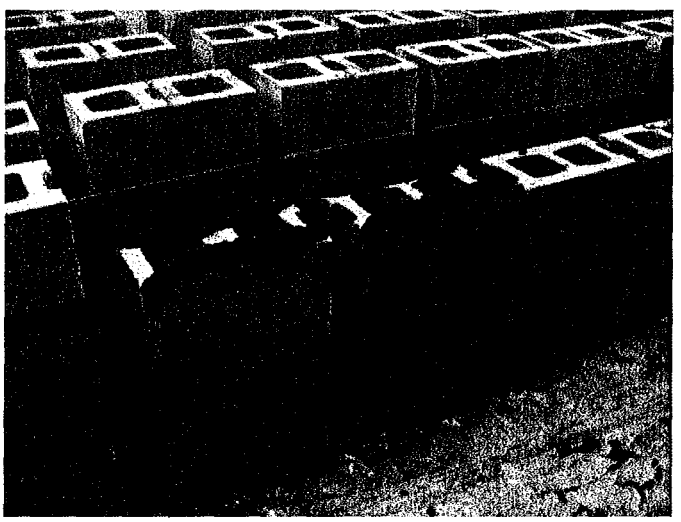

Figure 3.16 Prism construction

The mason did not have any difficulty constructing the prisms with the WGP or the polymers. The only problem he observed was that, with the polymer blocks, the width was not consistent so that he could only align them with one face of the block below. The mason also observed a significant weight difference between the blocks and commented that he could distinguish the ones with

polymers because they were much lighter and easier to lift than the regular blocks or those with WGP.

3.4.4 Capping for Compression Test

To ensure a level and uniform surface for compression testing, the blocks and prisms were hard capped with high strength gypsum cement capping material, known as hydro-stone, on the top and bottom, in accordance with ASTM C 1552 (2008a) and ASTM C 1314 (2007), respectively.

For the blocks, the hydro-stone paste was spread on a level steel surface coated with oil and then the block was placed on top and leveled. The capping was allowed to harden before the block was removed. The same procedure was followed for the other bearing surface of the block.

For the prisms, the bottom capping plate was a 76 mm steel plate and the top capping plate was also steel and 50 mm thick. First, the bottom of the prism was capped. This was accomplished by lifting the prism, with a rope around the bottom block, using a push forklift and setting it above the bottom capping plate, which was first leveled. Subsequently, the prism was leveled while suspended above the plate. The hydro-stone was then placed on the plate and the prism was lowered so that it just rested on it and the level was checked. If the prism was level, the hydro-stone was allowed to harden with the prism suspended partially by the forklift for approximately 20 minutes. Then, the prism was released and the hydro-stone allowed to cure for another 20 minutes before the top plate was added. The top plate was lowered manually, once a hydro-stone paste was placed, to cover the whole surface of the top block. The completed prisms where left overnight to cure before they were transported to the testing machine.

3.4.5 Instrumentation to Measure Elastic Modulus

To obtain the strain, linear potentiometers were attached to the surface of the block and prisms to measure the displacement. The linear potentiometers used were spring loaded, with a stroke of 12 mm and an accuracy of 2%. Figure 3.17a shows a close up view of a potentiometer. To ensure that the blocks were not damaged by drilling, which may affect their stiffness and strength, the potentiometers were attached to the surface of the blocks with custom made shelves, which were bonded using high strength structural epoxy (Sikator 31 Hi-Mod Gel).

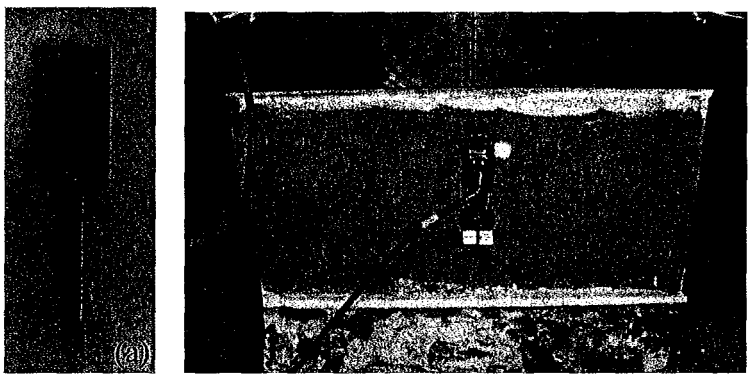

Figure 3.17 (a) linear potentiometer (b) linear potentiometer attached to block

For the blocks, potentiometers were attached to the centre of both faces of the block and the elastic modulus was determined from the average of their two readings. Figure 3.17b shows how the potentiometer was attached to a block. The gauge length across which the displacement was measured was approximately 70 mm.

Similarly for the prism, linear potentiometers were attached to the surface of the prism, as shown in Figure 3.18; however, the gauge length was 610 mm to measure displacements across all the joints. A total of four linear potentiometers was used, 2 on each side of the prisms and a trigger wire was used to span the joints.

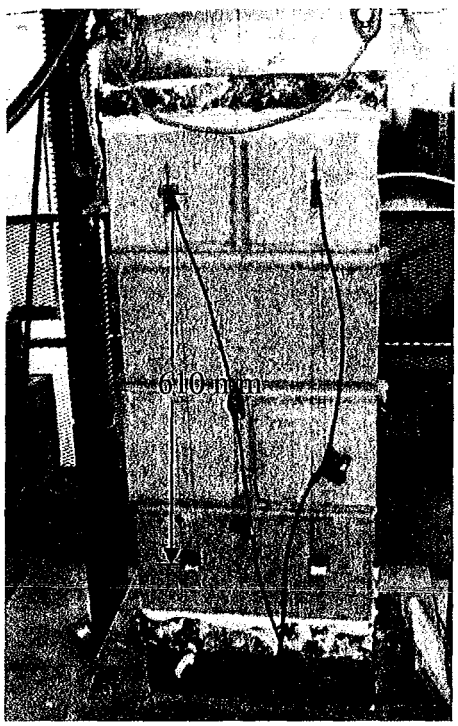

Figure 3.18 Linear potentiometers on prism

3.4.6 Preparation for ASR Test

The possibility of ASR expansion was tested according to ASTM C 1260 (2007). Strips were cut out of the concrete blocks to conform in size with the mortar bars normally tested. ASTM C 490 (2008) outlines the mold dimensions for the mortar bar test. The bars cut from the blocks were nominally 285 by 33 by 33 mm with a gauge length of 250 mm. Normally, the mortar bars are 25 mm by 25 mm in thickness, but 33 mm was chosen in this case to correspond to the block face shell thickness. The bars were cut from the blocks using a large diamond saw with a wet blade. Brass points, to be used to measure the length change of the bars, were bonded to the surface with epoxy. The length change was measure with a DEMEC mechanical strain gauge, as shown in Figure 3.19. Figure 3.20 shows a submerged mortar bar with the brass points. The bars were conditioned by immersing them in distilled water for 24 hrs in a convection oven at 80 $\pm$ 2°C.

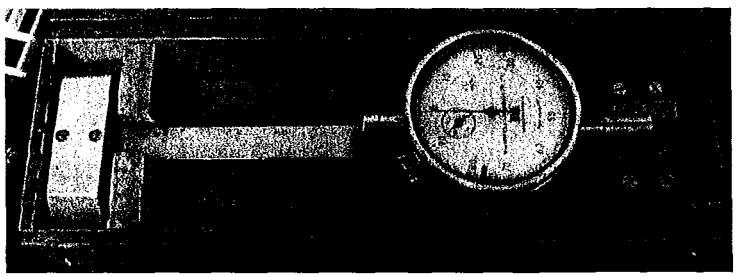

Figure 3.19 DEMEC gauge

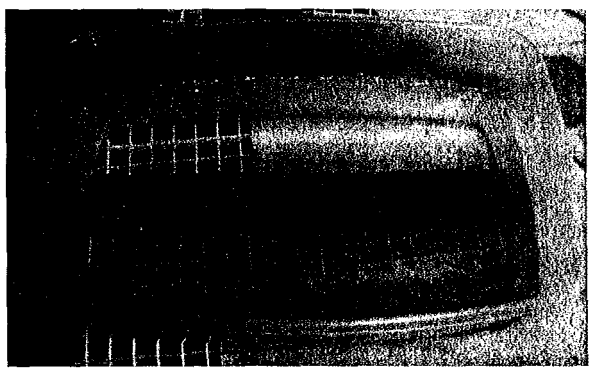

Figure 3.20 Submerged mortar bar with brass points

3.5 Test Methods

3.5.1 Mortar

3.5.1.1 Flow

Once the mortar was mixed and before it was used, the flow was tested. The flow of mortar is an indication of how well it will bond with the blocks. According to CSA 179 (2004), the flow must be between 100% and 115% to produce a good bond for mortar produced in the laboratory.

The flow was tested according to ASTM C 1437 (2007). The apparatus for testing consists of a flow table, standard calipers, tamping rod and 100 mm base

diameter cone. The mold filled, as shown in Figure 3.21a, then the table was dropped 25 times following the specifications. The diameter of the sample was then measured using calipers, as in Figure 3.21b. If flow exceeded the permitted limits; the mortar was mixed a little longer to allow for some of the excess water to evaporate.

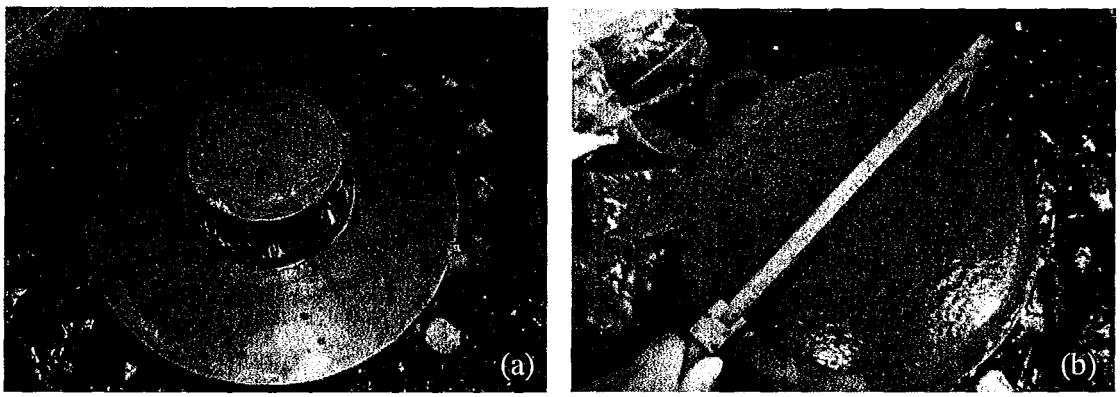

Figure 3.21 (a) Flow test apparatus (b) flow measurement

3.5.1.2 Compressive Strength

The compressive strength of mortar cubes is important for quality assurance and because it affects the properties of the masonry assemblage. For each mortar mix, 3 mortar cubes were made according to CSA A179 (2004). The standard requires that 6 cubes be made for each mix, but this was not possible due to the number of molds available. The mortar cube compressive strength was tested on the day the prisms were tested.

After molding the mortar cubes in standard 50 mm molds, the cubes were placed in a moist cabinet for 48 hrs. Then they were removed from the molds and from the moist room and stored in the same room as the prisms. After the prisms were tested, the mortar cube compressive strength was tested on the Tenius Olsen machine (maximum load 600 kN), shown in Figure 3.22. The cubes were centered on the machine and loaded to failure at a constant rate.

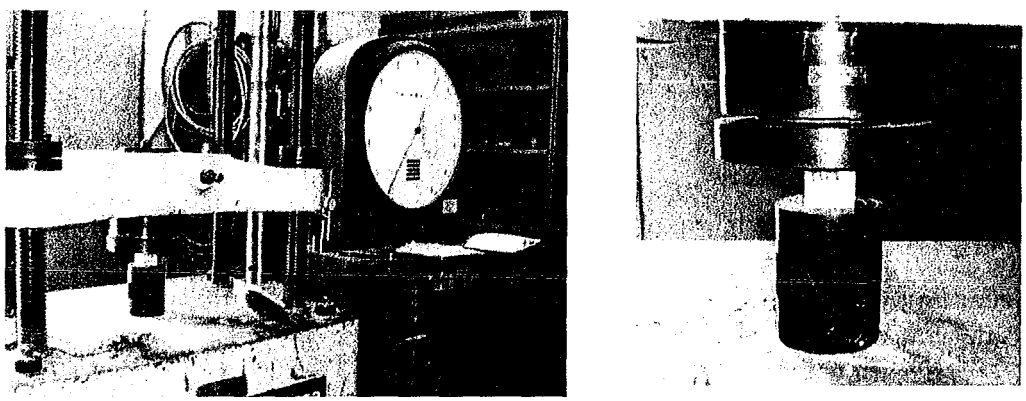

Figure 3.22 Compression test for mortar cubes

3.5.2 Blocks

The physical properties of the masonry units relate to their performance in assemblages and for which applications they can be used, therefore it is important to determine how these properties are affected by the addition of WGP or polymers. The individual block units were tested for water absorption, density, initial rate of absorption (IRA), compressive strength and modulus of elasticity. The test procedure is outlined in the following sections. The blocks tested consisted of stretcher and splitter blocks, as shown in Figure 3.23, of nominal size 200 mm by 200 mm by 400 mm.

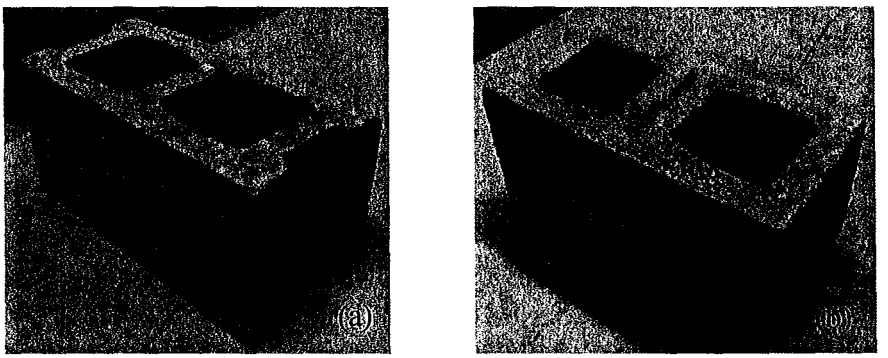

Figure 3.23 Block types: (a) stretcher (b) splitter

3.5.2.1 Density, Moisture Content and Water Absorption

The density, moisture content and water absorption of the blocks was determined in accordance with ASTM C140 (2008a). Each test was performed on 5 regular stretcher blocks and 5 splitter blocks for each of the 12 concrete mixes. Each block was weighed (W_r), to the nearest 0.001 kg, and then submerged in water for 24h. Then, the submerged weight (W_i) was obtained by weighing the specimen on a mesh attached to a scale, while the specimen was still fully submerged, as shown in Figure 3.24. The block was then allowed to drain for 1 min on a mesh and excess surface water was removed with a damp cloth, after which the specimen was weighed to determine its saturated weight (W_s). The blocks were then placed in an oven for a minimum of 48 hrs after which they were weighed to determine their oven dry weight (W_d).

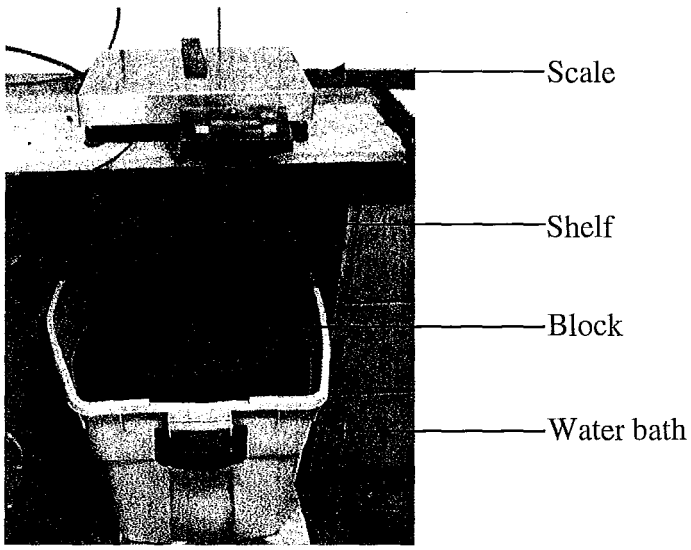

Figure 3.24 Setup for determining submerged weight

From the measured values, the following properties were calculated: moisture content (equation 3.1), density (equation 3.2) and water absorption (equation 3.3), as well as the net volume (equation 3.4) and net area (equation 3.5) of the specimens.

$$Moisture\ content\ (\%) = \frac{(W_r - W_d)}{(W_s - W_d)} \times 100 \qquad 3.1$$

$$Density\ (kg/m^3) = \frac{W_d}{(W_s - W_i)} \times 1000 \qquad 3.2$$

$$Absorption\ (\%) = \frac{(W_s - W_d)}{W_d} \times 100 \qquad 3.3$$

$$Net\ volume\ (mm^3) = \frac{W_d}{density} = (W_s - W_i) \times 10^6 \qquad 3.4$$

$$Average\ net\ area, A_n\ (mm^2) = \frac{net\ volume}{height} \qquad 3.5$$

3.5.2.2 Initial Rate of Absorption

The initial rate of absorption (IRA) is an indication of the ability of brick masonry to bond to mortar. The value must not be either too high or too low. A high value indicates that too much water is absorbed from the mortar by the brick, thereby drying out the mortar before it can properly hydrate. A low IRA value indicates that the brick will not absorb enough water from the mortar to form a

bond between the two materials (Drysdale & Hamid, 2005). Although this is also an important property for concrete masonry, IRA is not a standard test for concrete blocks so the standard test for brick masonry was followed.

The IRA was determined for 3 blocks, for each mix, based on the standard test for bricks, ASTM C 67 (2009). The bottom 1 mm of the blocks was submerged in a large tank, as shown in Figure 3.25. The blocks were placed in the tank individually for 1 min. After 1 min, the block was weighed (W_{IRA}). The IRA value is calculated by using equation 3.6.

Figure 3.25 Test set up for IRA

$$IRA\ (kg/m^2/min) = \frac{(W_{IRA} - W_d)}{\left(\frac{A_n}{1000^2}\right)} \qquad 3.6$$

3.5.2.3 Compressive Tests

The compressive strength, f_c' , of masonry units is an important property which determines whether the blocks may be used in structural or non structural applications. Five blocks were randomly selected from each block type to test for compressive strength. The compressive strength was tested at 160 day and after 1 year.

The compression test was performed in a reaction frame and the load was applied by a hydraulic jack through a load cell. The jack was operated by a hand pump. Two steel plates, with a total thickness of 152.4 mm (6 in), acted as a base for the blocks. Once a specimen was placed on the base plates and centered on the jack, a 127 mm (5 in) thick steel top plate was lowered onto the block to ensure uniform distribution of the load across the surface area of the block, since the loading head is smaller than a block. A spherical swivel was placed between the load cell and the top plate to ensure that the load was transferred axially to the block. Figure 3.26 shows the test set up.

The test was performed in accordance with ASTM C140 (2008a). The load was applied at a uniform rate, within the limits that were achievable with a

hand pump, although the rate was slowed at loads above 900 kN since the pump became more difficult to operate at these levels. Because of the hand pump it was not possible to fail the specimen within 1 to 2 minutes after achieving half of the expected strength. All specimens were loaded to failure and the maximum load, P_{max}, was recorded, The compressive strength was calculated using equation 3.7.

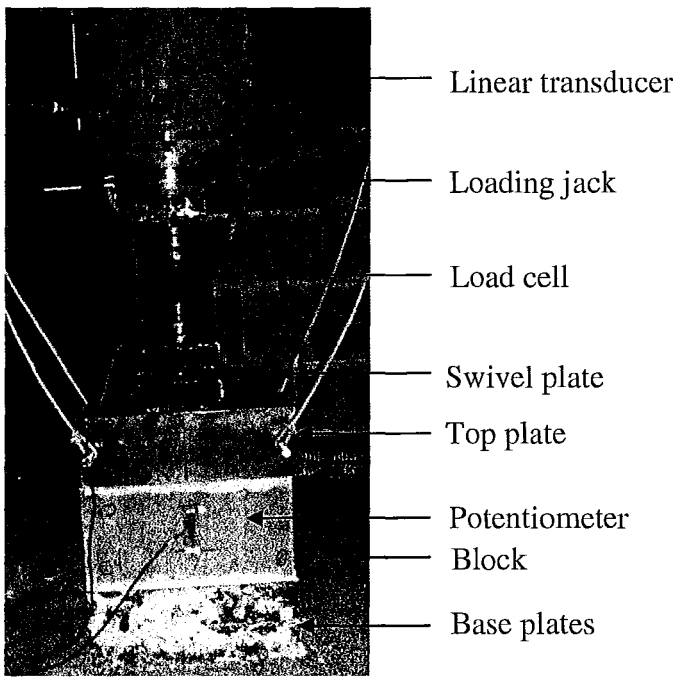

Figure 3.26 Compressive test setup

$$f_c' = \frac{P_{max}}{A_n} \qquad 3.7$$

3.5.2.4 Modulus of Elasticity

Typically, for masonry units, a secant elastic modulus is calculated based on the slope of the stress-strain line from zero stress to approximately 33% of the strength of the unit, to ensure that the linear portion of the curve is used (Drysdale & Hamid, 2005). For this study the readings below 5% of the strength were disregarded as required by the procedure for testing masonry prisms, in accordance with CSA S304.1 (2004) D.4.6.

Four blocks, of the five used to calculate compressive strength, were also used to determine the elastic modulus. Since the failure of masonry blocks is sudden, the potentiometers had to be removed between 50 and 70% of the failure load to ensure that they would not be damaged. For this reason, the first block tested for each mix was loaded to failure, so that 50 to 70% of the failure load could be estimated. Due to the nature of the instrumentation used and the difficulty of placing it on the blocks, some values of the modulus of elasticity were calculated from strains at strengths greater than 15% but lower than 50% of

the strength of the blocks. In all cases, this was still within the elastic range of the stress-strain graph. Also, in some instances, readings of one of the two potentiometers were found to be faulty and the value of only one could be used to estimate the elastic modulus. Since the readings of the two potentiometers were invariably close, this was considered acceptable.

3.5.2.5 Mortar Bar Test for ASR

The alkali silica reaction (ASR) is a major durability problem for concrete with waste glass. The accelerated test used in this study was the mortar bar test outlined in ASTM C 1260 (2007). The test was modified slightly since a portion of the concrete blocks was tested instead of making mortar bars. The blocks tested were three control blocks, three with 10% and three with 25% WGP blocks and three blocks with 15% LDPE aggregate.

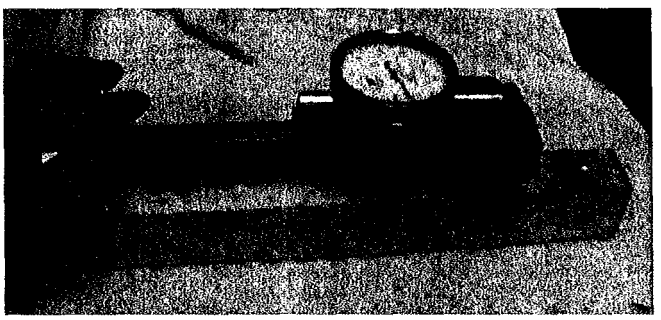

Figure 3.27 Mortar bar expansion reading with DEMEC

After conditioning, the bar was placed in a 1 mol/L NaOH solution in a 80 $\pm$ 2°C oven. Readings were taken periodically over a 14 day period to determine whether any expansion occurred using the DEMEC gauge, like in Figure 3.27. The test was continued for 30 days. According to ASTM C 1260 (2007), a specimen in considered nonreactive if after 14 days the expansion is less than 1%, a specimen is reactive if after 14 days the expansion is greater than 2%. If the expansion is between these criteria, the result of the test is inconclusive and the test should be continued beyond 14 days.

3.5.3 Prisms

Prisms were constructed to test the properties of the modified concrete, when it is used as an assemblage, so that its behaviour as a wall could be determined. The compressive strength and elastic modulus of the prisms was tested, as well as the bond strength between the blocks and the mortar.

3.5.3.1 Compressive Strength

The compressive strength of masonry prisms, f'_m, is a cost effective and convenient way to determine the performance of masonry without requiring full scale specimens. The compressive strength of 5 prisms for each of the 12 block

types was determined according to CSA S304.1 (2004) and ASTM C 1314 (2007). The prisms were tested six months after construction.

The compressive strength of the prisms was tested on the Riehile compression machine, which has a maximum capacity of 2500 kN. The test setup is shown in Figure 3.28. Once the prism was placed in the machine, it was leveled on the jack using 3 plumb-bobs. A 127 mm thick plate was placed on top of the prism. The prism was loaded at a constant rate until failure. The compressive strength was calculated from the maximum failure load, P_{max}, and effective cross-sectional area, A_e, of the prism (equation 3.8). For hollow masonry, the effective area is the area of mortar bedding, which is taken as two times the minimum face shell thickness multiplied by the length of one block. According to CSA S304.1 (2004) Annex D Table D.1, no correction factor was needed.

$$f'_m\,(MPa) = \frac{P_{max}}{A_e} \qquad 3.8$$

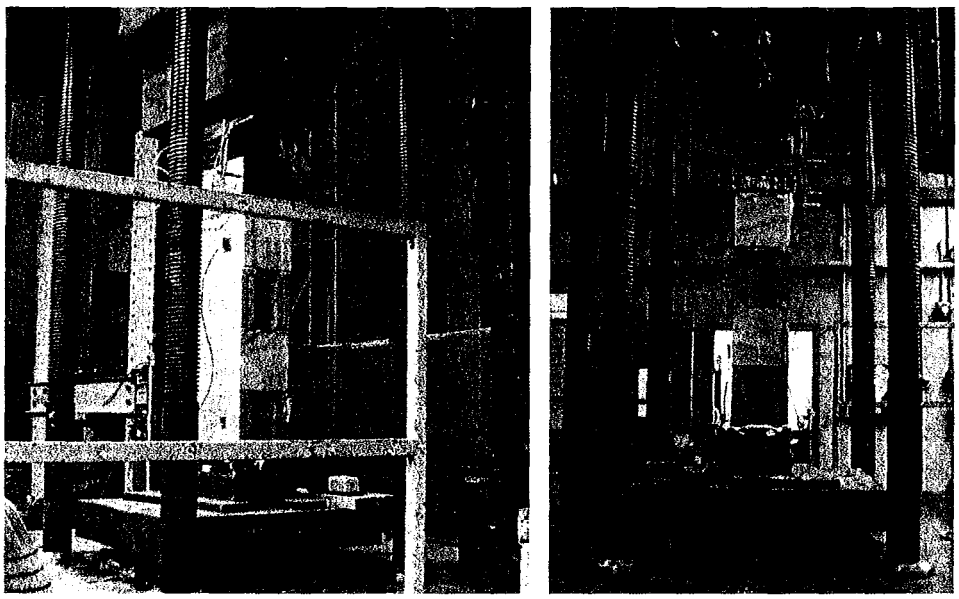

Figure 3.28 Prism compression test setup

3.5.3.2 Modulus of Elasticity

The modulus of elasticity, E_m, was also determined for all the prisms tested in compression from the displacement of the 4 potentiometers. The displacement was recorded up to approximately 50% to 70% of the compressive strength so that the potentiometers could be removed before prism failure.

The strain of the prisms was calculated by dividing the change in length of the potentiometers by the gauge length. The secant modulus was calculated from the average strain of the prisms. According to CSA S304.1 (2004) D.4.6, the secant modulus is determined by the slope of the stress strain graph between 5 to 33% of the prisms compressive strength. For some prisms, the range needed to be

modified to ensure that an accurate modulus was obtained, however the values used were always in the elastic range. It should also be noted that, in some cases, one or two of the linear potentiometers did not work properly, but for all the prisms, the elastic modulus was calculated from at least two potentiometer readings.

3.5.3.3 Flexural Tensile Bond Strength

The bond wrench test was used to determine the flexural tensile bond strength of masonry prisms by eccentric bending. The test procedure followed CSA S304.1 (2004) Annex E and ASTM C 1072 (2006). The test apparatus is depicted in Figure 3.29. This test was performed on each bond of the 2 stacked prisms for each block type, for a total of 6 bond tests per mix. The standard asks for a minimum of 15 joints to be tested, due to the variability of the test; however, due to space and time constrains, only 6 joints were tested for each type of block to give an indication of the bond strength. The bond wrench test was performed 5 months after prism construction.

The prisms were placed into the bond wrench apparatus with a forklift. The prism was raised so that the bottom of the top mortar joint was just above the top of the bottom clamping bracket. Then the bottom bracket was tightened so that all the bending tension was supported by the mortar joint. The top bracket with the lever arm was placed on the top block and the top bracket was clamped tightly. Due to the heavy load of the top bracket and the low bond strength of hollow prisms, a counterweight was applied, as shown in Figure 3.29, so that the joint would not fail before any additional load was applied. Then the load was applied at the end of the lever arm by slowly adding sand to a bucket. After failure, the top bracket was removed and the lower bracket loosened. Then the prism was raised so the second joint was above the lower bracket and the same procedure was repeated to test the joint.

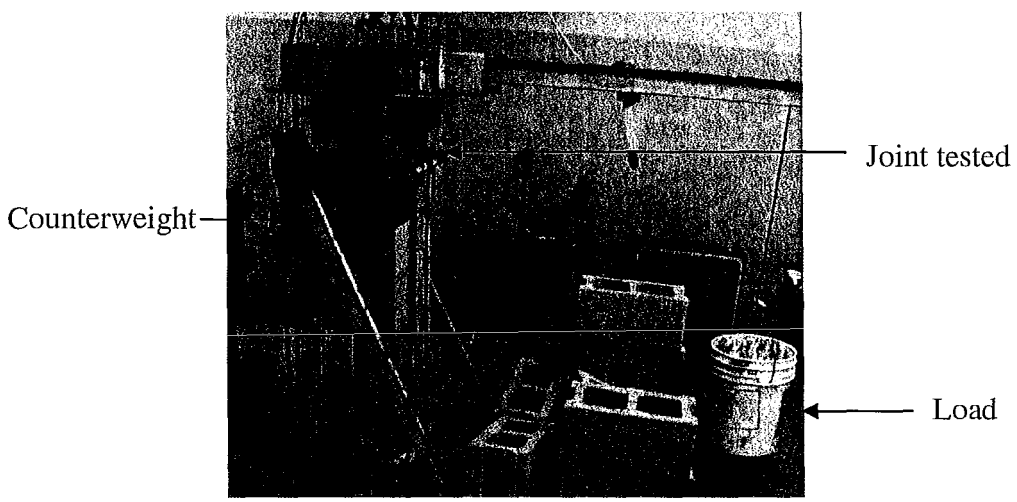

Figure 3.29 Bond wrench apparatus

The net flexural tensile strength, F_n, that causes the failure of the joint is calculated using equation 3.9. In the equation, P is the maximum load applied at the end of the lever arm and L is the distance from the centroid of the prism to the location where the load is applied, P_1 is the weight of the loading arm and L_1 is the distance from the centroid of the prism to the centroid of the lever arm and P_c is the load due to the counterweight and L_c is the distance from the centroid of the prism to the counterweight. The net bedded area, A_n, of the prism is used for hollow prisms and the sectional modulus, S, is calculated for the net bedded area.

$$F_n(MPa) = \frac{PL + P_1L_1 - P_cL_c}{S} - \frac{P + P_1 + P_c}{A_n} \qquad 3.9$$

CHAPTER 4 EXPERIMENTAL RESULTS

4.1 Introduction

The results of the experimental program, outlined in Chapter 3, are presented in this chapter. The effect of the replacement of sand with polymers and the replacement of cement with WGP on block and prism properties was determined and analyzed to conclude whether the results were statistically significant.

4.2 Statistical Analysis

In this study, the composition of concrete blocks was varied to determine the effect of using post-consumer waste on block properties. For this reason, statistical analysis was needed to determine whether these replacements are significant to the block properties for a certain level of confidence.

Hypothesis testing was the statistical inference tool used to determine the significance of the parameters tested. In statistics, a hypothesis is a statement about a parameter. In this chapter the parameters are the properties tested and the hypothesis is that there was a change in the parameter tested when the composition of the concrete blocks is changed. Hypothesis testing is used to determine the validity of the hypothesis. Since the sample size for each test was small, the variance of the tested samples is unknown; however the distribution is assumed to be at least partially normal (Montgomery & Runger, 2003). This corresponds to the use of Student's t-distribution to determine the validity of a hypothesis based on a function of the parameter tested, referred to as the test statistic. A null hypothesis is set so that, if it is true, there is no evidence of change or difference between the results. If the test shows that the null hypothesis should be rejected then the alternative hypothesis, that there is a difference between the results, must be true (Montgomery & Runger, 2003).

For the analysis, it is assumed that the observed results of the experiment are normally distributed, that there is no interaction between the results for the various replacement types and that the variance is the same for each replacement type (Montgomery & Runger, 2003). The F-distribution is used to check the hypothesis that the variance of one replacement is equal to the variance of another replacement. The null hypothesis for the f-test is that the variances are equal. The null hypothesis is true if the value of the test statistic given in equation 4.1 falls within the limit given in equation 4.2, where S_1^2 and S_2^2 are the variances of the two populations, and n_1 and n_2 are the number of samples tested. The confidence level of the statistical analysis is given by $100(1-\alpha)\%$.

$$F_0 = (S_1^2)/(S_2^2) \qquad 4.1$$

$$f_{\alpha/2,n_1-1,n_2-1} < F_0 < f_{1-\alpha/2,n_1-1,n_2-1} \qquad 4.2$$

If the statistic falls within the limit in equation 4.2, the variance can be assumed to be the same so that a pooled estimate for the variance may be used. The pooled variance, S_p^2, is given by equation 4.3. A hypothesis test may then be performed on the means, μ, of those two populations to determine if they are different. In this case, the test statistic is given in equation 4.4, where $\bar{X}_1$ and $\bar{X}_2$ are the means of the samples. If the test statistic, T_0, falls within the limit given in equation 4.5, then the hypothesis that the means are equal is true. If it does not fall within the limit, there is evidence that the mean values are different (Montgomery & Runger, 2003). Therefore there is a change in the block property due to the addition of that waste material at that level.

$$S_p^2 = \frac{(n_1-1)*S_1^2 + (n_2-1)*S_2^2}{n_1 + n_2 - 2} \tag{4.3}$$

$$T_0 = \frac{\bar{X}_1 - \bar{X}_2}{S_p * \sqrt{\frac{1}{n_1} + \frac{1}{n_2}}} \tag{4.4}$$

$$t_{\alpha/2, n_1+n_2-2} < T_0 < -t_{\alpha/2, n_1+n_2-2} \tag{4.5}$$

If the variance between the two populations is found to be unequal, an approximate method is needed to determine an estimate for the test statistic so the t-test may be performed. In this case, the test statistic is T_0^*, given in equation 4.6, for the degrees of freedom, ν, given in equation 4.7. The hypothesis that the means are equal is then tested to see if T_0^* falls within the limits given in equation 4.5, with n_1+n_2-2 replaced by ν. Although this is an approximate method, so statistical significance cannot be guaranteed, it does give an indication of the significance (Montgomery & Runger, 2003).

$$T_0^* = \frac{\bar{X}_1 - \bar{X}_2}{\sqrt{\frac{S_1^2}{n_1} + \frac{S_2^2}{n_2}}} \tag{4.6}$$

$$\nu = \frac{\left(\frac{S_1^2}{n_1} + \frac{S_2^2}{n_2}\right)^2}{\frac{\left(S_1^2/n_1\right)^2}{n_1 - 1} + \frac{\left(S_2^2/n_2\right)^2}{n_2 - 1}} \tag{4.7}$$

The methods described were used to determine if there is equality between block compositions on each block property tested for two populations and what

effect the mix modifications had on these properties. The goal of this analysis is to determine whether there is any statistical difference between the mean of one type of replacement and the mean of another type of replacement or control. In all cases, the confidence level was set as 95%, so $\alpha = 0.05$.

4.3 Contact Angle of Polymers

The contact angle is a measure of how a material interacts with a liquid. In this case, the contact angle of the polymers was determined when a drop of water was placed on their surface (Berg, 1993). Table 4.1 gives the measured contact angle for the three polymers used in this study.

Table 4.1 Polymer contact angle

Polymer	Mean (^{0})	Standard Deviation (^{0})	COV (%)
LDPE	95.8	1.2	1.3
HDPE	94.7	2.9	3.1
Grafted HDPE	94.5 or 67.7	5.8 or 4.3	6.1 or 6.3

There was no significant difference between the contact angle of the LDPE and the HDPE. Because the measured angles were over 90^0, it indicates that the LDPE and HDPE polymers are hydrophobic. The grafted polymer however has two contact angles since it is not a homogeneous material; that is, the grafting is spread over the surface of the polymer but does not cover the whole surface. Therefore, some locations on the surface of the grafted HDPE have the same contact angle as the ordinary HDPE while others have a lower contact angle, indicating a decrease in the hydrophobicity of the polymer. The grafting resulted in a decrease in the contact angle compared to the other polymers; however, the degree of grafting was not measured.

4.4 Units

The results of the tests performed on the masonry units are presented in this section. The properties tested were density, absorption, IRA, compressive strength and elastic modulus.

4.4.1 Dimensions

All the blocks had the standard nominal dimensions: 200 mm by 200 mm by 400 mm. The width (W), height (H), length (L), the face shell thickness (t_{fs}) and the web thickness (t_w) were measured according to ASTM C140 (2008a) Annex A. Table 4.2 and Table 4.3 summarize the average dimensions for 5 stretcher and 5 splitter blocks for each mix type. It was observed that the dimensions were larger when polymers were used compared to the control blocks. This was especially noticeable for the 15% polymer blocks.

Table 4.2 Summary of stretcher block dimensions (mm)

Mix	L	H	W	t_{fs}	t_w
C	390	189	190	33.1	26.6
LP3	390	190	190	33.1	26.6
LP6	390	189	190	33.1	26.3
LP9	391	189	191	33.5	26.7
LP15	392	189	191	33.8	27.0
HP3	390	189	190	33.8	26.3
HP6	390	190	189	33.2	26.5
HP9	391	190	191	33.6	26.9
HP15	392	189	191	33.3	27.1
GP3	389	190	190	32.8	26.8
G10	390	189	188	32.7	26.6
G25	390	189	190	32.9	26.4

Table 4.3 Summary of splitter block dimensions (mm)

Mix	L	H	W	t_{fs}
C	390	189	190	32.9
LP3	391	190	190	32.9
LP6	391	189	190	33.1
LP9	392	189	191	33.3
LP15	393	189	191	33.4
HP3	391	189	191	33.4
HP6	390	190	191	33.5
HP9	390	189	191	33.4
HP15	392	190	190	33.4
GP3	390	189	190	32.9
G10	390	190	189	33.0
G25	390	189	190	33.1

4.4.2 Weight and Density

For each of the 12 mixes, the oven dry weight and the density of 5 stretcher and 5 splitter blocks were tested. The results of the oven dry weight are presented in Table 4.4 with their coefficient of variance (COV). The density of each of the blocks in terms of mean value, standard deviation and COV is summarized in Table 4.5.

Table 4.4 Oven dry weight of blocks (kg)

Stretcher Blocks				Splitter Blocks			
Mix	Mean	Standard Deviation	COV (%)	Mix	Mean	Standard Deviation	COV (%)
C	16.30	0.12	0.73	C	17.79	0.11	0.60
LP3	15.87	0.04	0.26	LP3	17.25	0.13	0.74
LP6	15.26	0.12	0.76	LP6	16.45	0.13	0.78
LP9	14.77	0.08	0.54	LP9	16.08	0.13	0.81
LP15	13.97	0.10	0.75	LP15	15.28	0.11	0.69
HP3	15.86	0.03	0.17	HP3	17.28	0.04	0.21
HP6	15.23	0.05	0.32	HP6	16.60	0.06	0.38
HP9	14.68	0.10	0.67	HP9	15.92	0.06	0.37
HP15	13.78	0.18	1.31	HP15	15.04	0.19	1.25
GP3	15.62	0.13	0.82	GP3	16.99	0.12	0.72
G10	16.22	0.19	1.15	G10	17.74	0.12	0.68
G25	16.16	0.11	0.66	G25	17.58	0.08	0.48

Table 4.5 Density of blocks (kg/m^3)

Stretcher Blocks				Splitter Blocks			
Mix	Mean	Standard Deviation	COV (%)	Mix	Mean	Standard Deviation	COV (%)
C	2164.9	12.2	0.6	C	2156.3	8.1	0.4
LP3	2098.3	29.5	1.4	LP3	2096.6	8.8	0.4
LP6	2015.7	8.3	0.4	LP6	2004.2	5.7	0.3
LP9	1960.2	6.3	0.3	LP9	1936.3	11.0	0.6
LP15	1841.7	12.3	0.7	LP15	1836.1	10.6	0.6
HP3	2097.4	9.9	0.5	HP3	2093.0	2.6	0.1
HP6	2022.3	11.5	0.6	HP6	2019.2	4.1	0.2
HP9	1930.4	21.8	1.1	HP9	1924.5	7.1	0.4
HP15	1825.4	17.7	1.0	HP15	1823.7	17.2	0.9
GP3	2075.9	13.8	0.7	GP3	2063.7	14.4	0.7
G10	2146.3	16.7	0.9	G10	2151.6	12.1	0.6
G25	2140.1	4.2	0.2	G25	2130.2	9.1	0.4

The results given in Table 4.4 and Table 4.5 show that the variation of the weight and density of the blocks is very small, since the coefficient of variance is less than 1% in most cases and less than 1.5% for all the mixes. The variation for all the mixes is the same according to the f-test and there was no difference in the results between the splitter and stretcher blocks. From the statistical t-test analysis, for a 95% confidence interval, it can be seen that there is a significant change in the weight and density of the blocks, for all the mixes containing plastic compared to the control. Therefore, even low substitutions of 3% sand result in a decrease in the weight and density of the blocks. However, for the blocks with WGP replacing cement, there is no significant statistical effect on the weight of

the blocks or on the density for the 10% replacement while there is a slight effect on the density for the 25% WGP mix.

The effect of the substitutions was almost the same on the weight and density for the splitter and stretcher blocks so the following discussion focuses on the results for the stretcher blocks. For all the mixes with polymers, the weight and density decreased with the reduction in sand content. The effect of the LDPE and HDPE was similar at the same replacement level while the 3% grafted mix showed a slightly higher reduction in weight and density than the reduction achieved by the 3% LDPE and 3% HDPE mixes, although this difference is not statistically significant. For the LDPE mixes, the weight was 2.6%, 6.4%, 9.4% and 14.3% lower than that of the control for the 3%, 6%, 9% and 15% replacements, respectively, while the density reduction was 3.1%, 6.9%, 9.5% and 14.9%, respectively. For the same sand replacement levels for the HDPE, the reduction in weight compared to the control was 2.7%, 6.5%, 10.0% and 15.4% and the density reduction was 3.1%, 6.6%, 10.8% and 15.7%. The mix with 3% grafted polymer resulted in a weight of 4.2% and a density of 4.1% less than the control. For the WGP mixes, the weight reduction was less than 1% and the density reduction was less than 1.1%. Figure 4.1 summarizes the density of the block mixes in descending order and clearly shows the effect of polymers in reducing the density. According to CSA A165.1 (2004), the block density must be lower than 1700 kg/m^3 for the concrete masonry unit to be classified as lightweight. Although there was a noticeable reduction in density for the blocks with polymers, none of them had a density low enough to be classified as lightweight.

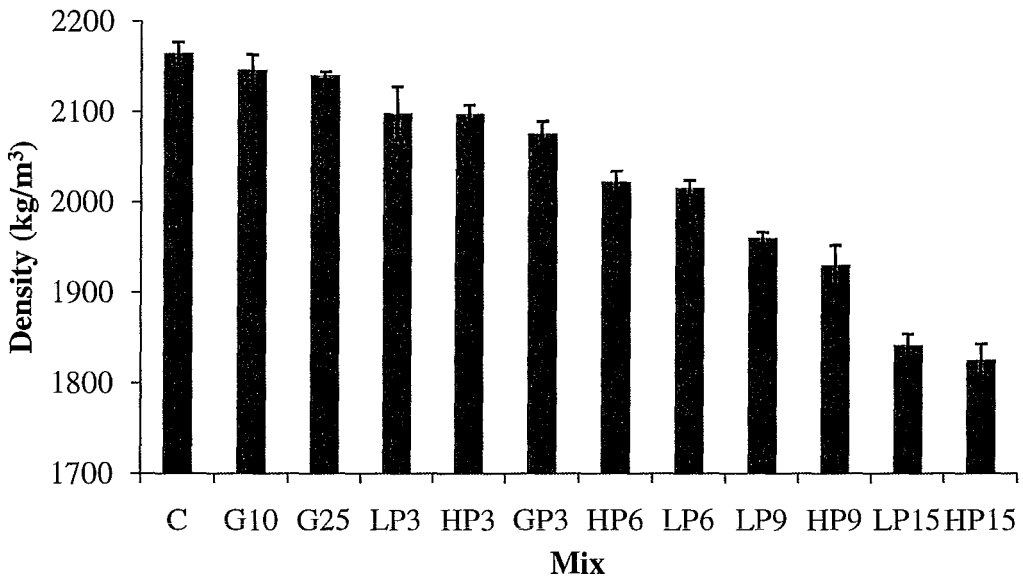

Figure 4.1 Density of the block mixes, from largest to smallest

4.4.3 Water Absorption

The water absorption was tested for each of the mixes for the same 5 stretcher and 5 splitter blocks used to determine the dry weight and density of the blocks. The mean water absorption, standard deviation and COV are presented in Table 4.6 for both the stretcher and splitter blocks.

Table 4.6 Absorption of the blocks (%)

Stretcher Blocks				Splitter Blocks			
Mix	Mean	Standard Deviation	COV (%)	Mix	Mean	Standard Deviation	COV (%)
C	5.0	0.1	2.9	C	5.1	0.2	3.2
LP3	5.2	0.2	4.1	LP3	5.5	0.2	3.9
LP6	7.1	0.3	4.2	LP6	7.5	0.3	3.3
LP9	7.3	0.2	2.5	LP9	8.0	0.2	2.8
LP15	8.1	0.6	7.9	LP15	8.3	0.4	4.7
HP3	5.4	0.2	4.4	HP3	5.5	0.3	5.5
HP6	6.9	0.3	4.8	HP6	6.9	0.2	2.2
HP9	7.7	0.1	1.3	HP9	7.8	0.2	3.1
HP15	10.4	0.4	4.4	HP15	10.4	0.6	5.4
GP3	6.2	0.3	4.2	GP3	6.4	0.4	5.5
G10	5.2	0.3	5.4	G10	5.1	0.2	4.0
G25	5.6	0.3	4.5	G25	6.0	0.4	7.4

The variation of the block absorption was not significantly different between the mixes, except for the 15% LDPE and 15% HDPE mixes, which had higher variation, according to the f-test. Most of the mixes had low COV values, which were less than 5%, so it can be concluded that there is little variation in the results, although they are more variable than the results for the density. For a confidence of 95%, the t-test showed that all the mixes, except two, produced a statistically significant, different result compared to the control mix. No significant deviation from the control absorption was observed for the 3% LDPE mix and the 10% WGP mix, so it can be concluded that these two mixes perform in the same manner as the control for water absorption. All the other replacement levels produced blocks with higher absorptions values than the control blocks. Both the stretcher and splitter blocks followed the same trend.

The water absorption increased with the addition of glass or polymers; however, the mixes with polymers affected the absorption more than the glass mixes. LDPE and HDPE blocks performed the same for the lower replacement levels, 3% and 6%; however, the HDPE blocks with 9% and 15% sand replacement result in a statistically higher water absorption then the LDPE blocks at the same replacement levels. This is possibly due to a higher porosity of the HDPE mixes at higher replacement levels or due to faster drainage of the LDPE

mixes at higher replacement levels. Also, the grafted mix had a higher absorption than both the 3% LDPE and 3% HDPE mix, which may be due to the lower hydrophobicity of the grafted polymer, compared to the low and high density polyethylene. Beyond 3% replacement with polymers, the absorption of the blocks becomes high. For mixes with 6%, 9% and 15% LDPE the absorption increased by 41%, 46% and 62%, respectively, compared to the control. The HDPE blocks performed worse with 8%, 37%, 53% and 107% increases in absorption compared to the control for the 3%, 6%, 9% and 15% mixes, respectively. The 3% grafted mix produced a 24% increase. The 25% WGP mix produced an increase of 13%, while the 10% WGP mix did not produce any significant change in the absorption. Figure 4.2 shows the absorption of the stretcher blocks in ascending order of absorption.

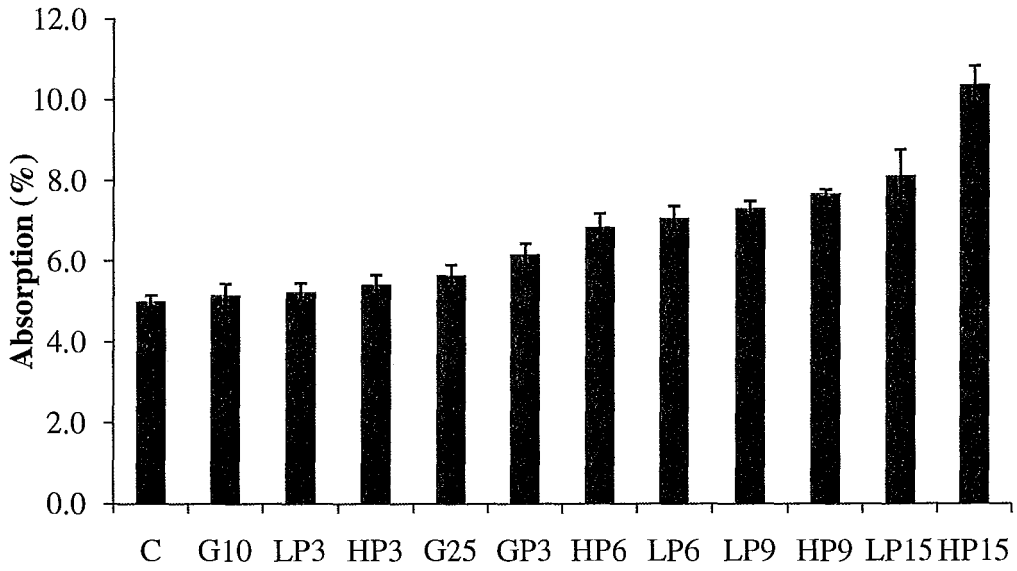

Figure 4.2 Water absorption

4.4.4 Initial Rate of Absorption (IRA)

The initial rate of absorption (IRA) was determined for 3 stretcher blocks of each mix type. Table 4.7 summarizes the results of the IRA of the blocks and gives the standard deviation and COV of the results.

Table 4.7 Initial rate of absorption (kg/m^2/min)

Mix	Mean	Standard Deviation	COV (%)
C	0.5	0.09	17.6
LP3	0.8	0.05	6.5
LP6	2.2	0.42	19.3
LP9	2.4	0.42	17.3
LP15	2.6	0.46	17.8
HP3	0.7	0.06	8.4
HP6	2.3	0.38	16.4
HP9	2.1	0.16	7.6
HP15	6.0	0.40	6.7
GP3	1.1	0.23	20.8
G10	0.7	0.19	29.6
G25	0.7	0.06	8.8

From Table 4.7 it can be seen that the results of this test are highly variable where the COV value tends to be high, for most of the mixes varying between 17% and 30%. This indicated that the number of samples is not representative and more samples are needed. All the mixes produced a statistically significant increase in the IRA of the blocks compared to the control, except for the 10% WGP mix.

Similar to water absorption, the IRA was more affected by the presence of polymers in comparison to the replacement of cement with WGP. For the 3% sand replacement level, the HDPE polymer produced blocks with lower IRA than the LDPE, at 6% and 9% the two polymers can be considered statistically the same, while at the 15% replacement level the HDPE had a much higher IRA than the 15% LDPE blocks. The grafted material; however, produced a higher IRA than both the LDPE and HDPE at the same replacement level. The increase in IRA was 60%, 338%, 383% and 412% due to the LDPE in comparison to the control at the 3%, 6%, 9% and 15% replacement levels, respectively. Similarly, the HDPE produced an increase of 38%, 368%, 329% and 1090% at the 3%, 6%, 9% and 15% replacement levels, respectively. It should be noted that the IRA results for the 15% polymer blocks are higher than anticipated due to cracks in the webs of these mixes, formed when the blocks were de-molded. The grafted polyethylene produced an increase of 121% at only 3% sand replacement. While the 25% WGP mix resulted in a 41% increase in IRA. Figure 4.3 shows the results of the IRA test, with the mixes arranged in order from lowest IRA value to highest.

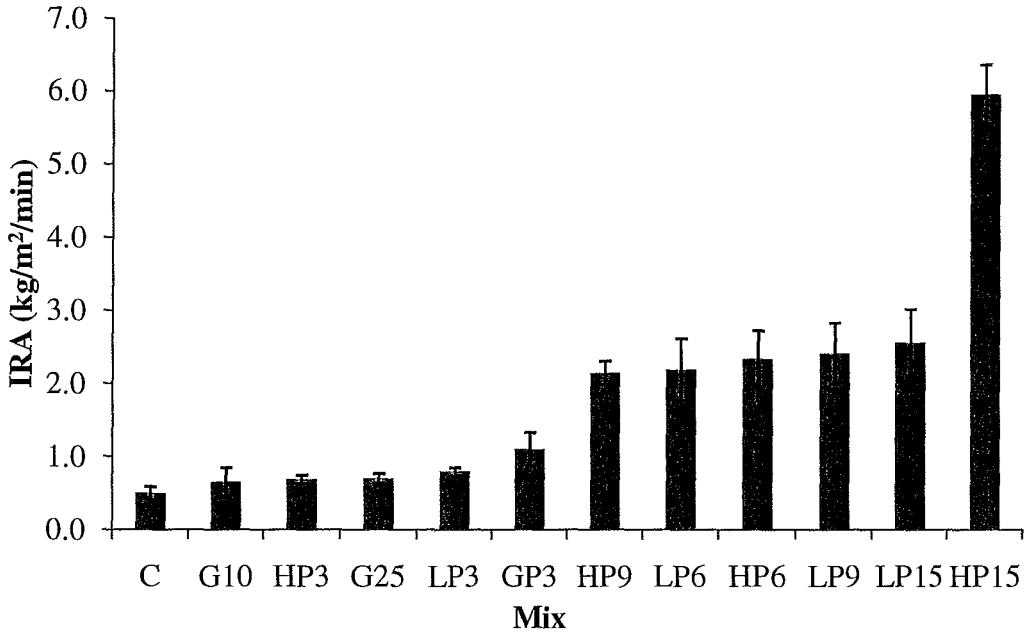

Figure 4.3 IRA results in ascending order

4.4.5 Compressive Strength

Compressive strength is one of the most important characteristics used to assess the quality of the blocks produced. The average compressive strength of the 5 blocks tested for each of the 12 mixes is given in Table 4.8, with the corresponding standard deviation and COV.

Table 4.8 Compressive strength of the blocks (MPa)

Mix	Mean	Standard Deviation	COV (%)
C	32.5	1.7	5.3
LP3	25.9	0.9	3.5
LP6	15.7	1.6	9.9
LP9	14.2	0.4	2.6
LP15	9.7	1.0	10.2
HP3	25.2	1.9	7.7
HP6	19.4	2.9	15.0
HP9	16.0	1.9	11.8
HP15	10.0	1.7	17.0
GP3	24.4	2.4	9.9
G10	28.9	1.4	4.8
G25	27.3	2.2	8.2

The results show a good coefficient of variation, although the COV increases with the addition of both the LDPE and HDPE. CSA S304.1 (2004) Clause 5.1.3.4.2 states that the COV of the blocks must not exceed 15%. This was satisfied by all the mixes except the 15% HDPE mix. The t-test was used to determine if there was any effect on the compressive strength due to the replacement of sand with polymers, and cement with WGP at a confidence level of 95%. In all cases, it was determined that there is a definite statistical difference for all of the 11 modified mixes compared to the control and in all cases the replacement produced blocks with lower strength than the control.

Increasing the content of either the polymers or WGP resulted in reduced strength, although the reduction with polymers was more dramatic. A t-test was used to show that the HDPE and LDPE mixes had no conclusive strength difference at the 3%, 9% and 15% sand replacement levels. While at the 6% replacement level, LDPE had statistically lower strength than the HDPE. Moreover, the 3% grafted blocks were statistically the same as the 3% LDPE and 3% HDPE blocks. Also, from a t-test, it was determined that there was no statistical difference between the compressive strength of the 10% WGP and 25% WGP block. The compressive strength of the blocks with LDPE decreased by 20%, 52%, 56% and 70% at the 3%, 6%, 9% and 15% replacement levels, respectively, compared to the control. Similarly, the compressive strength of the blocks with HDPE decreased by 22%, 40%, 51% and 69% at the 3%, 6%, 9% and 15% replacement levels, respectively, compared to the control. The blocks with 3% grafted polymer showed a decrease of 25% compared to the compressive strength of the control. While the 10% WGP and 25% mixes produced blocks with compressive strength 11% and 16%, respectively, lower than the control. Figure 4.4 shows the block compressive strength in order of decreasing strength.

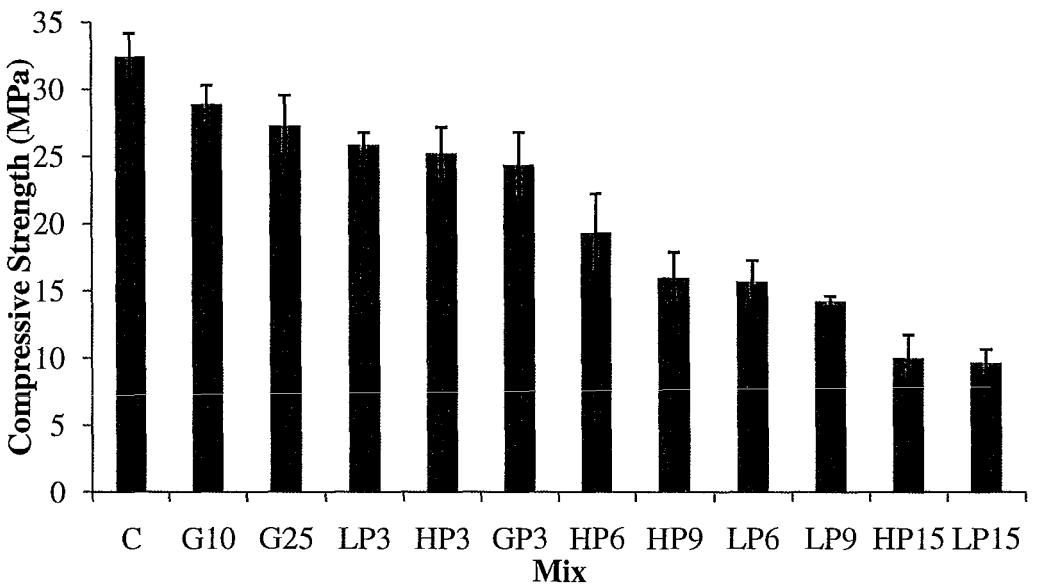

Figure 4.4 Compressive strength of blocks arranged by descending strength

The 4 day compressive strength was tested at the block plant and the results are presented in Figure 4.5. Since the 4 day compressive strength test was tested in a different facility using a slightly different method then for the other compression tests, the results can only be discussed in general. It is evident that the blocks gained strength between day 4 and day 160. The compressive strength for the polymer blocks did not change significantly in this time period.

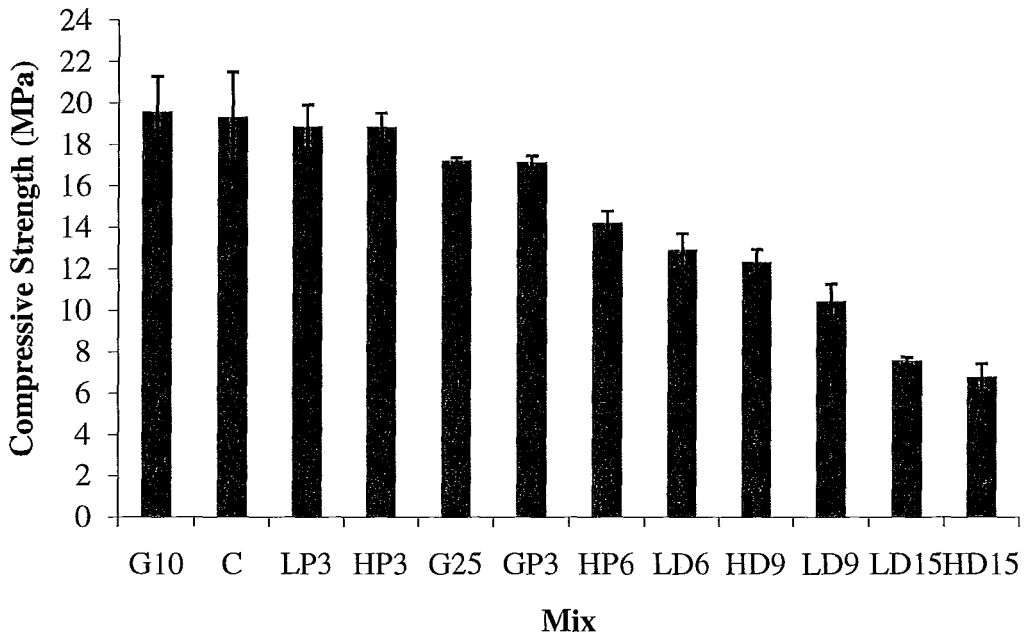

Figure 4.5 Day 4 compressive strength of blocks by descending strength

The compressive strength of the blocks was also tested one year after casting for the control blocks, the 10% WGP and the 25% WGP blocks. Three blocks were tested for each mix. The results are presented in Table 4.9.

Table 4.9 Compressive strength (MPa) after one year

Mix	Mean	Standard Deviation	COV (%)
C	30.7	0.1	0.4
G10	30.9	1.6	5.1
G25	25.7	0.3	1.3

The compressive strength of the blocks after one year was compared to the results of the compressive test presented in Table 4.8 using statistical analysis. It was determined that the variation was different for the compressive strength of the original control and 25% WGP blocks. To compare the results, the modified t-test was used. The variation was the same for the 10% blocks tested at both ages. The strength of the control blocks and the 25% WGP blocks was found to be

statistically the same at the original tested age of 160 days and at one year, while the 10% WGP blocks showed an improvement in strength with age. The compressive strength of the 10% and 25% WGP blocks was compared to the control strength at one year. The compressive strength of the 10% WGP blocks was found to be statistically the same as that of the control blocks. Although the compressive strength of the 10% WGP blocks was not higher than that of the control blocks at one year, there was a noticeable improvement in their strength with time. For the 25% WGP blocks, the compressive strength was lower than that of the control, which indicates that there was no improvement of strength with time for these blocks.

The blocks tested generally followed the same failure modes. The blocks failed by popping out the face shells in a conical manner, as shown in the two views in Figure 4.6. Due to some eccentricity in the loading or non-uniformity in the block properties across the section, shear failures, like those shown in Figure 4.7, were also fairly common. However, the side at which the eccentric failure occurred varied indicating that there was no bias in the experimental setup.

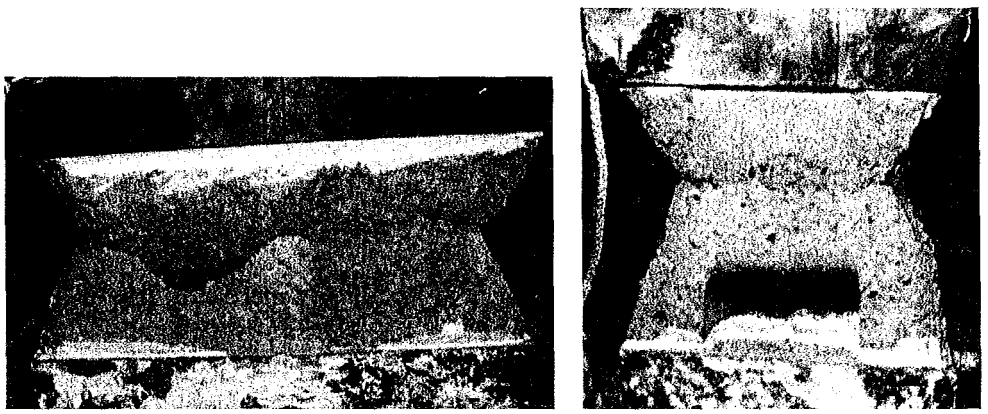

Figure 4.6 Typical failure of concrete masonry unit in compression

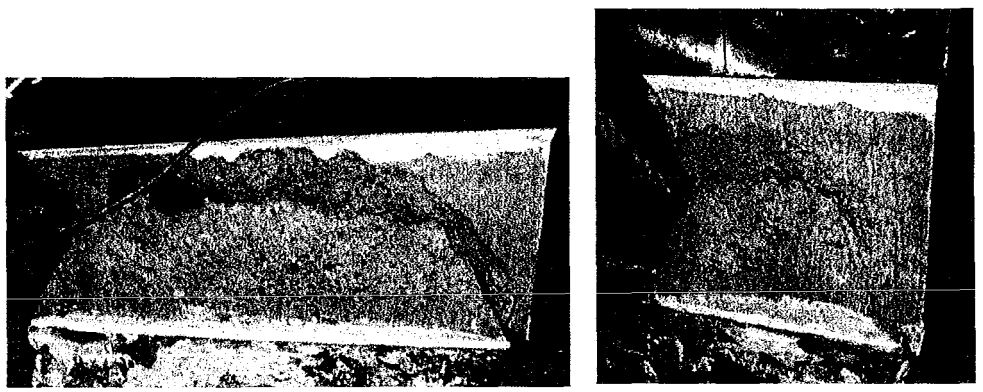

Figure 4.7 Other typical compressive of concrete masonry unit in compression

4.4.6 Modulus of Elasticity

The elastic modulus was determined from the average of two linear potentiometers attached to the surface of the blocks tested in compression. Since the potentiometers needed to be removed before failure, one block was tested to failure first then the other four were used to measure the elastic modulus. The stress strain curves of the linear potentiometers used to measure displacement and their average are shown in the range of 5% to 33% of the failure load in Figure 4.8 for a control block and in Figure 4.9 for a 9% HDPE block. Example plots for each block type are shown in Appendix A. the stress strain plots clearly demonstrate the degradation of the elastic modulus with the addition of polymers. Table 4.10 summarizes the mean, standard deviation and COV of the results for the elastic modulus.

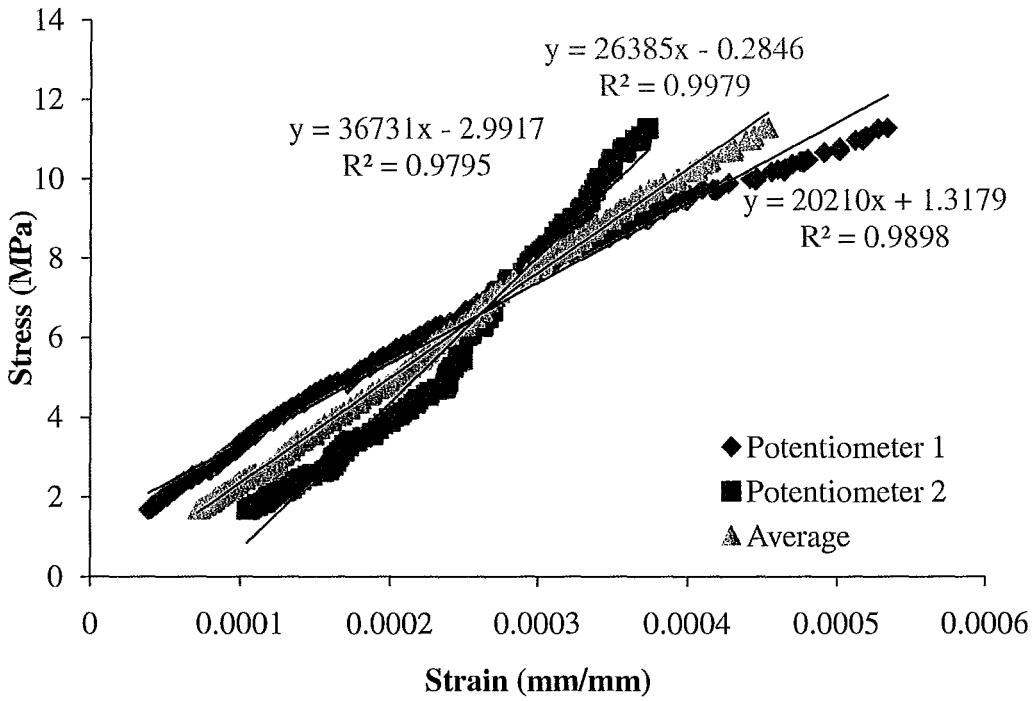

Figure 4.8 Example of stress strain curves for control concrete block from 5% to 33% of maximum stress

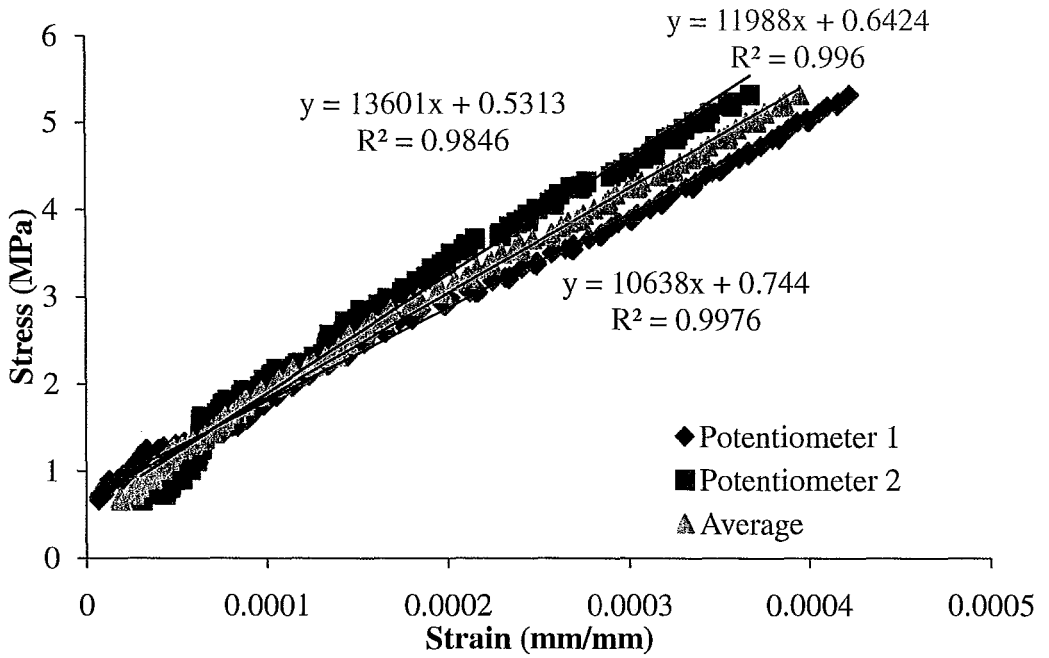

Figure 4.9 Example of stress strain curves for 9% HDPE concrete block from 5% to 33% of maximum stress

Table 4.10 Elastic modulus of blocks (GPa)

Mix	Mean	Standard Deviation	COV (%)
C	26.7	1.0	3.7
LP3	27.9	1.5	5.6
LP6	21.9	5.3	24.4
LP9	12.7	1.8	14.1
LP15	9.4	1.1	11.4
HP3	20.4	0.9	4.5
HP6	17.4	1.2	6.8
HP9	12.5	1.4	11.1
HP15	7.8	1.0	12.8
GP3	19.7	2.3	11.5
G10	22.9	1.9	8.2
G25	23.8	2.1	8.9

The COV results for the elastic modulus of the blocks are more variable than the results obtained for the compressive strength. This is due to the method of determining the elastic modulus with the linear potentiometers over a small gauge length and the variability in the composition of the blocks. The blocks with higher polymer content, 9% and 15%, showed more variability than the other mixes, which is likely due to inconsistency of the polymer distribution throughout

the blocks. The 6% LDPE blocks had a high coefficient of variance and high standard deviation so the results of the test for this mix type is not representative for the mix. From the t-test, it can be conclusively shown that the 3% LDPE and the 25% WGP mix have no significant effect on the elastic modulus of the blocks, while all the other mixes resulted in a reduction in the elastic modulus, when the results are compared to the results for the control blocks.

No significant difference was found, using the t-test, for the polymers at the 6%, 9% and 15% sand replacement levels. There was an indication that the results for the elastic modulus of the 6% LDPE and the 6% HDPE were the same, which is probably more accurate than that the elastic modulus of the 6% LDPE and the control are the same. There was also no statistical difference between the results for the 10% WGP blocks and those for the 25% WGP blocks. There was, however, a statistical difference between the elastic modulus of the 3% LDPE and both the 3% HDPE and the 3% grafted blocks, with the 3% LDPE blocks having a higher modulus than the other two. There was no conclusive difference between the modulus of the 3% HDPE and the 3% grafted blocks. In general, the elastic moduli of the blocks decreased with the addition of the replacement materials, except for the 3% LDPE and the 25% WGP mixes. The 6%, 9% and 15% LDPE blocks had a 18%, 53% and 65%, respectively, lower elastic modulus than the control, while the elastic modulus of the 3%, 6%, 9% and 15% HDPE blocks was 24%, 35%, 53% and 71% lower than the control, respectively. The 3% grafted material added to the blocks decreased the elastic modulus by 26%, while the 10% WGP decreased it by 14%. Figure 4.1 shows the value of the average elastic modulus of each block mix and its corresponding standard deviation arranged in order of decreasing elastic modulus.

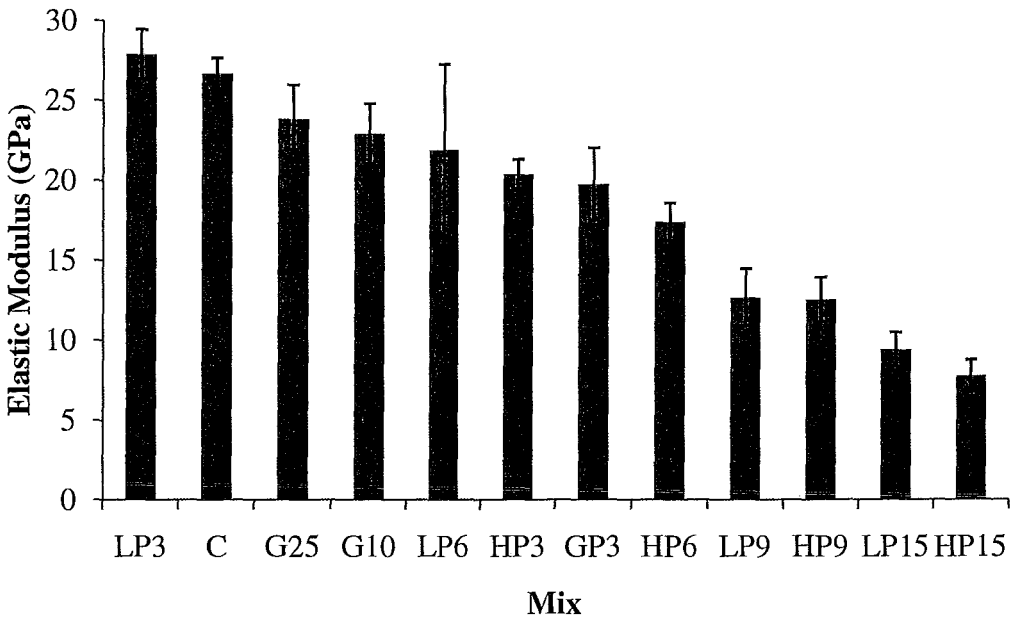

Figure 4.10 Elastic modulus of blocks sorted by decreasing modulus

4.4.7 ASR Mortar Bar Test

The possibility of an expansive ASR reaction was determined using the mortar bar test (ASTM C 1260 (2007)). Three bars were tested for the control, the 10% WGP and the 25% WGP blocks. Three bars were also tested for the 15% LDPE to assess the effect of highly alkali solution on the blocks with a high polymer content. An expansion of less than 1%, corresponding to strain less than $1x10^{-3}$ mm/mm, after 14 days is an indication that ASR expansion is unlikely to occur according to ASTM C 1260 (2007). If the expansion is between 1 and 2%, or strain is less than $2x10^{-3}$ mm/mm, there is potential for ASR and, if it is above 2%, the ASR expansion is likely.

The mortar bars were first placed in an oven at a constant temperature of 80°C, in distilled water, for 24 hrs to obtain the zero reading. For 30 days, the bars were submerged in a 1 M NaOH solution with length measurements taken periodically. The strains of the mortar bars are plotted in Figure 4.11. From the plots, one can observe that the results are highly variable. This was especially evident for the 25% WGP bars, while the 10% WGP bars showed the lowest variability. The highest expansion was seen in the 25% WGP bars while the other bars showed less expansion. Statistical analysis of results at day 14 revealed that, 15% LDPE and 25% WGP bars have statistically higher expansion than the control. The 10% WGP bars had a statistically lower expansion than the control bars, which shows that the 10% WGP bars performed better than the control bars. From the results of this test there is no indication that any of the bars will experience ASR expansion since none of the bars exceeded the 14 day expansion criterion after 30 days.

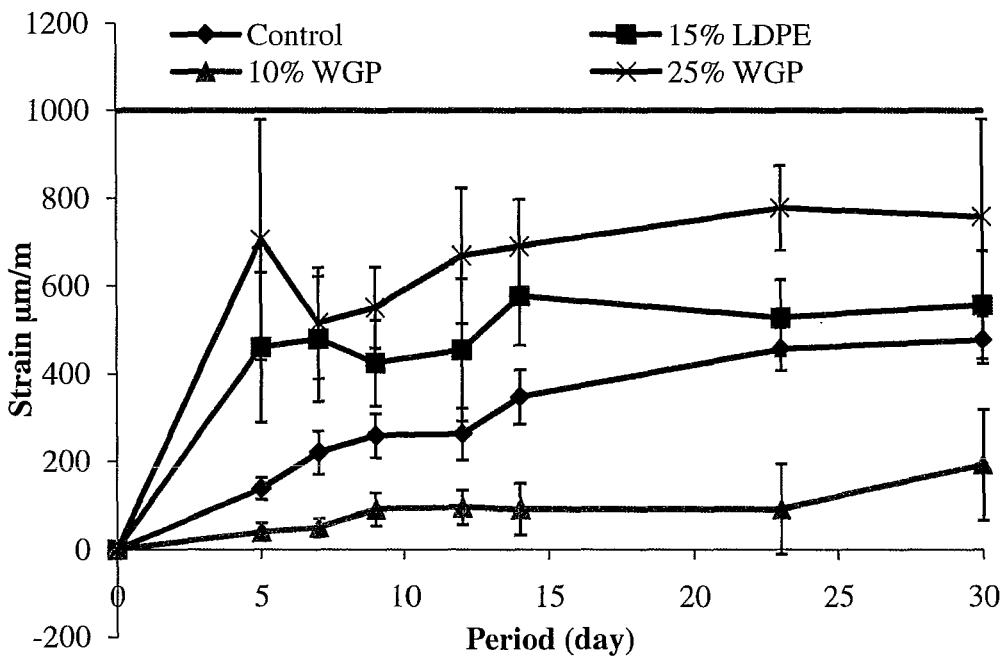

Figure 4.11 Mortar bar strain

4.5 Mortar

Mortar has a significant influence on the properties of a masonry assemblage. For this reason, the wet properties and compressive strength of the mortar is needed to determine its effect on the assemblage and to ensure it is of good quality. Moreover, these tests ensure that there is consistency between the mortar batches. In total, 16 mortar batches were made. Batches 1 to 12 were used to construct the prisms tested in compression and batches 13 to 16 were used to construct the prisms for the bond wrench test. This section assesses the flow of the wet mortar and the compressive strength of the hardened mortar cubes.

4.5.1 Flow

The flow of the wet mortar is used as a quality control. The flow must be within 100% to 115%, according to CSA A179 (2004), otherwise the mortar will have poor workability. Table 4.11 gives the initial flow values of each of the mortar batches used to construct the prisms tested in this study. The flows were acceptable in most cases. The three mortar batches which had flows slightly higher than 115% were mixed for a couple of minutes longer to allow some of the water to evaporate, thereby reducing the flow.

Table 4.11 Flow of wet mortar (%)

Batch	Flow	Batch	Flow
1	114	9	119
2	113	10	114
3	109	11	115
4	113	12	106
5	116	13	108
6	112	14	118
7	109	15	114
8	111	16	107

4.5.2 Compressive Strength

For S type mortar, the minimum 28 day compressive strength should be 12.5 MPa, according to CSA A179 (2004) Table 6. Three cubes were tested in compression on the day the corresponding prism was tested. The compressive strength of the cubes tested and the average batch strength is given in Table 4.12. The compressive strength of the cubes does not vary significantly, as indicated by the COV which not greater than 5.9%. Figure 4.12 plots the average compressive strength of each of mortar batches.

Table 4.12 Mortar cube compressive strength (MPa)

Batch	Cube 1	Cube 2	Cube 3	Mean	Standard Deviation	COV (%)
1	28.7	30.0	29.7	29.5	0.7	2.4
2	27.6	27.1	25.4	26.7	1.1	4.2
3	28.1	30.5	29.5	29.4	1.2	4.2
4	24.7	24.6	24.8	24.7	0.1	0.4
5	30.2	32.0	32.0	31.4	1.0	3.3
6	28.4	28.4	26.2	27.7	1.3	4.6
7	27.1	29.1	26.6	27.6	1.3	4.8
8	37.4	39.8	35.4	37.5	2.2	5.9
9	32.6	33.2	32.2	32.7	0.5	1.7
10	37.4	37.8	38.5	37.9	0.6	1.5
11	25.5	25.7	26.2	25.8	0.4	1.5
12	25.9	27.2	28.3	27.1	1.2	4.3
13	27.1	27.3	28.3	27.6	0.6	2.3
14	30.3	28.6	29.2	29.4	0.9	3.0
15	37.7	35.8	39.5	37.7	1.9	5.0
16	37.3	38.0	39.1	38.1	0.9	2.5
	Total Mean			30.7		
	Standard Deviation			4.7		
	COV (%)			15.3		

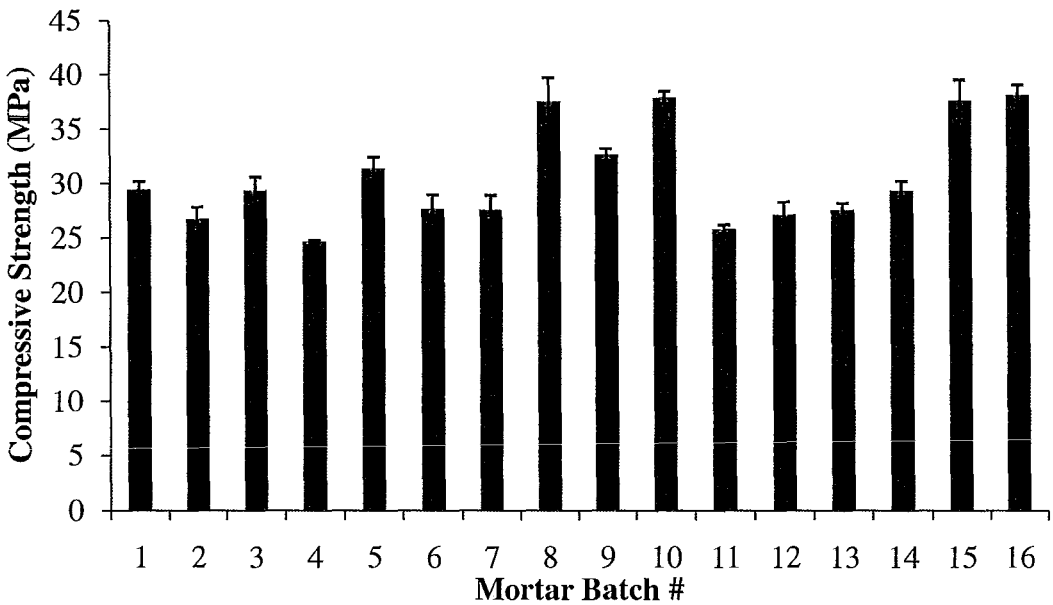

Figure 4.12 Mortar cube average compressive strength

There was no significant variation between the cube strength within one batch and, according to the f-test, most of the batches had the same variation. The t-test was used to compare the mortar batches. Table 4.13 includes a summary of which mortar batches are statistically comparable to each another.

Table 4.13 Statistical comparison of mortar cube compressive strength

Batch	Statistically Comparable to
1	3, 5, 6, 7, 14
2	3, 4, 6, 7, 11- 13
3	1, 2, 5-7, 12-14
4	2, 6, 7, 12
5	1, 3, 9, 14
6	1-4, 7, 11-14
7	1-4, 6
8	10, 15, 16
9	5
10	8, 15, 16
11	2, 6, 12
12	2, 3, 4, 6, 11, 13, 14
13	2, 3, 6, 12
14	1, 3, 5, 6, 12
15	8, 10, 16
16	8, 10, 15

The failure mechanism of the mortar cubes was the typical conical failure. Crushing of a mortar cube and the failed cube are shown in Figure 4.13.

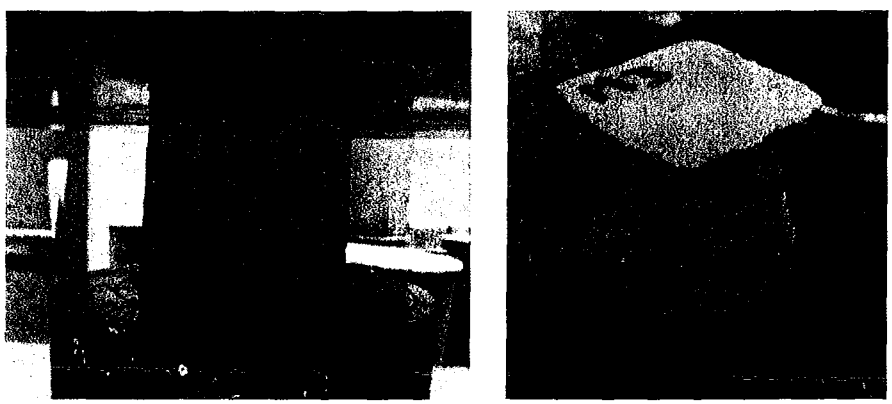

Figure 4.13 Failure of mortar cube in compression

4.6 Prisms

4.6.1 Compressive Strength

The compressive strength was tested for 5 prisms, constructed 4 units high in a running bond pattern, for each block mix. The results of the tests are given in Table 4.14.

Table 4.14 Compressive strength of prisms (MPa)

Mix	Mean	Standard Deviation	COV (%)
C	25.6	2.8	10.9
LP3	28.3	0.8	2.8
LP6	18.4	0.4	2.0
LP9	14.7	0.8	5.2
LP15	9.7	0.9	9.0
HP3	25.0	0.9	3.4
HP6	21.9	0.5	2.1
HP9	17.2	0.6	3.7
HP15	10.2	0.8	8.0
GP3	24.3	0.5	2.3
G10	27.2	1.3	4.7
G25	27.7	1.8	6.4

As can be seen in Table 4.14, the variance in the compressive strength results was less than 15%. Although it was higher for the control concrete blocks than for the modified blocks, this was likely due to some problems experienced with operating the machine to test these prisms. There was an electrical problem in the machine which resulted in an increased rate of loading, which was a concern when it occurred near the failure load of a specimen. The COV was also higher for the 15% polymer mixes, but this was expected since some of the blocks used to construct these prisms had more extensive cracking initially than other blocks, resulting in less uniform prisms. Due to the large variance in the control concrete prisms, the assumption that the variances between the control prisms and the polymer prisms were equal was proven to be false, using an f-test. This required the statistical analysis to be based on the estimated t-test, using equation 4.6. However, the variance between the control and the glass mixes was concluded to be the same, so these prisms were compared using the regular t-test (equation4.4). Conclusively, there was no difference between the compressive strength of the control prisms and the 10% and 25% WGP prisms. Using the estimated t-test, it was determined that the compressive strength of the 3% LDPE, 3% HDPE and 3% grafted prisms was the same as that of the control; however, since an approximate statistical analysis was employed, this was not conclusive. Similarly, it was shown that the other polymer mixes resulted in a reduction of the compressive strength of the prisms, compared to the control.

Although the 3% polymer mixes did not show any difference in compressive strength to the control, the 3% LDPE prisms had statistically higher compressive strength than both the 3% HDPE and the 3% grafted material prisms, which were found to perform in the same way. For both the 6% and 9% replacement levels, the LDPE prisms had lower strength than the HDPE prism at the same level. At the 15% replacement level, the LDPE and the HDPE performed the same. Also, no significant difference in compressive strength was found for the 10% and 25% WGP prisms. The mixes that had an effect on the compressive strength were the 6%, 9% and 15% mixes with either LDPE or HDPE. The LDPE showed a decrease in compressive strength of 28%, 43% and 62% at the 6%, 9% and 15% levels, respectively, while the HDPE caused a 15%, 33% and 60% decrease at the 6%, 9% and 15% levels, respectively, compared to the control. The results are presented graphically in Figure 4.14.

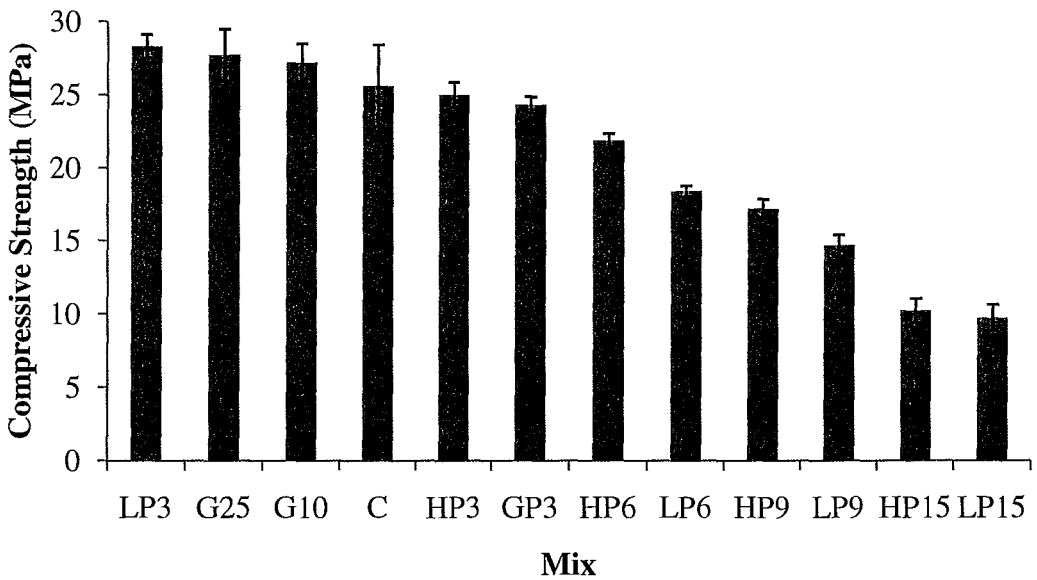

Figure 4.14 Compressive strength of prisms from highest to lowest strength

Visual examination of the results plotted in Figure 4.15, indicate that some of the prism strengths are greater than the blocks for the same type of block mix. However, from the t-test it was determined that the block strength was statistically the same as the prism strength for each mix at a 95% confidence level, except for the control and the 3% LDPE blocks. The control blocks had a conclusively higher compressive strength than the control prisms. The 3% LDPE blocks did not have the same variance so there is only an indication that the block strength was lower than the prism strength for that mix. The prism strength was high and statistically the same as that of the blocks due to the high mortar strength used to construct the prisms, which was very close to or higher than the block strength, as illustrated by Figure 4.15.

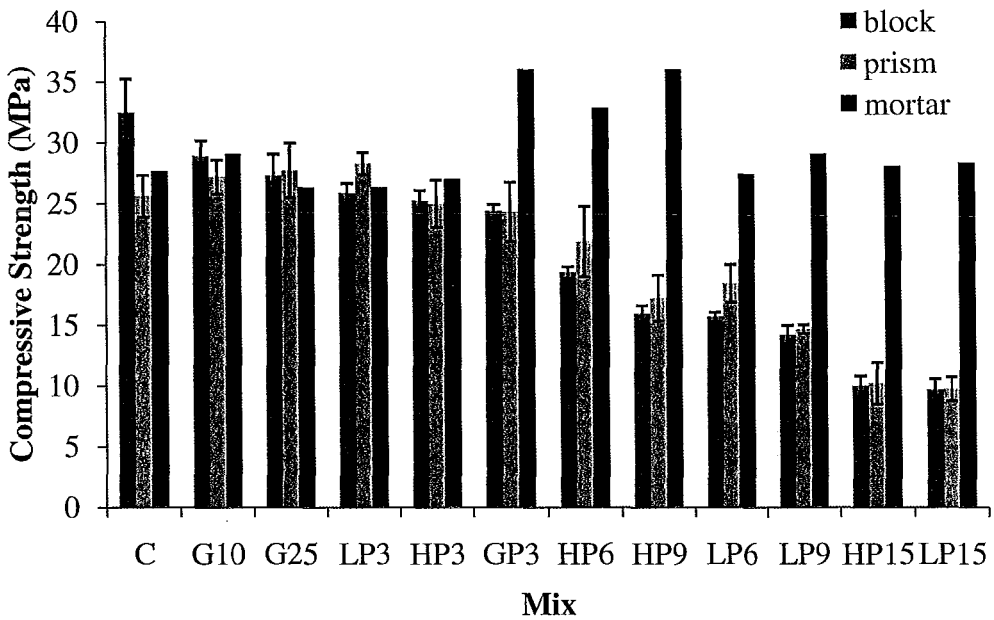

Figure 4.15 Compressive strength of prisms and blocks

The typical compressive failure of the prisms was face shell splitting as seen in Figure 4.16. The initial cracks formed in either the top or the bottom of a web and propagated through the block and the other courses. The first cracks usually formed in the second block from the bottom, as in Figure 4.16b, or the top block, since these had the thinnest webs because they were the blocks cut to form the running bond pattern. For the control prism and the prisms with WGP, the failure was quite sudden after the cracks had propagated through one or two of the courses; however, for the prisms with polymers, the failure was not as sudden and the cracks could be observed opening up a few millimeters before failure, as the failed 6% LDPE specimen in Figure 4.16 demonstrates. For the 15% LDPE and 15% HDPE prisms, as well as for some of the 9% LDPE and 9% HDPE prisms, a different failure mode was observed. The failure of these prism occurred as a combination of face shell splitting and shear, like the 15% HDPE prism shown in Figure 4.17. The initial cracks formed in the webs and propagated outwards; however, at some point, they deviated and the crack continued through the face shell and mortar joints of the blocks. This is likely due to a weak plane that formed in the block, which had locally higher polymer content due to some clumping of the polymer particles. Significant expansion of the cracks was observed before failure in these cases and, from the partial plot of the stress-strain curves, given in Appendix B, there seems to be considerable ductility in these prisms compared to the regular masonry prisms.

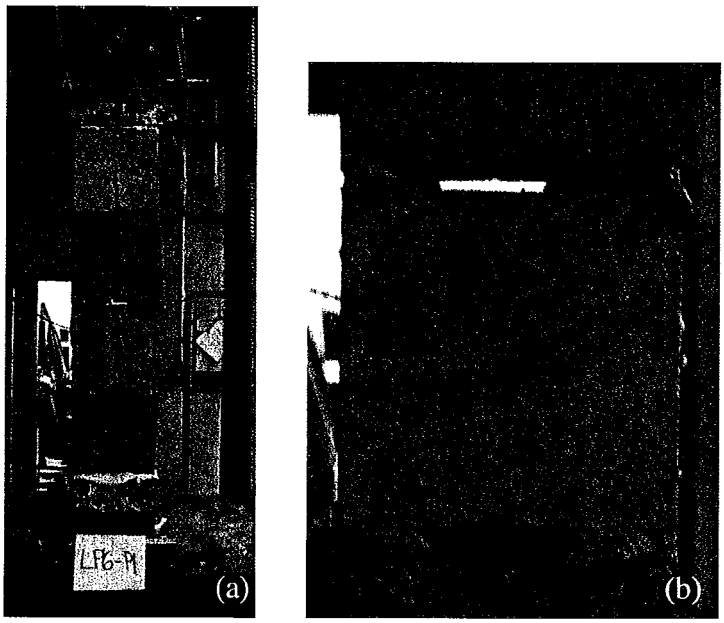

Figure 4.16 Typical failure pattern of masonry prism in compression

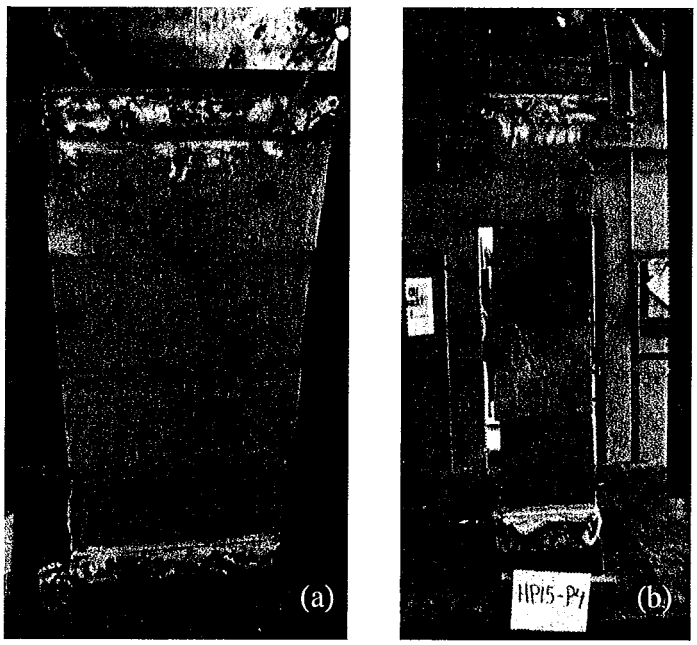

Figure 4.17 Failure pattern of prisms with 15% LDPE or 15% HDPE in compression

4.6.2 Modulus of Elasticity

The elastic modulus was tested for all five of the prisms in compression. It was determined, for each prism, from four linear potentiometer readings. An example of the stress strain curves used to determine the elastic modulus of the prism is given in Figure 4.18 for a control prism and in Figure 4.19 for a 9%

HDPE prism. Further examples are provided in Appendix B. It should be noted that the slope of the stress strain curves decreases with the addition of polymers. Table 4.15 gives the average result of the 5 prisms for each of the mixes with the corresponding standard deviation and COV.

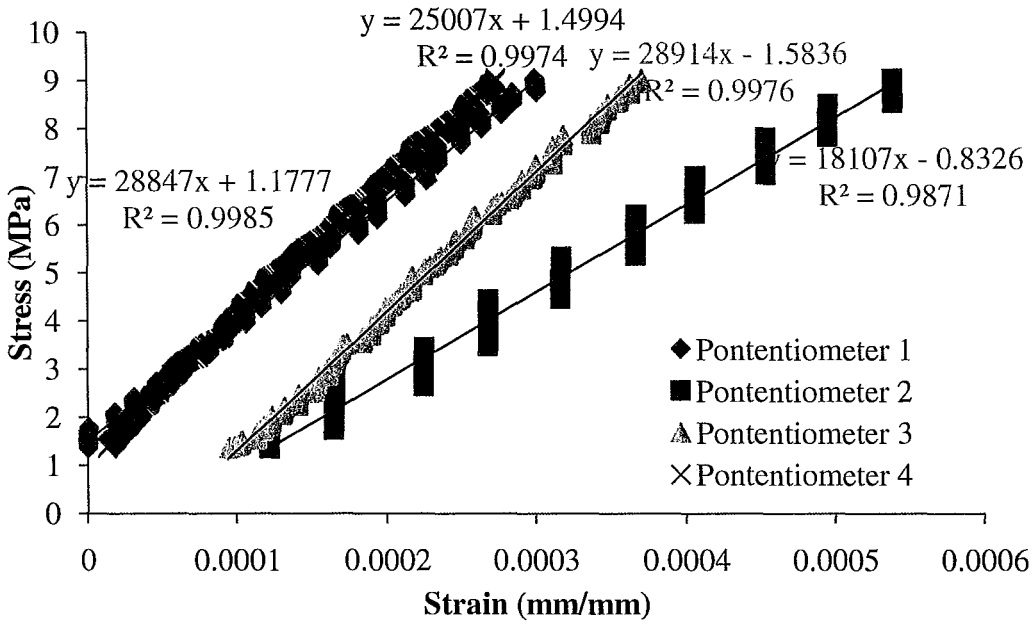

Figure 4.18 Example of stress strain curve for one control prism from 5% to 33% of failure load

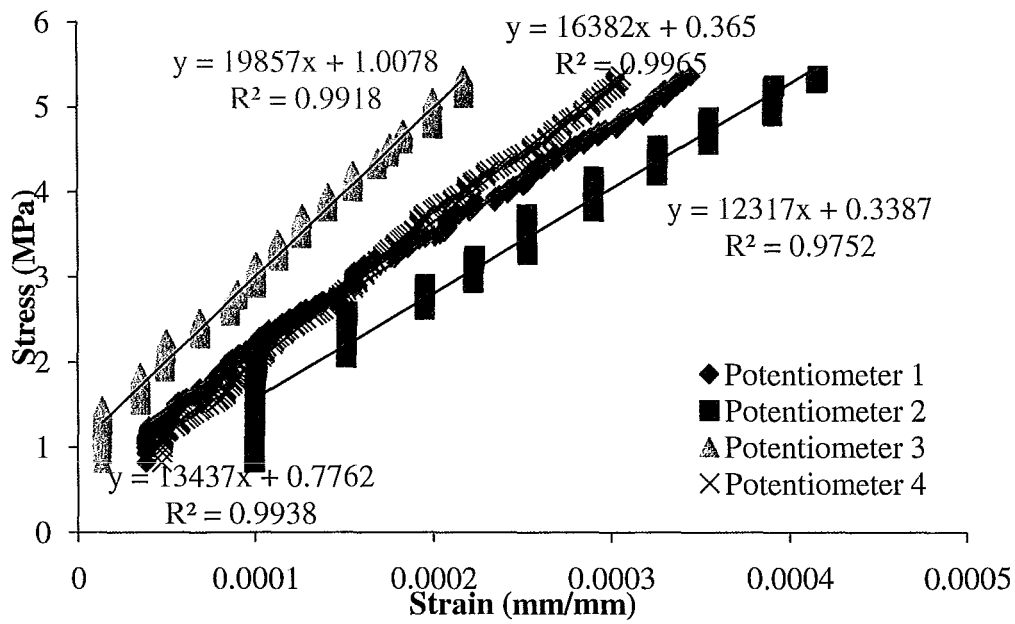

Figure 4.19 Example of stress strain curve for one 9% HDPE prism from 5% to 33% of failure load

Table 4.15 Elastic modulus of prisms (GPa)

Mix	Mean	Standard Deviation	COV (%)
C	26.0	3.1	12.1
LP3	24.8	1.2	4.8
LP6	18.6	0.9	5.1
LP9	13.8	0.6	4.5
LP15	10.3	1.1	11.2
HP3	23.2	0.8	3.4
HP6	19.8	1.1	5.5
HP9	14.8	2.0	13.7
HP15	9.1	0.6	6.9
GP3	26.4	2.2	8.3
G10	24.6	1.1	4.7
G25	23.8	1.1	4.7

The variance of the elastic modulus of the prisms is less than 15%. Similar to the compressive strength, the COV is high for the control prism results in comparison to the other mixes. The variance of the control prism elastic modulus is the same as the variance of most of the other mixes, except that of 6% and 9% LDPE and 3% and 15% HDPE, according to the f-test. Where the variance can be considered the same, the t-test was used and, where the variance was not the same, the estimated t-test was used to determine the significance of the results. Comparing the elastic modulus of each of the modified prisms to that of the control, the same pattern of results as for the compressive strength of the prisms was observed. There was no significant difference between the elastic modulus of the control and that of the 3% LDPE, 3% HDPE, 3% grafted, 10% WGP and 25% WGP, but there was a significant decrease in the elastic modulus for the other mixes.

Comparing the effect of the modifications, it was observed that the 3% LDPE and 3% grafted mixes had elastic moduli that were statistically the same while that of the 3% HDPE prisms was lower. At all other levels there was no significant difference between the LDPE and the HDPE prisms. Also, there was no conclusive difference between the elastic modulus of the 10% WGP and that of the 25% WGP prisms. Of the mixes that had a significant effect on the elastic modulus of the prisms, the LDPE reduced the modulus by 28%, 47% and 60% for the 6%, 9% and 15% replacement levels, respectively, while the HDPE produced a decrease of 24%, 43% and 65% for the 6%, 9% and 15% replacement levels, respectively. The graphical representation of the elastic modulus for each of the mixes is given in Figure 4.20.

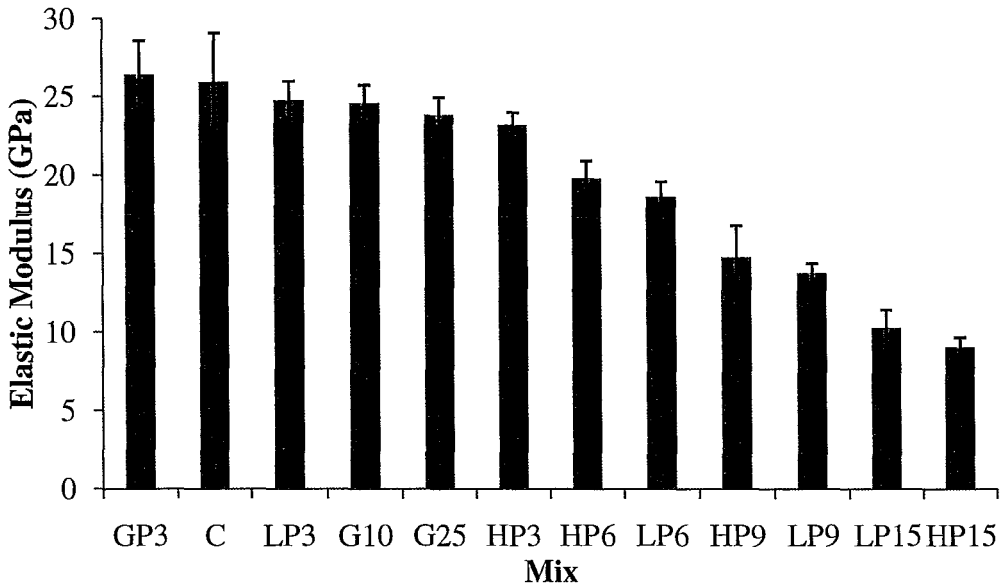

Figure 4.20 Elastic modulus of prisms in order of decreasing modulus

4.6.3 Flexural Tensile Strength (Bond Wrench)

The tensile strength of the bond between the concrete blocks and the mortar was tested using the bond wrench test. Six mortar joints were tested for each block mix. Since the bond wrench is a very variable test, the standard ASTM C1072 (2006) test requires a minimum of 15 joints to be tested. For this reason the results of this test were expected to be highly variable. Table 4.16 summarizes the average bond strength of each of the mixes tested.

Table 4.16 Bond tensile strength (MPa)

Mix	Mean	Standard Deviation	COV (%)
C	0.18	0.04	23.3
LP3	0.14	0.09	63.5
LP6	0.45	0.16	36.3
LP9	0.22	0.09	40.0
LP15	0.14	0.02	15.7
HP3	0.12	0.01	11.5
HP6	0.52	0.21	40.6
HP9	0.53	0.11	20.6
HP15	0.25	0.14	55.3
GP3	0.42	0.11	26.3
G10	0.26	0.07	25.9
G25	0.28	0.11	40.3

As expected, these results are very variable, with the maximum coefficient of variation over 60%. It was also expected that the variation would not be the same between the mixes, so most of the results were analyzed using the estimated t-test. There was evidence that the control bond strength was different from the bond strength of 6% LDPE, 15% LDPE, 3%, 6% and 9% HDPE and 3% grafted. There was no evidence of any difference between the control and the bond strength of the 3% LDPE, 9% LDPE, 15% HDPE 10%WGP and 25% WGP mixes. Where there was statistical difference between the results, the control had lower bond strength than the 6% LDPE, 15% LDPE, 6% HDPE, 9% HDPE and 3% grafted prisms, but higher bond strength than the 3% HDPE prisms.

There was no significant difference between the 3% LDPE and the 3% HDPE prisms, but there was conclusive evidence that the 3% grafted prisms had higher bond strength than the 3% LDPE and the 3% HDPE prisms. The 9% LDPE prisms had a lower bond strength than the 9% HDPE prisms, but at all other levels, there was no difference between these two polymer types. There was no evidence of any difference in bond strength between the 10% and 25% WGP prisms. The 3% HDPE prisms had a bond strength 34% lower than the control and the 15% LDPE had bond strength 21% lower, while all the other mixes produced an increase in bond strength. The 6% LDPE prisms had a bond strength 153% higher than the control. Also, the HDPE prism had 191% and 197% higher bond strength than the control at the 6% and 9% replacement levels. While the 3% grafted mix produced bond strength 134% higher than the control. Figure 4.21 clearly shows the large variation in the bond strength for the various mixes.

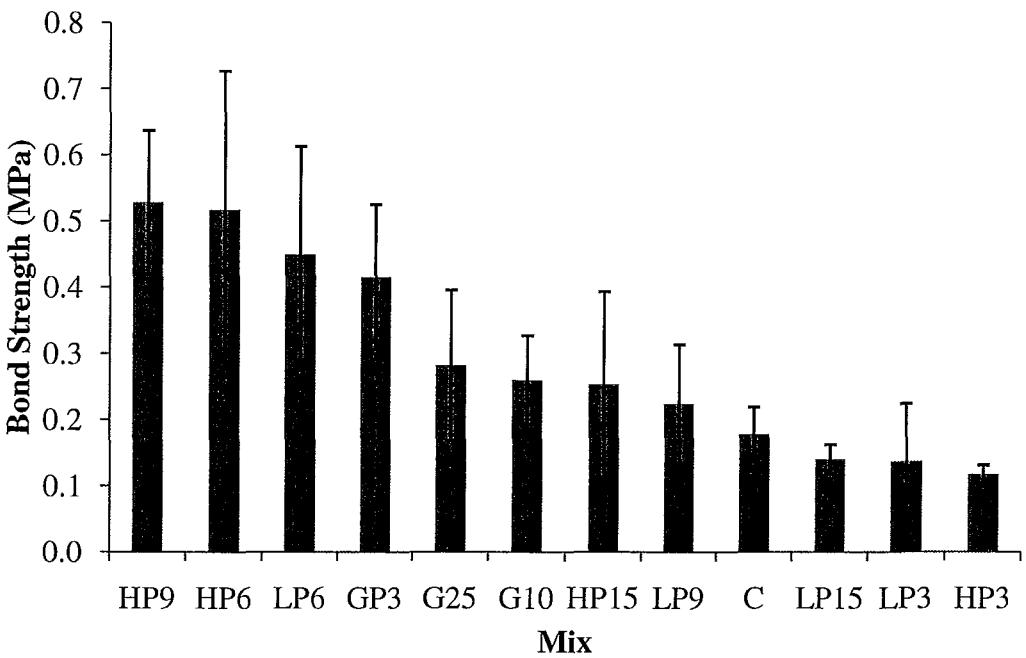

Figure 4.21 Bond tensile strength sorted from highest to lowest strength

There were three failure modes observed for the bond test. Either the mortar joint failed at the top interface between the mortar and block, or at the bottom interface, or at both the top and bottom interface simultaneously. Figure 4.22 shows the failure modes. Figure 4.22c shows the failure occurring at the top and bottom of the mortar joint and block interface and then passing through the mortar. In all cases, the failure occurred at the interface of the mortar and block.

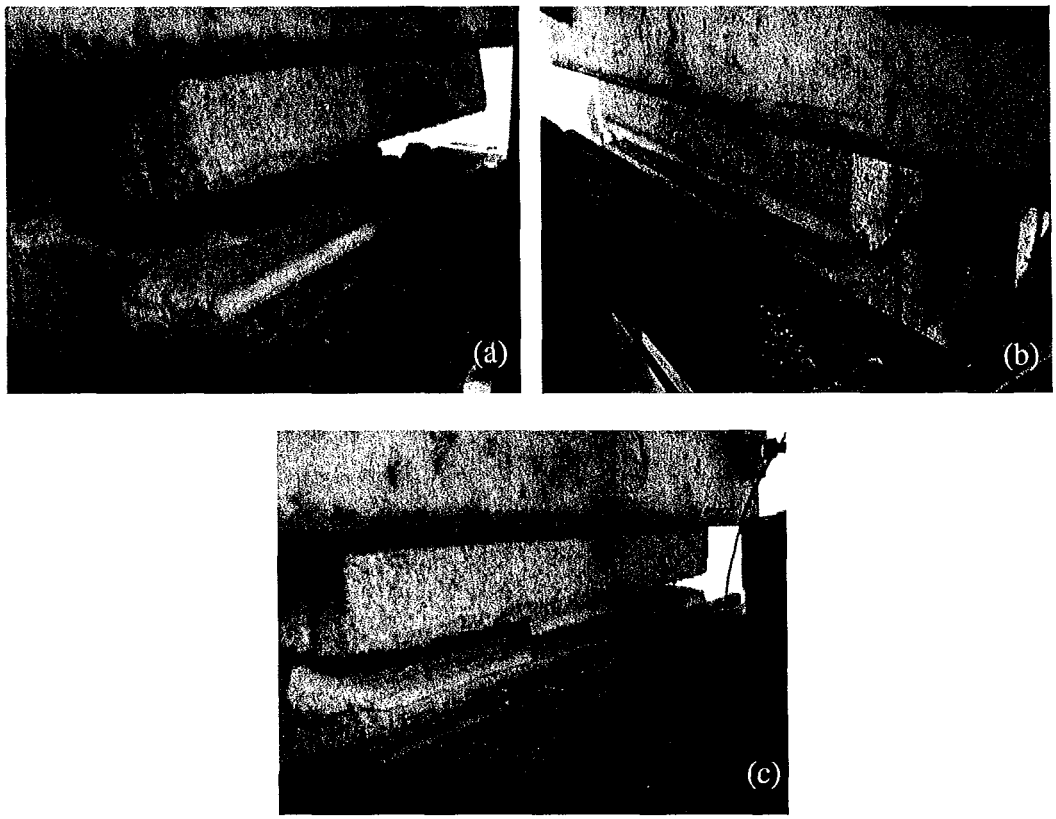

Figure 4.22 Failure of mortar joint in tension

CHAPTER 5 REGRESSION ANALYSIS AND DISCUSSION

5.1 Introduction

This chapter presents several regression models to study the effects of using polymers as sand replacement or WGP as cement replacement in concrete blocks. The models are based on multiple linear regression analysis and show the effects of these replacements on the physical and mechanical properties of the blocks and prisms.

5.2 Linear Regression Analysis

Linear regression analysis is a useful tool to determine the relationship between two or more variables. Regression analysis generates a probabilistic model, $\hat{y}$, that represents the response variable, y, as a linear function of the regressor variables, x_i, and unknown parameters, β_i, plus an error term, ϵ. Equation 5.1 gives the general equation for multiple linear regression. For simple linear regression the equation simplifies to only the first two terms plus the error term. The multiple linear regression can also be modified to include interaction terms, $x_i x_j$, and higher order effects, x^n (Montgomery & Runger, 2003)

$$y = \beta_0 + \beta_1 x_1 + \ldots + \beta_k x_k + \epsilon \qquad 5.1$$

The regression analysis best fit model is determined when the square of the residuals is minimized. For multiple linear regression this is most easily achieved by using a matrix approach as shown in equation 5.2. $\widehat{\boldsymbol{\beta}}$, in equation 5.3, is the least square estimate for $\boldsymbol{\beta}$, and is used to obtain a fitted model, $\hat{\boldsymbol{y}}$. The difference between the actual observed values of y and the fitted model are the residuals of the model, e. The residuals describe the error in the fit of the model (Montgomery & Runger, 2003).

$$\boldsymbol{y} = \boldsymbol{X\beta} + \boldsymbol{\epsilon} \qquad 5.2$$

$$\widehat{\boldsymbol{\beta}} = (\boldsymbol{X'X})^{-1}\boldsymbol{X'y} \qquad 5.3$$

Hypothesis testing can be used to determine the model adequacy and its significance. To be able to apply hypothesis testing, the error term of the model must be normally and independently distributed with a mean of zero and a variance of σ^2 (Montgomery & Runger, 2003). Normal probability plots for the residuals and plots of the residuals versus the regressor variables give a good indication of whether the residuals are normally distributed and independent. Ideally the normality plot must form a straight line, while the error for the residual plots must be randomly scattered (Montgomery & Runger, 2003).

A hypothesis test is performed to determine whether a linear relationship actually exists between y and x. This requires the determination of whether at least one of the parameters is not equal to zero. The null hypothesis states that all

of the coefficients, β_0 to β_i, are equal to zero and no relationship exists between the response variable, y, and the independent variables, x_i. If the criterion for the rejection of the null hypothesis is satisfied, then at least one of the coefficients, β_i, is not equal to zero, so at least one regressor variable contributes significantly to the model.

The criterion for accepting or rejection the null hypothesis comes from an analysis of variance (ANOVA) and the F-probability distribution. So the test statistic, F_0, is the mean sum of squares of the regression divided by the mean sum of squares of the residuals. If F_0 is greater than $f_{\alpha/2,\ p,\ n-p}$, where n is the number of observations of y and p is the number of regressor variables, then the null hypothesis should be rejected. The coefficient of multiple determination, R^2, is an indication of how well the model fits the data and is calculated by dividing the sum of squares of the regression by the total sum of squares (Montgomery & Runger, 2003).

Confidence intervals on each of the regression coefficients enable the determination of which parameters are significant to the model. So for a certain confidence level, 100(1-α)%, the confidence interval on the coefficient β_j, for j=0,1,..p is given by equation 5.4, where $\sqrt{\hat{\sigma}^2 C_{jj}}$ is the standard error of the regression coefficient $\hat{\beta}_j$. If the confidence interval contains zero then the regression coefficient may be zero and is not significant to the model.

$$\hat{\beta}_j - t_{\frac{\alpha}{2},n-p}\sqrt{\hat{\sigma}^2 C_{jj}} \leq \beta_j \leq \hat{\beta}_j + t_{\frac{\alpha}{2},n-p}\sqrt{\hat{\sigma}^2 C_{jj}} \qquad 5.4$$

In this study, regression was used to determine the effect of modifying the block composition on the properties of the blocks and prisms for a 95% confidence level, α=0.05. The procedure outlined in this section was employed. For the blocks the absorption, density and compressive strength were related to the block composition using regressor variables for the polymer content, x_1, and glass content, x_5. The properties were also related to the type of polymer used by the indicator parameters, x_2, x_3 and x_4. The variables for the block regression are given in Table 5.1. It should be noted that block type, x_6, was not incorporated for the compressive strength and elastic modulus models. For the prisms, multiple linear regression was used to establish a model relating the block strength, mortar strength and density to the compressive strength of the prisms. A model is also presented relating the block elastic modulus and mortar strength to the prism elastic modulus. The variables for the prism regression are different than for the block properties and are discussed in the corresponding sections.

Table 5.1 Variables for linear regression for concrete blocks

	x_1	x_2	x_3	x_4	x_5	x_6
	% Polymers	**LDPE**	**HPDE**	**grafted**	**% WGP**	**Block type**
Level	0	0 other	0 other	0 other	0	0 stretcher
	3	1 LDPE	1HDPE	1 grafted	10	1 splitter
	6				25	
	9					
	15					

5.3 Regression Models for Blocks

5.3.1 Density

The parameters given in Table 5.1 were used to fit a model for the density of the blocks tested. Data for each mix was used and the variables looked at content of polymers, content of WGP, the type of polymer and whether the block was a splitter or stretcher block. The model is presented in equation 5.5. The density is represented by $\hat{y}_d$ and all 4 regressor variables were used to produce the model. The R^2 value of the model is 0.979 indicating that the model fits almost all the variation in the data.

$$\hat{y}_d = 2163.5 - 21.9x_1 - 5.9x_2 - 12.5x_3 - 24.6x_4 - 1.0x_5 - 6.9x_6 \quad 5.5$$

The residual plots for the actual densities measured and all the regressor variables are given in Figure 5.1. The results indicate that the fit is good since no obvious pattern is evident and the residuals are fairly evenly distributed about the mean of zero. However, there are some observations that can be made. For the e (residuals) versus $y_{density}$ plot, the error is randomly distributed, but there are a couple of points which show a higher variation than the rest. The residuals for the 9% polymer content in the plot of x_1 appear to be more negative than the others, which indicates that the model predicts higher densities for these blocks than were observed. For x_2, x_3 and x_4, the error is distributed with the same variation for all three polymer types. The error of the 25% WGP blocks is lower than in the 10% WGP blocks, which shows that the model is better able to predict the density of the 25% WGP block in comparison to the 10% WGP blocks. The distribution for the residuals for the type of the block, x_6, is very good.

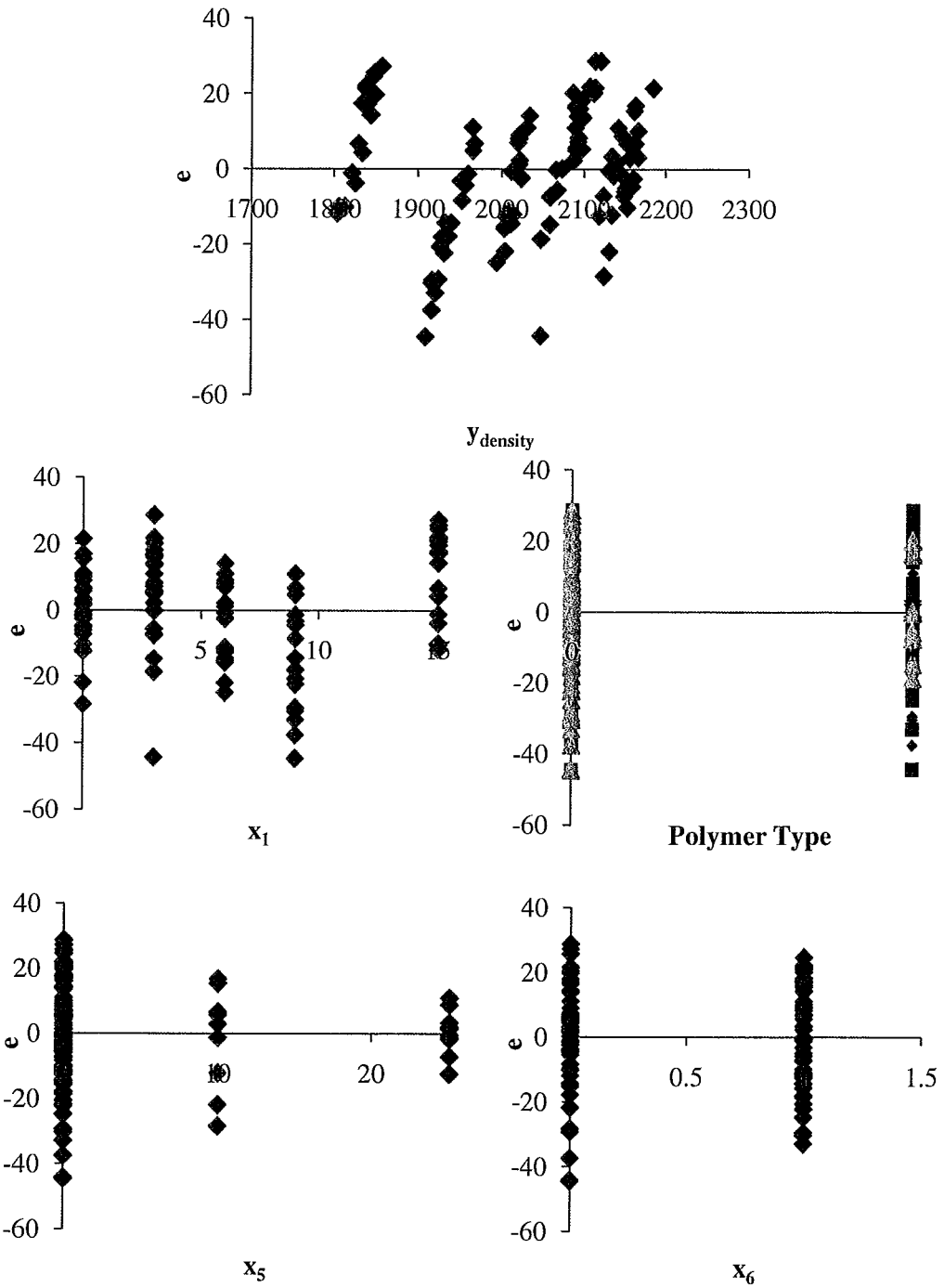

Figure 5.1 Residual plots for block density model

An ANOVA table is presented in Table 5.2. Since the F_0 values is much greater than $f_{\alpha/2,k,n-p}$=3.604, where α=0.05, k=6 and n-p=113, the model is

significant for the variables used to fit the model and at least one of the coefficients is not zero,.

Table 5.2 ANOVA results for block density

Variation	Sum of Squares	DOF	Mean Square	F0
SSR	1473657	6	245609.5	895.3
SSE	31000	113	274.3	
SST	1504657	119		

From the ANOVA table, it is known that at least one of the coefficients in not zero, so to determine, which coefficients are significant and which are likely to be zero, the confidence interval on the coefficients was determined. The confidence intervals on the coefficients were obtained using equation 5.4 and the coefficients and their corresponding interval are presented in Figure 5.2. Although β_0 is not presented in Figure 5.2, because it is a lot larger in comparison to the other coefficients, it is significant to the model. The LDPE polymer type is not significant to the model and HDPE is unlikely to be very influential because the confidence interval is very large and close to zero. The polymer content and the grafted polymer type are the most influential to the model. The block type has a large confidence interval so it likely does not have a large effect on the density. In general, increasing the polymers content causes a linear decrease in density, while an increase in WGP also decreases the density but not to the same degree.

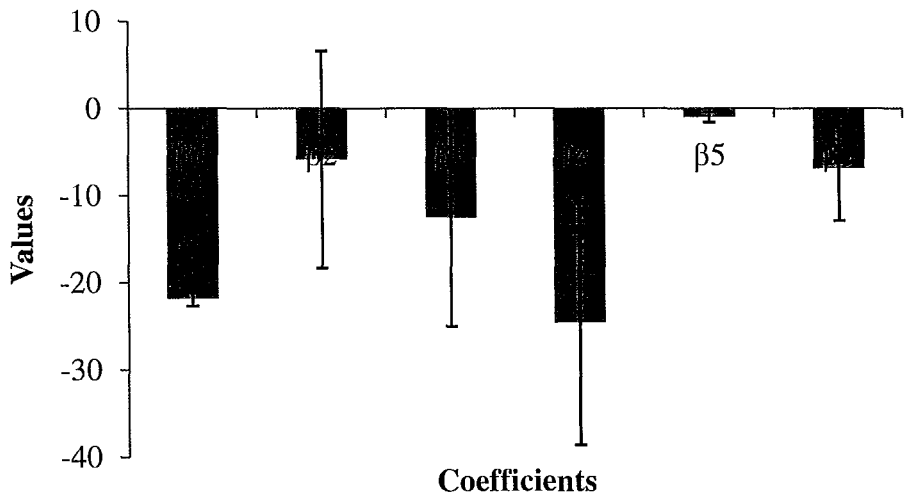

Figure 5.2 Coefficients for block density

5.3.2 Absorption

Similarly to the density, a model for the block absorption was fitted using linear regression and the regressor variables are given in Table 5.1. The model for the absorption, $\hat{y}_{abs}$, is presented in equation 5.6 for all the parameters. The R^2

value of the model is 0.870, which suggests that the parameters used represent 87% of the total. Figure 5.3 shows the residual plots for all the parameters.

$$\hat{y}_{abs} = 4.89 + 0.31x_1 - 0.45x_2 + 0.07x_3 + 0.40x_4 + 0.03x_5 + 0.18x_6 \qquad 5.6$$

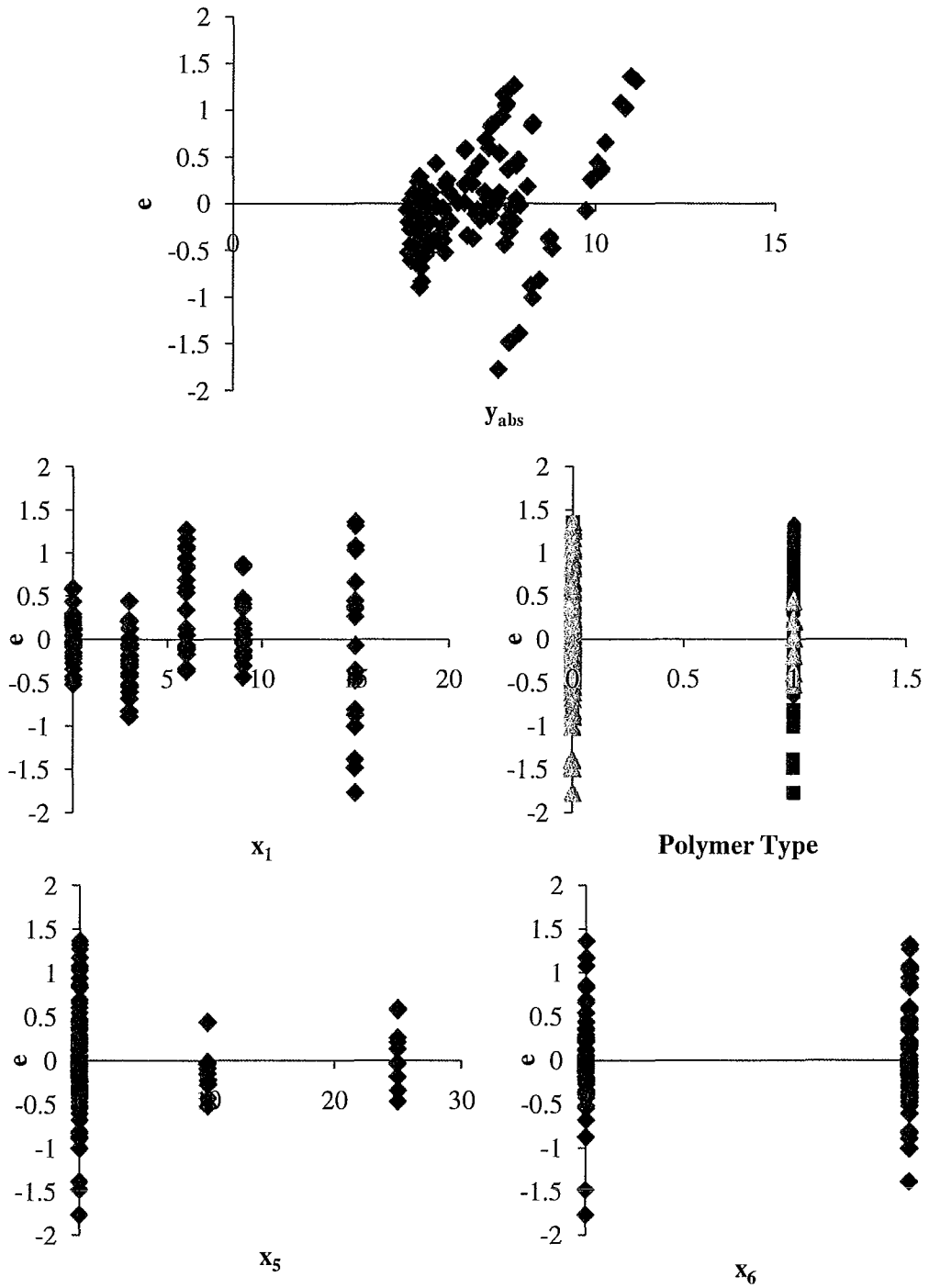

Figure 5.3 Residual plots for block absorption model

There is room for improvement in this model and it can be seen in the residual plots. The plot of the residuals versus the absorption shows a good relationship for most of the data, however, there are a number of points that form a clearly linear relation at the higher absorption values. This is likely where the low fit in the model manifests. The variation for the error versus x_1 is good for all the replacement levels except for the 15% replacement level. This is due to the higher absorption in these blocks because of the extensive cracking caused when the blocks were manufactured. Comparing x_2, x_3 and x_4, the variation for the residuals is good, but there are some outliers for the LDPE and HDPE polymer types. The variation in the residuals is consistent for the 10% and the 25% WGP blocks (x_5), as well as for the splitter and stretcher blocks (x_6).

An ANOVA table is presented in Table 5.3 for the absorption regression model. The analysis shows that the model is significant for the variables used to fit the model and at least one of the coefficients is not zero since the F_0 values is much greater than $f_{\alpha/2,k,n-p}=3.604$, where $\alpha=0.05$, $k=6$ and $n-p=113$.

Table 5.3 ANOVA results for block absorption

Variation	Sum of Squares	DOF	Mean Square	F0
SSR	252.5	6	42.1	125.6
SSE	37.9	113	0.3	
SST	290.4	119		

According to the ANOVA table, the model contains at least one non-zero coefficient. The level of confidence was determined for each coefficient using Student's t-distribution and a level of confidence of 95%. The coefficients and level of confidence are presented in Figure 5.4. The intercept of the model, β_0 is not presented in the graph since it is very large in comparison to the other coefficients, but it was significant to the model. From the confidence intervals, x_1, x_2 and x_5 are influential to the model, although x_2 appears only slightly relevant to the model since at the 95% confidence level the confidence interval is very large. As expected, the main factor influencing block absorption is the polymer content regardless of polymer type.

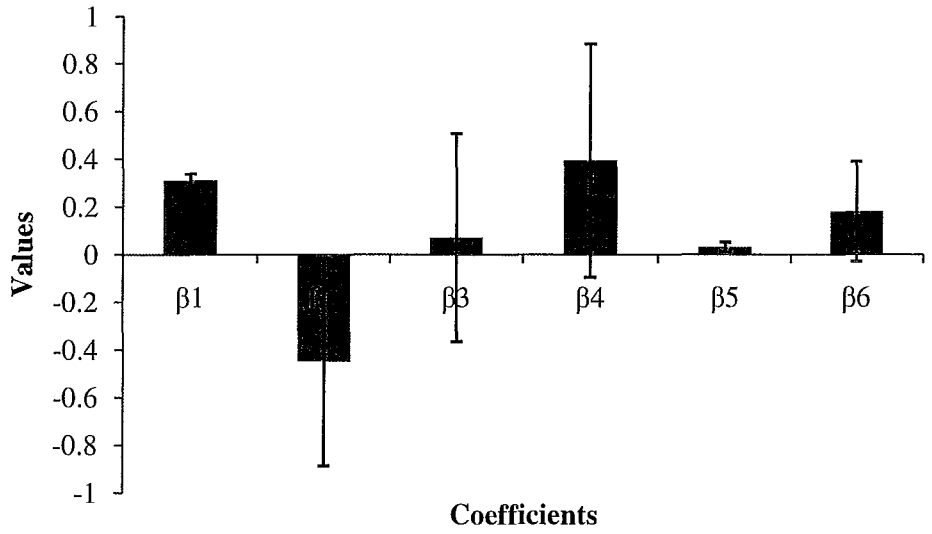

Figure 5.4 Coefficients for block absorption

5.3.3 IRA

The IRA of the blocks was modeled using linear regression. The model, $\hat{y}_{IRA}$, is presented in equation 5.7. The R^2 value of the model is 0.772, which is low. This indicates that additional parameters may need to be added to improve the model or that linear regression is not the right approach to model this data. Figure 5.3 shows the residual plots for all the parameters in the model.

$$\hat{y}_{IRA} = 0.53 + 0.27x_1 - 0.78x_2 + 0.01x_3 - 0.24x_4 + 0.01x_5 \qquad 5.7$$

There is some indication that the mean of the residuals is zero but that the variation is not equal at every level of the regressor variables. This can be seen from the distribution of the residual plot in Figure 5.5. For the y_{IRA} plot, there are outliners which lie significantly away from the e=0 axis when the IRA values are high. The distribution of the lower IRA error is randomly distributed and fits the model better. For the residual plot of the polymer content the variation is clearly increasing as the polymer content increases. This variation needs to be reduced to improve the model. A wide variation in the distribution of the error is seen for the plots of residuals versus x_2, x_3 and x_4, but is lower for x_4. To check how well the error fits a normal distribution, a normality plot was used, Figure 5.6. Since there are outliers on the normality plot that deviate significantly from a straight line, there is sufficient evidence to show that the assumption of normality of the residuals is false.

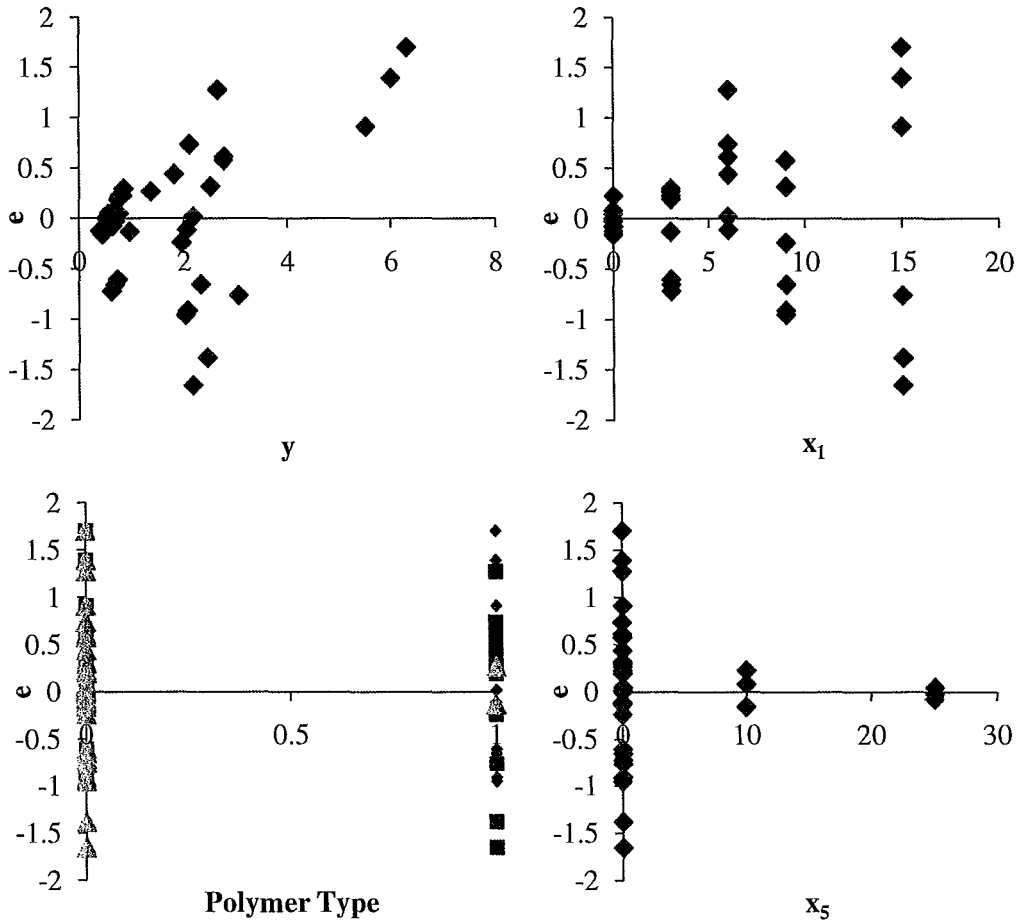

Figure 5.5 Residual plots for block IRA model

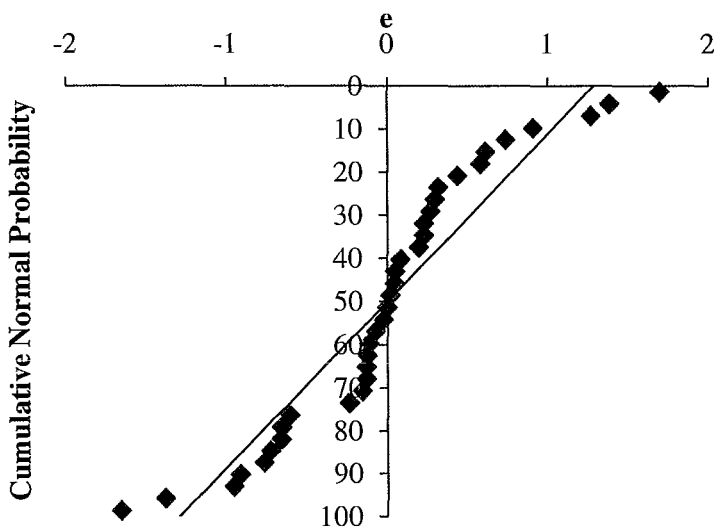

Figure 5.6 Normality plot for the residual for the IRA model

An ANOVA table is presented in Table 5.4 for the IRA regression model. The analysis shows that the model is significant for the variables used and at least one of the coefficients is not zero since the F_0 values is greater than $f_{\alpha/2,k,n-p}=3.026$, for $\alpha=0.05$, k=5 and n-p=30.

Table 5.4 ANOVA results for block IRA

Variation	Sum of Squares	DOF	Mean Square	F0
SSR	61.0	5	12.2	20.4
SSE	18.0	30	0.6	
SST	79.0	35		

Since according to the ANOVA table the model contains at least one non-zero coefficient, the level of confidence was determined for each coefficient. The coefficients and level of confidence are presented in Figure 5.7. Only the interval for β_1 does not contain zero so x_1 is the only regressor variable which affects the model. Therefore, IRA is only affected by the polymer content. It is odd that β_0 is also inconsequential since this means that, according to the model, the control blocks have zero IRA. This result is due to the effect of the very high IRA for the 15% LDPE and the 15%. The model would likely be improved if the 15% LDPE and 15% HDPE data were removed.

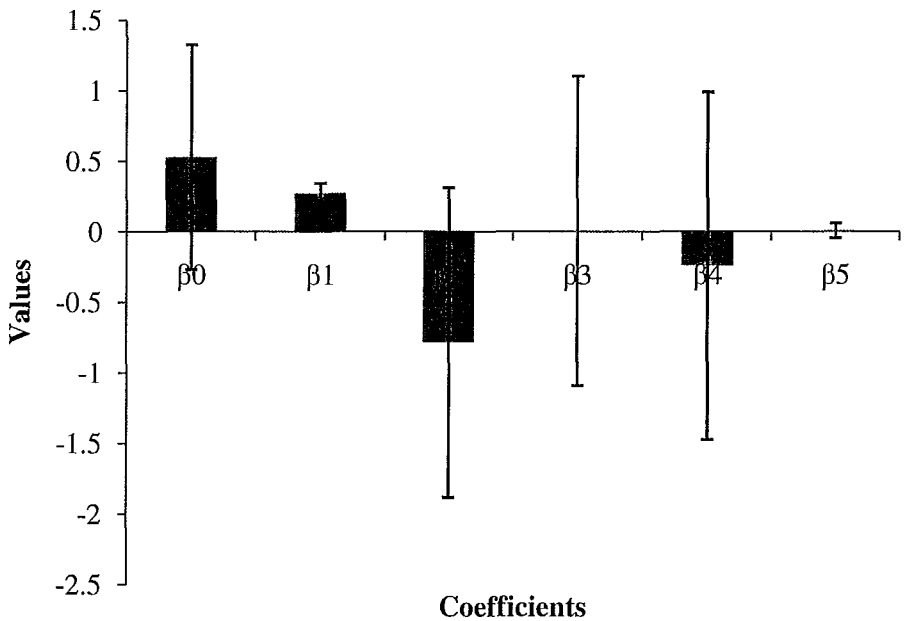

Figure 5.7 Coefficients for block IRA

5.3.4 Compressive Strength

Using multiple linear regression a block compressive strength model, $\hat{y}_{comp}$, (equation 5.8) was found. The model attempts to find the effect of polymer content, polymer type and WGP content on the strength of the concrete blocks. The fit of the model is good since the R^2 value is 0.905. The residual plots for this model are shown in Figure 5.8.

$$\hat{y}_{comp} = 31.77 - 1.22x_1 - 5.37x_2 - 4.09x_3 - 3.75x_4 - 0.19x_5 \quad 5.8$$

The residual plot for the compressive strength, y_{comp}, is well distributed with no visible trends. It appears that there are two outliers, but they do not vary too far from the mean, so they are unlikely to significantly affect the model. The spread of the residuals is fairly good for the x_1, x_2, x_3 and x_4 regressor variables. The spread of the error for x_5 is not as good. A residual plot was also constructed for the error versus the density since this is possibly a lurking variable, which is a variable that is not included in the regression but may have an effect the model. The error in this case is slightly more negative in the mid range for the density, but otherwise it is randomly scattered and therefore is unlikely to improve the model.

The ANOVA table, shown in Table 5.1, indicates that there is at least one coefficient that is significant to the model, since F_0 is a lot greater than $f_{\alpha/2,k,n-p}$=2.817, for α=0.05, k=5 and n-p=53. The confidence intervals on the regression coefficients shows that the intercept, β_0, and the coefficient for x_1, x_2, x_3 and x_4 are not zero, while x_5, the glass content, may not be significant to the model since its confidence intervals is close to zero. All the coefficients except for the intercept are shown in Figure 5.9. The model is most significantly affected by the polymer type, especially the LDPE polymer. As expected the WGP does not affect the strength of the blocks, which is in agreement with the results of the statistical analysis in Chapter 4.

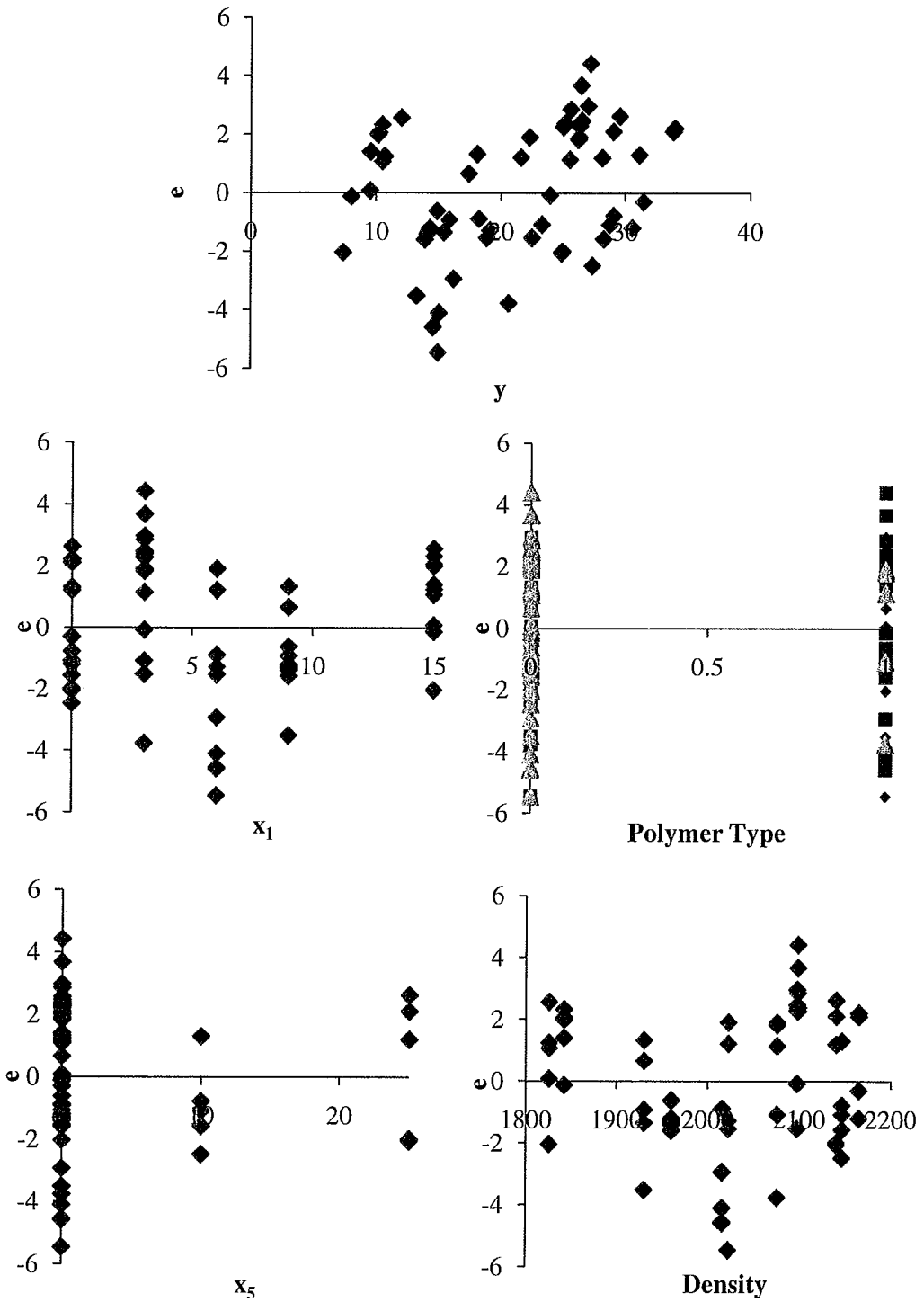

Figure 5.8 Residual plots for block compressive strength model

Table 5.5 ANOVA results for block compressive strength

Variation	Sum of Squares	DOF	Mean Square	F0
SSR	2891.1	5	578.2	101.3
SSE	302.4	53	5.7	
SST	3193.5	58		

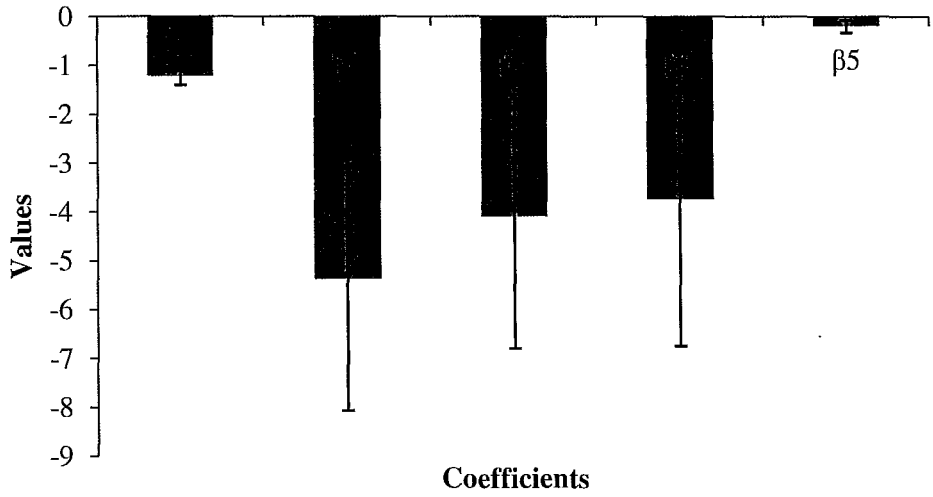

Figure 5.9 Coefficients for block compressive strength

5.3.5 Modulus of Elasticity

The regression model for the elastic modulus, $\hat{y}_E$, of the blocks is presented in equation 5.9. The fit of the model is good with R^2 equal to 0.845.

$$\hat{y}_E = 25.619 - 1.316x_1 + 3.255x_2 - 0.260x_3 - 1.932x_4 - 0.010x_5 \qquad 5.9$$

The residual plots for the model and its parameters, shown in Figure 5.10, indicate that the model does not fit all the data. This is especially evident in the plot of y_E where there are a couple of outliers at the upper right corner of the plot that deviate significantly from the other error values, which have a good spread. Also, there appears to be a slight u-shaped pattern in the plot of the elastic modulus. From the residuals versus x_1 plot, it is clear that for the 9% polymer replacement the error does not have the same variation since it is more negative than the other values. This indicates that for the 9% polymer content the model over estimates the elastic modulus. For the LDPE, there is a larger spread for the error than for the other polymer types as shown in the plot of e versus x_2, x_3 and x_4. The residuals for the glass do not meet the requirements of a mean of zero and equal variation. There are indications that the assumptions for the residuals are not true in all cases, which suggests that the model may need to be re-evaluated. Removing some of the outliers appears to be the best option for improving the

model for linear regression, since no other discernable patterns are evident in the residual plots.

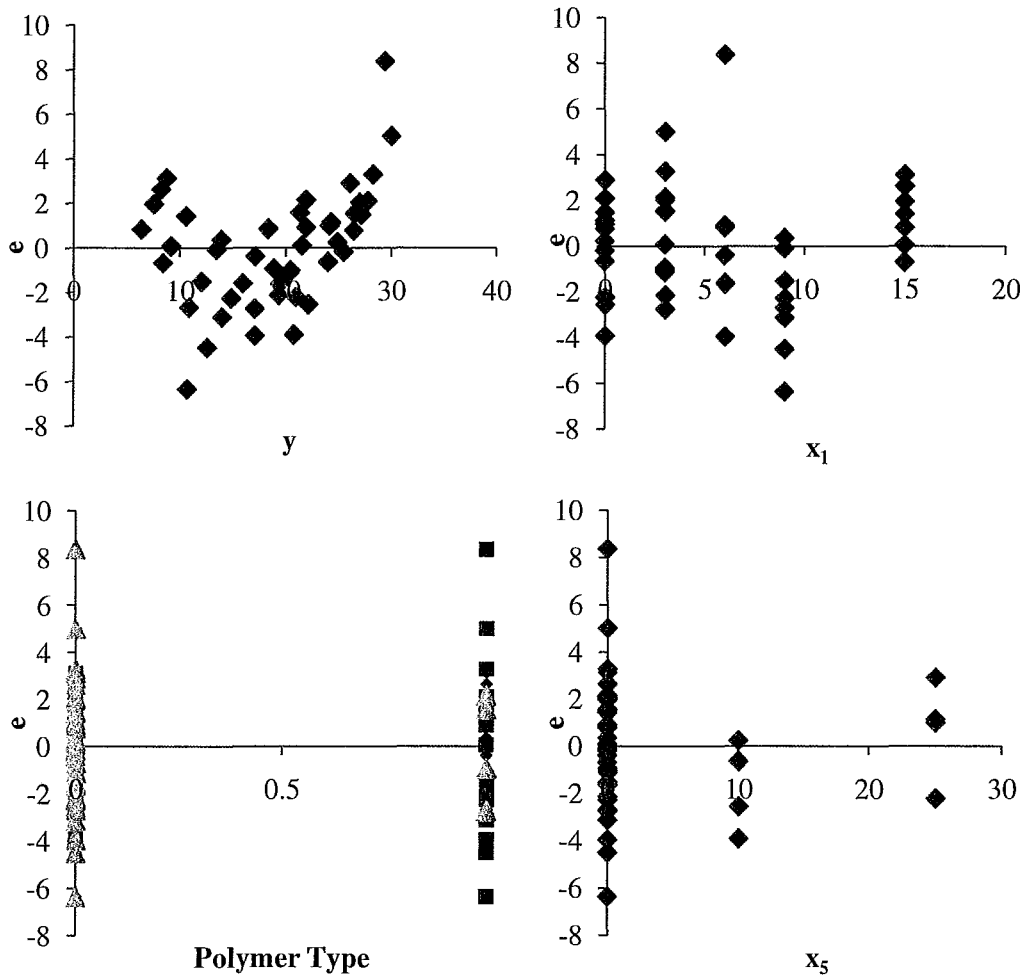

Figure 5.10 Residual plots for block modulus of elasticity model

The ANOVA table in Table 5.6 indicates that at least one of the coefficients of the model is not zero and therefore significant. The F_0 for the analysis is 60.25, which is greater than $f_{\alpha/2,k,n-p}$= 2.895, for α=0.05, k=3 and n-p=41. The confidence intervals on the coefficients show that the polymer type and the WGP content are not important to the model and that the polymer content is the only factor affecting the model. This is shown graphically in Figure 5.11.

Table 5.6 ANOVA results for block modulus of elasticity

Variation	Sum of Squares	DOF	Mean Square	F0
SSR	1701.5	5	340.3	44.7
SSE	312.3	41	7.6	
SST	2013.7	46		

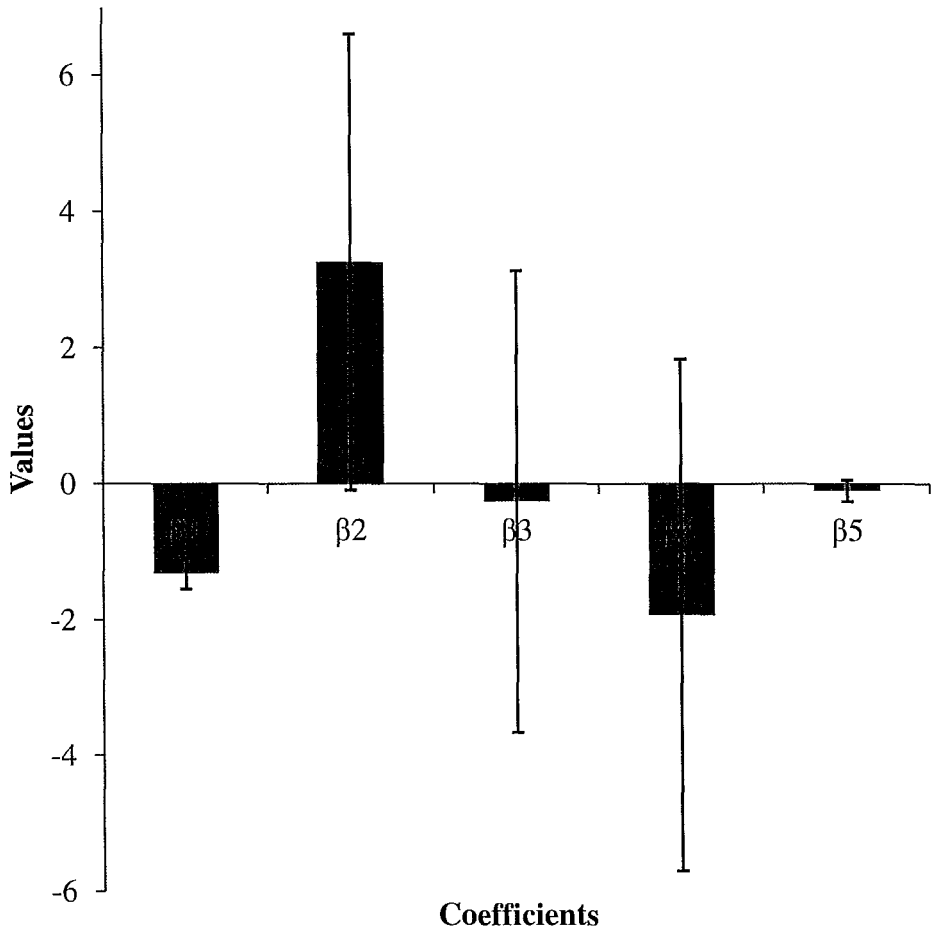

Figure 5.11 Coefficients for block modulus of elasticity

5.4 Regression Models for Prisms

5.4.1 Compressive Strength

A regression model was determined using the multiple linear regression approach. Due to correlation of some of the data, such as the block strength and block density, a stepwise regression approach was used to determine which regressor variables were to be included into the model (Montgomery & Runger, 2003). The model for the prism compressive strength, $\hat{y}_{f'_m}$, is presented in equation 5.10. For this model the regressor parameters were the block compressive strength, f'_{block}, the mortar compressive strength, f'_{mortar}, and the square of the block compressive strength, $(f'_{block})^2$. The R^2 value was 0.954, which indicates that the model fits the data very well. The residuals for the model are plotted in Figure 5.12.

$$\hat{y}_{f'_m} = 7.490 + 2.723 f'_{block} - 0.189 f'_{mortar} - 0.047 (f'_{block})^2 \quad 5.10$$

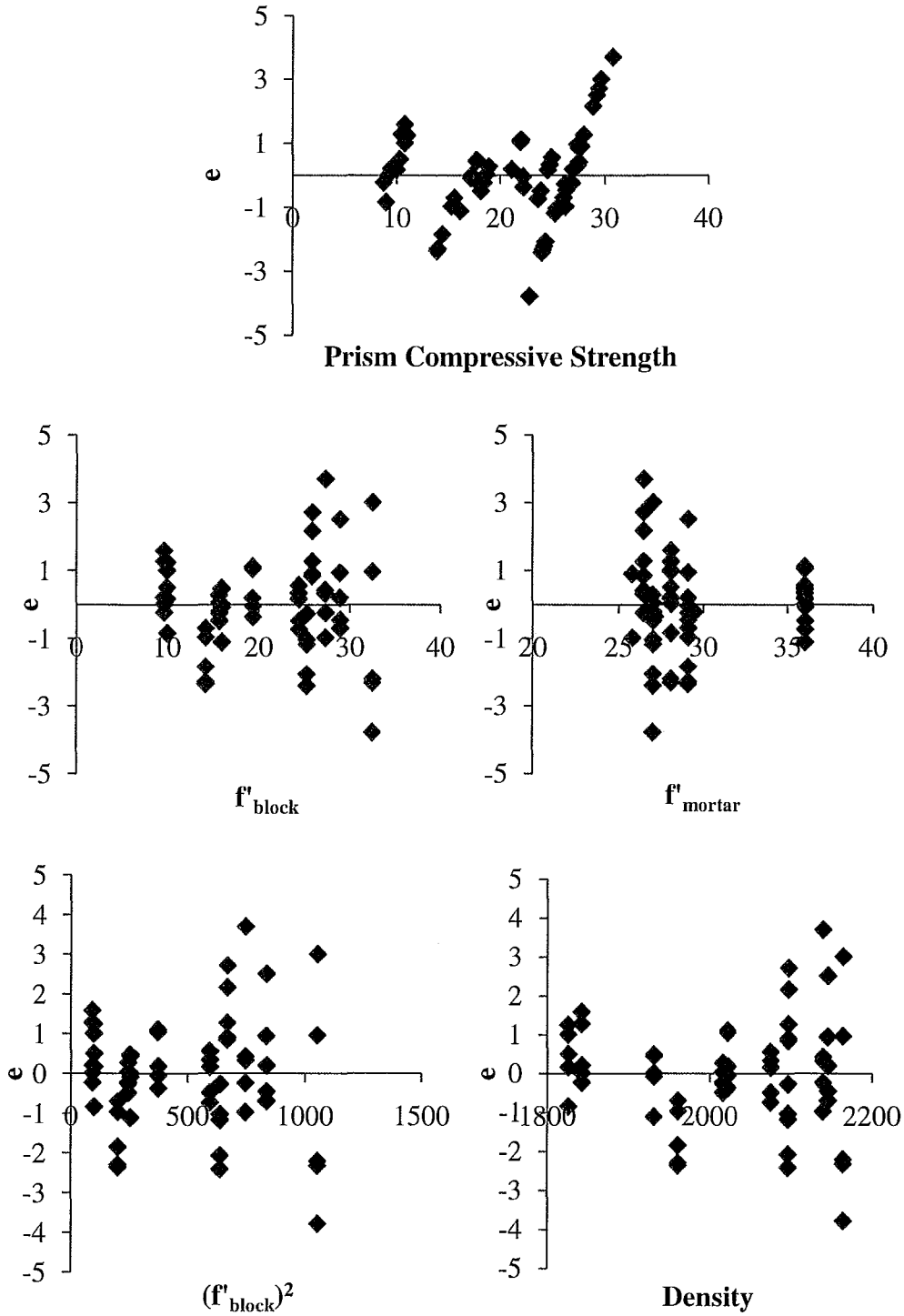

Figure 5.12 Residual plots for prism compressive strength model

In the plot of the residuals versus the compressive strength, the variation of the residuals is very good, except for a few outliers. For the error compared to

the compressive strength of the blocks, the variation is good, but there is some increase in the variation as the strength of the blocks increases. The spread is acceptable for the mortar strength although the variation is lower at the higher mortar strength. The square of the compressive strength also shows good variation. The residuals are also plotted against the block density since it may also be relevant to the model even though it was not included. From the plot, a similar spread of the residuals is evident for the density as for the block compressive strength. There are no new trends so including the density should not improve the model. There are no discernable trends in the residual plots which would aid in improving the regression model.

The ANOVA table (Table 5.7) indicates that there is at least one coefficient that is not zero in the model which affects the regression, since the F_0 value is very high. So the confidence interval on the coefficients was determined. The coefficients and the corresponding interval are plotted in Figure 5.13. The graph shows that all the coefficients are significant to the model. The block strength is the most influential factor while the square of the compressive strength is much less influential.

Table 5.7 ANOVA results for prism compressive strength

Variation	Sum of Squares	DOF	Mean Square	F0
SSR	2402.66	3	800.89	391.84
SSE	114.46	56	2.04	
SST	2517.12	59		

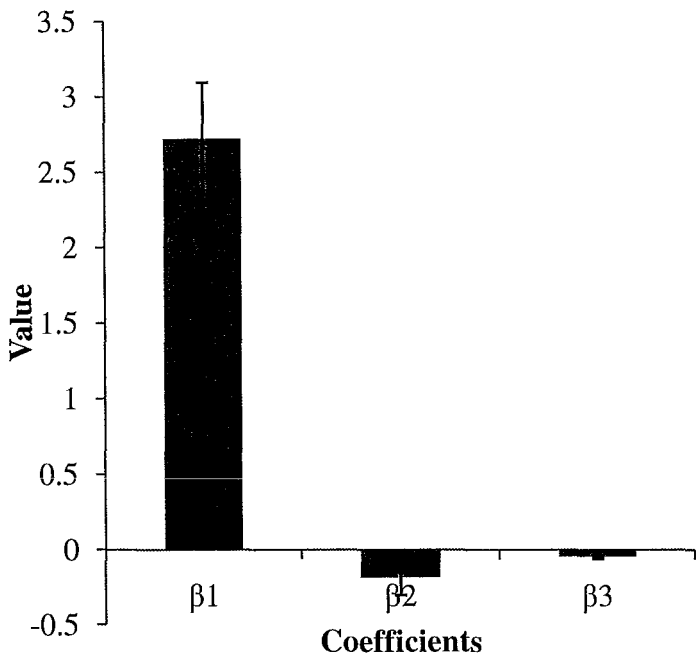

Figure 5.13 Coefficients for prism compressive strength model

5.4.2 Modulus of Elasticity

A linear regression model was determined for the elastic modulus of the concrete prisms tested using the same stepwise approach as for the compressive strength of the prisms. The model, $\hat{y}_{E_m}$, is presented in equation 5.11. The regressor variables were the polymer content, x_1, and the polymer type, x_2, x_3 and x_4, as well as the elastic modulus of the blocks, E_{block}, and the compressive strength of the blocks, f'_{block}. The fit of this model was very good, which is indicated by an R^2 of 0.945. The residual plots for the model are given in Figure 5.14

$$\hat{y}_{E_m} = 8.3 - 0.4x_1 + 1.6x_2 + 2.0x_3 + 5.9x_4 + 0.3E_{block} + 0.3f'_{block} \qquad 5.11$$

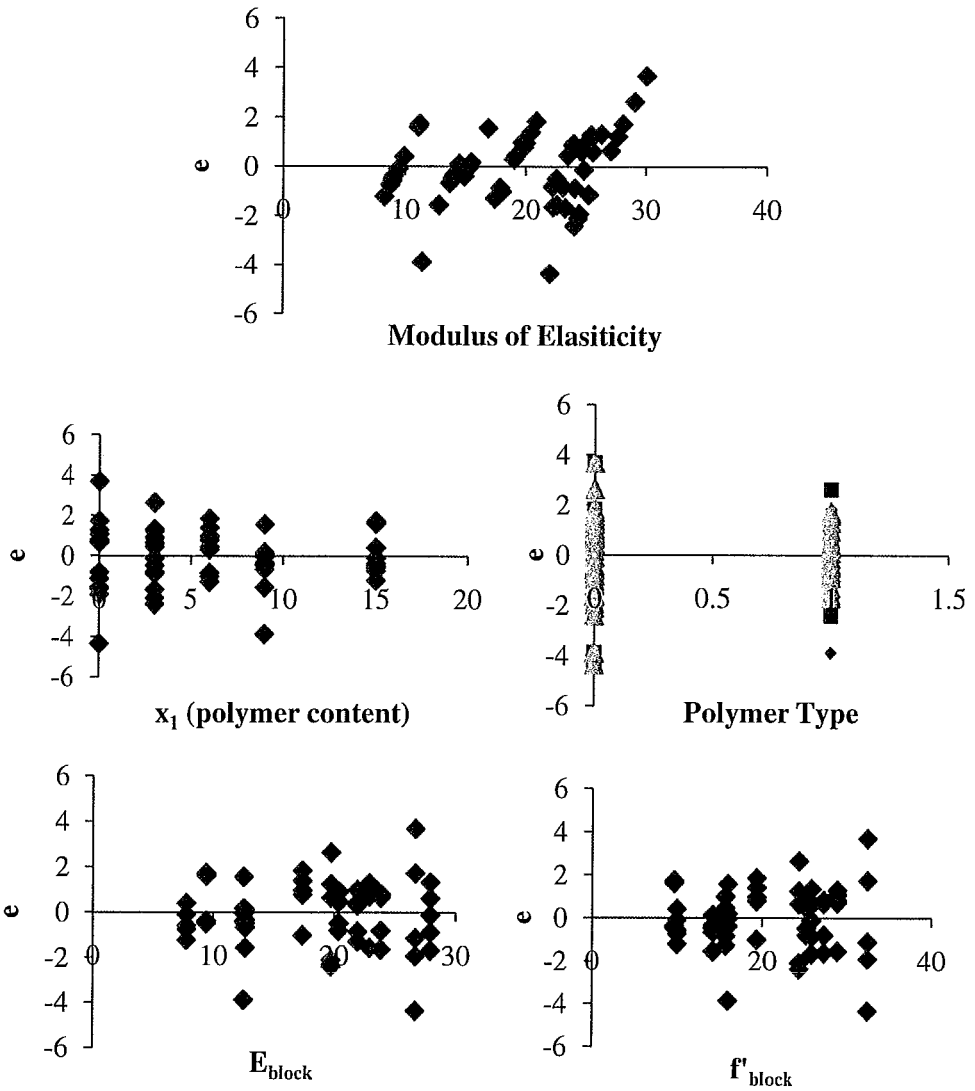

Figure 5.14 Residual plots for prism modulus of elasticity model

The spread of the error is very good for the plot of the residuals versus the prism elastic modulus, although some of the error points are found to be variable. For the regressor variables used in the model, the plots of the variation are very close to the ideal distribution, indicating that the assumptions of the model are closely met. Figure 5.15 presents the residual plots of the mortar strength and block density that were not used in the model. The residuals provide a well behaved plot of both of these factors, indicating that there is no evidence that their inclusion would benefit the model.

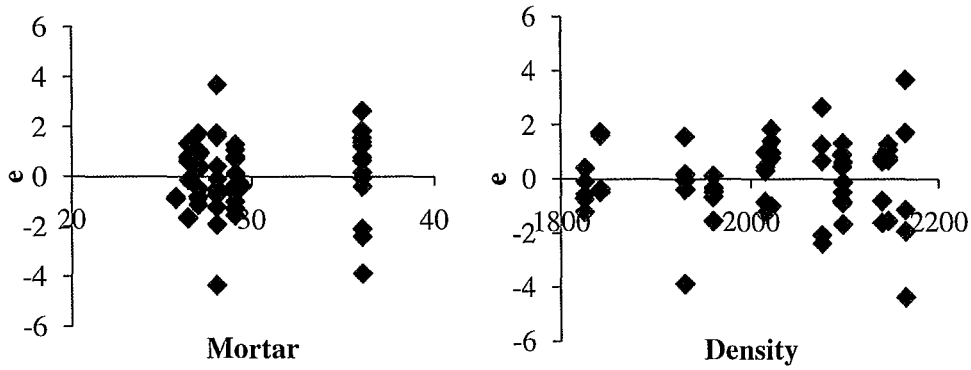

Figure 5.15 Residual plots of parameters not used in model

To determine if any of the coefficients in the model were significant an ANOVA table was used and is presented in Table 5.1. The analysis shows that at least one of the coefficients was relevant to the model. The plot of the coefficients and their 95% confidence interval (Figure 5.16) shows that all the factors influence the model, except the LDPE polymer. The grafted polymer type seems to have the greatest effect on the elastic modulus of the prisms, followed by the HDPE polymer type and polymer content. The polymer content leads to a decrease in the elastic modulus while the other factors have a positive effect on the modulus.

Table 5.8 ANOVA results for prism modulus of elasticity

Variation	Sum of Squares	DOF	Mean Square	F0
SSR	2116.81	6	352.802	152.095
SSE	122.94	53	2.31962	
SST	2239.75	59		

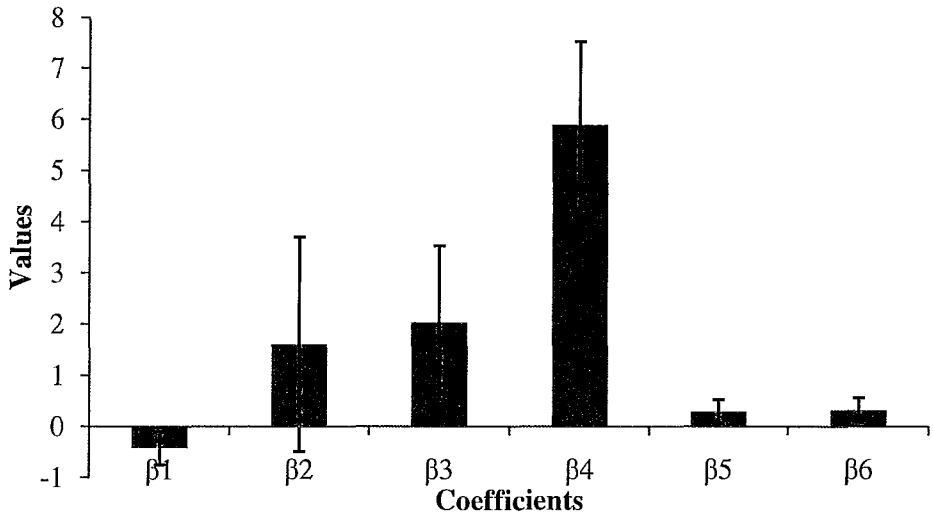

Figure 5.16 Coefficients for prism modulus of elasticity

5.5 Discussion

The experimental program was established to determine the effect of polymer aggregates on block properties and the viability of replacing a portion of the Portland cement with WGP to produce blocks with adequate properties but lower impact on the environment. This section provides a synthesis of the results and determines the effects of these materials on the properties of the block absorption, density, compressive strength and the prism compressive strength, elastic modulus and bond strength.

5.5.1 Waste Glass Powder as Cement Replacement

The WGP was used to replace cement by 10% and 25%, by weight. The results presented are very encouraging and show that glass is a viable material to use for this purpose. The 10% WGP replacement had very little effect on the block and prism properties tested while the 25% WGP replacement had a minor effect.

The 10% WGP concrete blocks had the same density and weight as that of the regular concrete blocks. The 25% had the same weight but a slightly lower density than the control blocks. The regression model for the density of the blocks indicates that there is a small reduction in density with the addition of WGP. The work of Shayan and Xu (2006) showed that the density of hardened concrete was affected by WGP. They determined that the density of the concrete was 5% lower for 20% cement replacement and 3% lower for 30% cement replacement.

The water absorption of the blocks was not affected by the addition of 10% WGP but increased by about 13% for the addition of 25% WGP. The IRA for the 25% WGP blocks also increased. This indicates that the capillary pores of the 10% WGP blocks are comparable to those of the control. The IRA of the 10% WGP blocks suggests that these blocks would have similar mortar bond as the regular blocks. Additional tests on the porosity and the durability are needed to

ensure these blocks can be used for outdoor exposure. The regression model shows that the WGP content increases the absorption but does not affect the IRA.

The compressive strength of the blocks was affected by both the 10% and 25% replacement of cement with WGP. In both cases, the strength of the blocks was lower than that of the control blocks. But there was no statistical difference between the compressive strength of the 10% and 25% WGP. The mean strength reduction was between 11% and 16% compared to the control, which is significant; however, the strength is still high enough to be used in structural applications. As with other pozzolanic materials, the compressive strength for the WGP blocks is expected to develop with time. It was not possible to test the blocks at 28 days, laboratory time and space constraints, but it can be assumed that the compressive strength would have been lower at that age than it was at the tested age of 160 days. This was shown by previous research into wet-cast concrete, where the compressive strength of concrete with WGP improved in strength from 28 days to 90 days (Shayan & Xu, 2006; Shao et al. 2000). The blocks were tested at 160 days so they are expected to have achieved most of their ultimate compressive strength, although some studies have indicated strength gain in concrete with WGP even at 270 days (Shayan & Xu, 2004). The compressive strength of the 10% WGP blocks at one year concurs with this, while the control and 25% WGP did not gain any strength. From the tests on the compressive strength the WGP blocks are expected to perform very well in construction as far as strength is concerned.

The elastic modulus of the blocks was also tested. The 10% and 25% WGP blocks showed higher variability than the control blocks and had statistically the same elastic modulus. The elastic modulus was slightly lower for the 10% WGP blocks than for the control blocks, but the 25% WGP blocks were statistically the same to the control. The higher variability makes it difficult to accurately judge the effect of the WGP on the elastic modulus. However, according to the regression model the WGP caused a slight reduction in the elastic modulus.

For the prism compressive strength the average strength of both of the 10% and 25% WGP prism was higher than the average for the control prisms but no statistical difference was found between them. This shows that good strength can be achieved by replacing some of the cement with WGP. There is some indication that the glass blocks increased in compressive strength with time since the 10% WGP blocks tested at one year were statistically comparable to the control blocks although they had lower compressive strength when tested at the earlier age of 160 days. Also, the compressive strength of the prism was statistically the same as that of the blocks, whereas, in general, prisms have lower strength (Drysdale & Hamid, 2005).

There was no difference between the elastic modulus of the prisms with WGP and the control prisms. The failure of the WGP prisms and the control prisms was exactly the same and in both cases the failure was brittle. The WGP content was insignificant to the regression model. This is a good indication that

for mechanical properties the WGP blocks will perform in the same manner as concrete blocks and can therefore be used for the same applications.

The bond wrench test was performed on 6 mortar joints for prisms with WGP. This is a very variable test so only general observations may be made about the effect of the glass on the bond strength. However, no statistical difference was found between the bond strength of the WGP and the control blocks.

Since glass is made of an amorphous silica material there is the possibility of an ASR reaction when it is used in concrete. For this reason, the mortar bar test was used to determine if there was any expansion in the mixes with WGP. The test is an accelerated ASR test used to determine the susceptibility of aggregates to ASR expansion. Since the glass for this study was a powder used as a pozzolanic material, the mortar bar test may not be indicative of reactivity in the concrete blocks (Kozlova, Millrath, Meyer, & Shimanovich, 2003). Also, instead of making mortar, according to the standard test, pieces of the blocks were tested, which may also affect the results. Other studies have indicated that the mortar bar test is not the most accurate method to determine ASR reactivity and has been known to give false positive results due to the extreme conditions it induces; however, it has the advantage of being quick and easy to perform (Kozlova et al., 2003). Bars from the 10% and the 25% WGP blocks were tested using the mortar bar test. None of the bars exceeded the ASTM C 1260 (2007) 14 day limit even after 30 days. This is a good indication that there is no detrimental ASR expansion occurring, although the expansion of the 25% WGP bars was larger than that of the control bars. This is consistent with work by other studies, where WGP used within mortar bars to replace cement did not cause expansion greater than the 14 day expansion limit, even at replacements as high as 30% (Shao et al., 2000; Shayan & Xu, 2004; Shayan & Xu, 2006; Schwarz et al. 2008).

From an analysis of the results and regression models for the properties of the blocks, there is very little effect of the concrete blocks when the cement is replaced by 10% or 25% with WGP. Only the absorption, density and elastic modulus of the blocks were affected by the addition of WGP, but even in those cases not to a large extent. All the properties indicated that the WGP blocks perform in the same way as, or very similarly to, the control blocks.

5.5.2 Effect of Polymer Addition

The polymers used in this study were used to replace a portion of the sand by 3%, 6%, 9% and 15% to make concrete blocks. From the analysis of the results and the regression models, the polymer content seems to be a major factor which affects the block properties tested.

The density of the blocks was significantly affected by the addition of polymers. As the polymer content increased, the density decreased. From the regression model, the polymer content was the most influential on the block density. For all the sand replacement levels with polymers the density of the blocks was decreased by a significant amount. The trend for the effect of density agrees with previous research on other polymers used to replace sand for concrete

production (Ismail, Saim, & Saleh, 2003; Ismail & Al-Hashmi, 2008); however, Marzouk et al. (2007) did not find any significant effect on density at sand replacement levels below 30% using PET waste. For masonry it may be beneficial to reduce the density, and thereby the weight, of the blocks to easy transport and placement.

The water absorption and the IRA of the blocks were both significantly affected by the polymer content. An increase in the polymer content resulted in a dramatic increase in the absorption and IRA. For both properties, the polymer content was the main influencing factor in the regression models. Ismail et al. (2003) also found an increase in absorption using polystyrene beads in concrete, which they attributed to voids created within the concrete due to the inclusion of polymers. IRA follows the same trend.

The compressive strength of the blocks is significantly reduced by adding polymers into the mix. In the statistical analysis, even 3% replacement of sand with polymers produced a statistically significant reduction in strength. For higher replacement levels, the strength decreased dramatically and the blocks produced were not suitable for structural applications. This is due, in part, to the low compressive strength of the polymer particles, as well as due to the cracking caused during manufacturing of the higher content polymer blocks. The structure of the 9% and 15% polymer blocks was weakened by cracks in the webs caused by expansion of the blocks after de-molding, which was likely caused by the pressure generated between the hydrophobic particles and the water in the block mix. Research by Ghaly and Gill (2004), Gavela et al. (2004), Ismail and Al-Hashmi (2008) and others agrees with these trends; however the reduction in strength was not as significant up to 20% sand replacement.

The elastic modulus of the blocks was also significantly affected by the presence of polymers, although polymer content was not the only influential factor. The increase in polymer content led to a decrease in the elastic modulus. A similar decrease was noted in the work of Ghaly and Gill (2004) for regular wet-mix concrete at w/c of 0.54; however the reduction was only about 15% for the 15% plastic concrete whereas it was reduced by over 50% for the 15% polymer blocks tested.

The prism compressive strength was also reduced with the addition of polymers; however, in the regression model this is taken into account in the block compression variable. The prism compressive strength was not as affected by the polymer content as the block compressive strength. The 3% polymer prisms performed well.

The elastic modulus of the prisms was also decreased with the addition of polymers. For the regression model in this case the polymer content caused a reduction in the elastic modulus.

The bond wrench test produced variable results. The 6% and 9% polymer blocks performed well in this test. Although a regression model was not determined, it appears that the higher IRA for the polymers than that of the

control aided in producing a better bond for these prisms. However, when the IRA increased to a certain level it negatively affected the bond strength.

In general, the addition of polymers produced a negative effect on the properties of the block. The 3% polymer mixes usually performed well and there is indication that these blocks can be used for structural applications. Although the 6% and 9% mixes may be acceptable for some non-structural applications, the 15% polymer mixes would not be adequate for any application since the properties for these mixes are very poor and cracks were apparent after de-molding.

5.5.3 Effect of Polymer Type

In this study, 3 polymers types were used LDPE, HDPE and grafted HDPE. It is desirable to determine whether the polymer type affected the block and assemblage properties, to what extent these properties are affected and which polymer type performed the best.

No statistical difference was found between the 3 polymer types for density however the polymer type was found to affect the regression model for the grafted polymer. The polymer type did not affect the absorption, IRA or elastic modulus of the blocks, nor the compressive strength of the prisms. All 3 polymer types; however, produced a decrease in the compressive strength of the blocks. The grafted polymer was most influential in the regression model for the elastic modulus of the prisms. These trends are consistent with the results for PET aggregate (Marzouk et al., 2007), mix post-consumer plastic waste (Ghaly & Gill, 2004) and polypropylene (Gavela et al., 2004).

It was theorized that grafting the polymer to reduce its hydrophobic nature would improve the properties of the blocks made with polymers. However, the results of the experimental program show that there was no significant improvement on the properties of the blocks, when 3% grafted HDPE was used, over the same property when 3% LDPE or 3% HDPE was used. The concentration of 3% was too low to impact the properties of the blocks since there is no indication that the hydrophobicity of the polymers affects the block properties at the 3% sand replacement level. The concentration of grafted polymer would need to be higher to evaluate the effect of the hydrophobic nature of the polymers.

CHAPTER 6 COMPRESSIVE STRENGTH MODEL FOR POLYMER CONCRETE BLOCKS

6.1 Introduction

From the results of this study and the work of others, including Gill & Ghaly (2004), Gavela et al. (2004) and Marzouk et al. (2007), the compressive strength of concrete is reduced with the addition of polymer aggregate. This chapter presents a compressive strength model for polymer concrete blocks that accounts for the amount of polymer added to the concrete mixture, it postulates that the polymers have zero strength and can be treated as air voids.

6.2 Porosity versus Compressive Strength of Concrete

Studies on regular concrete have shown that the compressive strength is related to the porosity of the concrete. The strength is related to the total volume of voids which includes the pores in the cement paste, the voids in the aggregate and the entrained air (Kearsley & Wainwright, 2002). Several relationships have been presented to describe this relationship with varies degrees of correlation. It has been suggested that the model which best suits the results is affected by type of concrete, total porosity, w/c, degree of hydration and pore size distribution (Rößler & Odler, 1985; Kearsley & Wainwright, 2002).

The following set of relationships has been developed for various materials other than concrete; however Kearsley and Wainwright (2002) and Kumar and Bhattacharjee (2003) have attempted to use them to describe the relationship between concrete compressive strength and its porosity. Equation 6.1 was developed by Balshin (1949) for the relationship of porosity to strength for porous metal-ceramic materials (Rößler & Odler, 1985; Kearsley & Wainwright, 2002):

$$f_c' = f_{c,0}'(1-p)^n \qquad 6.1$$

Where f_c' is the compressive strength of the concrete, $f_{c,0}'$ is the compressive strength at zero porosity, p is the porosity and n is an empirically determined constant. Equation 6.2 was developed by Ryshkevitch (1953) for porous sintered alumina and zirkonia, where k is an empirically determined constant. (Rößler & Odler, 1985; Kearsley & Wainwright, 2002):

$$f_c' = f_{c,0}' \cdot e^{-k \cdot p} \qquad 6.2$$

The formula developed by Shiller (1959) was based on the strength and porosity of gypsum paste (Rößler & Odler, 1985). Shiller's equation is presented in equation 6.3 (Kearsley & Wainwright, 2002), where k_s is an empirical constant and p_0 is the porosity at zero strength:

$$f_c' = k_s \cdot \ln\left(\frac{p_0}{p}\right) \quad 6.3$$

Finally, Hasselmann (1962) developed a linear relation between strength and porosity for polycrystalline refractory materials, equation 6.4, where k_H is an empirical constant (Rößler & Odler, 1985; Kearsley & Wainwright, 2002):

$$f_c' = f_{c,0}' - k_H \cdot p \quad 6.4$$

Looking at cement pastes, Rößler and Odler (1985) found that all the equations may be used, although a linear relation works best. For foamed concrete, Kearsley and Wainwright (2002) achieved a strong correlation between the strength and porosity of the concrete. Their results were best described by equation 6.2. The R^2 value for their model was 0.936.

Other works looked at additional factors. Hoff (1972) incorporated density and w/c into the relation. Kumar and Bhattacharjee (2003) did not obtain a good correlation between their experimental data and the results of the above equations for regular concrete. However, when they included the mean pore radius within their relation the correlation improved.

6.3 Model Determination

The equations given above are based on the porosity (%) and the compressive strength of concrete with 0% porosity. For the use of polymers in concrete blocks it is assumed that adding polymers is the same as adding voids into the concrete. Therefore, the percentage of sand replaced by polymers, LDPE, HDPE or grafted HDPE, can be considered the percentage of voids added to the blocks. So a block with 3% sand replaced by polymer aggregate is taken as having 3% porosity. Since the size of the polymer aggregate is much larger than the size of pores within the cement paste and voids in natural aggregate it is assumed that the porosity increase is due to the addition of polymers is much greater than the original porosity. Thus, relatively, the original porosity can be considered negligible, that is control blocks, which have no polymer aggregate, are assumed comparatively to have no voids. Therefore, $f_{c,0}'$ is assumed equal to the compressive strength of the control blocks. A mean compressive strength of 32.5 MPa, which corresponds to the control blocks, was taken as $f_{c,0}'$.

The empirical constants equations 6.1 to 6.4 were determined by minimizing the difference between the experimental compressive strength and the compressive strength calculated using the equations. Accordingly, equation 6.1, 6.2 and 6.4 become equation 6.5, 6.6 and 6.7, respectively. Equation 6.3 was found to be unsuitable for the proposed assumptions. The models where fitted for all the data for the blocks with polymers without distinguishing between polymer type. The empirical constants were determined from the experimental data so they are only applicable to the results of this experimental program. The constants

would need to be reevaluated for a different data set. A plot of the experimental data with the three models is shown in Figure 6.1.

$$f_c' = f_{c,0}'(1-p)^{8.35} \quad 6.5$$

$$f_c' = f_{c,0}' \cdot e^{-8.73 \cdot p} \quad 6.6$$

$$f_c' = f_{c,0}' - 190.8 \cdot p \quad 6.7$$

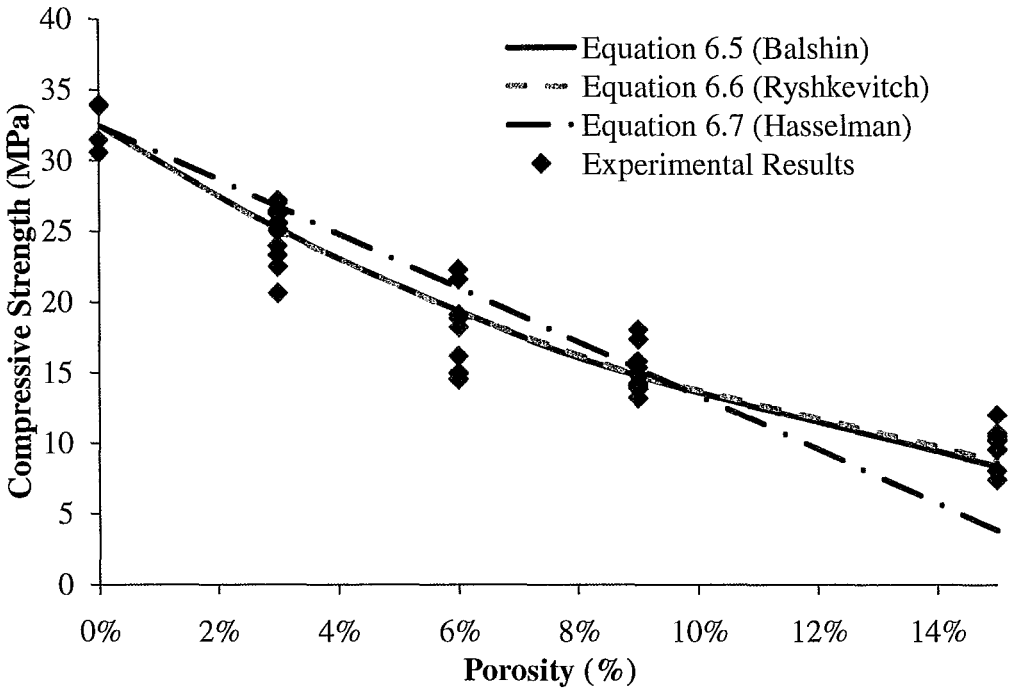

Figure 6.1 Compressive strength versus porosity

For the blocks tested, the fit of the models to the experimental data for the compressive strength was determined using the coefficient of determination, R^2. For equation 6.5 (Balshin) R^2 was equal to 0.919, for equation 6.6 (Ryshkevitch) R^2 was 0.921 and for equation 6.7 (Hasselmann) R^2 was 0.855.

6.4 Proposed Model

Both the Balshin (equation 6.5) and Ryshkevitch (equation 6.6) equations fit the data very well as shown by the high R^2 values. The Hasselmann (equation 6.7) equation does not predict the data as well and from Figure 6.1 it can be seen that model does not predict the compressive strength well at higher porosities. Either the Balshin equation or the Ryshkevitch equation may be used to predict the compressive strength of concrete masonry blocks which contain polymer aggregate. These equations work well at low and high polymer contents (from 0%

to 15%). From this analysis it can be concluded that the there is a relationship between compressive strength and polymer content. These results indicate that the assumption that the polymer aggregates added can be considered as voids is reasonable.

The model can be refined by considering additional factors, such as size of the polymer aggregate and by accounting for the voids already present in the concrete. Furthermore, refinement can be expected by accounting for the type of polymers and the contact angle of the polymers.

CHAPTER 7 CONCLUSIONS AND RECOMMENDATIONS

7.1 Introduction

This chapter outlines the conclusions that were drawn from the results presented in the previous chapters into the use of WGP and polymers to make concrete blocks.

7.2 Waste Glass Powder as Cement Replacement

Glass powder was used to replace either 10% or 25% by weight of the cement used to make concrete blocks. The effects of this replacement are summarized.

7.2.1 Block Properties

From the experimental program, the following effect on the block properties was observed:

1) The density of the block was not affected by the replacement of cement with WGP.
2) The absorption of the blocks was not affected by the 10% replacement of cement with WGP. However, the absorption increased by 13% when 25% of the cement was substituted.
3) The IRA of the blocks was not affected by the 10% replacement of cement with WGP. However, at 25% WGP the IRA increased by 41%
4) There was no statistical difference between the compressive strength of the blocks with 10% and 25% WGP; however both types of blocks had lower strength than the control blocks. The blocks with WGP were between 11% and 16% lower in strength than the control blocks.
5) The results for the elastic modulus yield a 14% lower modulus than the control for the 10% WGP blocks, while the 25% WGP blocks show no statistical difference with the control blocks.

7.2.2 Assemblage Properties

For the blocks with WGP, the following was concluded for the assemblage properties:

1) The compressive strength was the same for the prisms with 10% and 25% WGP and for the control, based on statistical analysis. Both the prisms with 10% and 25% achieved strengths of approximately 27 MPa.
2) Although the mean elastic modulus of the prism with WGP was lower than that of the control, statistically there was no difference.
3) The bond strength of the prisms was very variable so there was no evidence of any difference between the bond strength of the control prisms and the prisms with 10% and 25% WGP.

In conclusion, the prism properties tested show that both the 10% and 25% blocks produced prisms with comparable strength, elastic modulus and bond strength to the control prisms.

7.2.3 Alkali-Silica Reaction

The results of the expansion measurements for ASR are variable but the following conclusions can be made:

1) Neither the 10% nor 25% WGP bars showed expansion exceeding the allowable limit, even up to 28 days of testing.
2) The 10% WGP bars showed statistically lower expansion than the control bars.
3) The 25% WGP bars showed statistically higher expansion than the control bars but the expansion is within the acceptable limits set by ASTM C 1260 (2007).

7.2.4 Concluding Statement

There is no indication that replacing 10% of the cement with WGP will produce negative effects on masonry properties; in fact, for all the properties tested, the blocks with 10% WGP were comparable to the control blocks. There is also no indication that these blocks will undergo detrimental ASR expansion. The 25% WGP blocks performed well for all properties except for water absorption and showed slightly higher expansion than the control. The results suggest that the 25% blocks would also perform well, although some additional testing is recommended to confirm this.

7.3 Polymer Aggregate

Two types of polymers, LDPE and HDPE were used to replace sand at 3%, 6%, 9% and 15% by volume. Also, blocks were made with 3% of sand replaced with a grafted HDPE polymer. This section will summarize the effect of these replacements on unit and prism properties of the blocks in comparison to the control blocks.

7.3.1 Block Properties

The block properties were affected by the addition of polymers in the following manner:

1) At 15% sand replacement with polymer aggregate, it was difficult to produce uncracked blocks and most of the resulting blocks developed cracks within the webs. The 9% polymer blocks had some cracks while the 3% and 6% were visually comparable to the control blocks.
2) The density of the blocks decreased with the replacement of sand with polymers. A notable decrease in density was observed even at low sand substitutions. At 3% replacement of sand with polymer aggregate, the density was approximately 3% less than the control, while at 15% replacement, the density was approximately 15% lower than the control.
3) The water absorption of the blocks increased significantly with the addition of polymer aggregate. Although, the 3% LDPE blocks had comparable water absorption values to the control blocks, all the other blocks with polymers had higher absorptions.

4) The IRA was significantly affected by the addition of polymers and increased in all cases with the increased polymer content.
5) The polymer content had a negative impact on the strength of the blocks. At 3% polymer content, the strength decreased between 20% and 25%, at 6% the strength decreased between 40% and 52%, at 9% the strength decreased between 50% and 56%, and at 15% the strength decreased approximately 70% compared to the control block strength. This shows that even small replacements of sand with polymer material results in a significant decrease in strength.
6) A model developed to account for the polymer content revealed that the polymers can be treated as voids; however the relation is not linear.
7) The results show that the elastic modulus of the blocks with 3% LDPE is statistically the same as that of the control. All the other blocks with polymers result in a lower elastic modulus than the control.
8) The HDPE and LDPE blocks performed similarly and, in general, there is no strong evidence to choose one over the other.

In summary, the block properties are significantly affected by the substitution of sand with polymer aggregate. Strength is drastically reduced by the addition of even small amounts of polymer so this might not be viable for structural applications. Acceptable blocks may be achieved with either 3% or 6% sand replacement; however, at higher replacement values, the production of the blocks with hydrophobic polymers becomes difficult.

7.3.2 Assemblage Properties

The following conclusions were deduced regarding the effect of polymers on the properties of masonry assemblages:

1) The compressive strength of the prisms made with the 3% polymers, for all polymer types, was the same as the compressive strength for the control prisms, based on statistical analysis. Further addition of polymers resulted in a decrease in the compressive strength. At 9% sand replacement, the compressive strength decreased more than 30%.
2) The failure mechanism of the prisms with high polymer content was different than that of the regular prisms.
3) The modulus of elasticity of the prisms is not affected by a 3% replacement of sand; however, it decreases significantly with replacement levels greater than 6%.
4) The results of the bond strength test yielded some unexpected results. It was found that the 6% LDPE, 15% LDPE, 3%, 6% and 9% HDPE and 3% grafted prisms had higher bond strength than the control prisms. There is evidence that this result is related to the IRA of the blocks and that the blocks with intermediate IRA values had the highest bond strength.

For the results of the experimental program, it was found that the 3% replacement of the sand with polymers will produce adequate prisms. A

substitution by 6% also seems feasible, however higher replacement levels will result in a significant loss in compressive strength.

7.4 Recommendations and Future Research

The goal of this research was to determine the feasibility of replacing either the sand or cement in concrete blocks with post-consumer waste in order to improve the sustainability of the industry. The experimental program aimed to establish the quantity of cement which may be replaced with finely ground WGP and to determine the quantity and type of polymer which can be used to replace sand. From the experimental work presented, several recommendations can be made:

1) WGP may be used as a replacement for cement up to 25%; however a reliable and cost effective source needs to be determined to obtain the glass powder.
2) The cost of collecting, sorting and crushing WG into a fine powder needs to be compared to the cost of using other pozzolanic materials to replace a portion of the cement.
3) This study did not use waste polymers to make concrete blocks; therefore waste polymers should be used in further studies to meeting the goals of improving the sustainability of block production. However, first a reliable source of polymer waste is needed.
4) The sorting of waste polymers based on type and ensuring adequate grading needs to be addressed if waste polymers are used to replace sand.

From the results of this thesis, the following areas for future research have been identified:

1) For WGP replacing cement blocks, in-depth investigation of the possibility of ASR needs to be assessed.
2) The degree of hydration and the hydration product of the blocks with WGP should be evaluated in order to determine how well the WGP acts as a pozzolan. The degree of hydration of the WGP blocks should then be compared to blocks made with other pozzolanic materials to assess the performance of the WGP as a supplementary cementing material.
3) Future work needs to look at other possible types of polymers that can be used to make concrete blocks. Thermosetting polymers or polymer fibers may be valid options.
4) Chemical treatments of polymer aggregates may improve their performance in concrete. Larger concentrations of grafted material need to be evaluated to determine whether this type of treatment improves the block properties, since the amount of grafted material used in this study was too low to show any change in the block characteristics.
5) The particle size of the polymer aggregate is another factor that may affect the properties of the blocks but was not studied in this project.
6) This study focused on the physical and mechanical properties of the concrete blocks; however the durability and chemical properties of the blocks need to

be assessed to determine their quality and performance. This should include freeze-thaw testing, chemical resistance, etc.

The research presented is an initiative to develop more sustainable construction materials. As can be seen from the work presented, good quality blocks may be produced by replacing part of the usual raw materials of concrete with post-consumer waste materials, thereby reducing the impact of block manufacturing on the environment.

REFERENCES

ASTM C 67, (2009). Standard Test Methods for Sampling and Testing Brick and Structural Clay Tile. *American Society for Testing and Materials*: West Conshohocken.

ASTM C 140(a), (2008). Standard Test Methods for Sampling and Testing Concrete Masonry Units and Related Units. *American Society for Testing and Materials*: West Conshohocken

ASTM C 490, (2007). Standard Practice for Use of Apparatus for the Determination of Length Change of Hardened Cement Paste, Mortar, and Concrete. *American Society for Testing and Materials*: West Conshohocken.

ASTM C 618, (2008). Standard specifications for coal fly ash or calined pozzolan for use in concrete. *American Society for Testing and Materials*: West Conshohocken.

ASTM C1072, (2006). Standard Test Method for Measurement of Masonry Flexural Bond Strength. *American Society for Testing and Materials*: West Conshohocken.

ASTM C 1260, (2007). Standard Test Method for Potential Alkali Reactivity of Aggregates (Mortar-Bar Method). *American Society for Testing and Materials*: West Conshohocken.

ASTM C 1314, (2007). Standard Test Method for Compressive Strength of Masonry Prisms. *American Society for Testing and Materials*: West Conshohocken.

ASTM C 1437, (2007). Standard Test Method for Flow of Hydraulic Cement Mortar. *American Society for Testing and Materials*: West Conshohocken.

ASTM C 1552(a), (2008). Standard Practice for Capping Concrete Masonry Units, Related Units and Masonry Prisms for Compression Testing. *American Society for Testing and Materials*: West Conshohocken.

ASTM D 5725, (2008). Standard Test Method for Surface Wettability and Absorbency of Sheeted Materials Using an Automated Contact Angle Tester. *American Society for Testing and Materials*: West Conshohocken.

ASTM D 5946, (2009). Standard Test Method for Corona-Treated Polymer Films Using Water Contact Angle Measurements. *American Society for Testing and Materials*: West Conshohocken.

Babu, K. G., & Babu, D. S. (2003). Behaviour of lightweight expanded polystyrene concrete containing silica fume. *Cement and Concrete Research, 33*(5), 755-762.

Babu, S. D., Ganesh Babu, K., & Wee, T. H. (2005). Properties of lightweight expanded polystyrene aggregate concretes containing fly ash. *Cement and Concrete Research, 35*(6), 1218-1223.

Babu, D. S., Ganesh Babu, K., & Tiong-Huan, W. (2006). Effect of polystyrene aggregate size on strength and moisture migration characteristics of lightweight concrete. *Cement and Concrete Composites, 28*(6), 520-527.

Berg, J. C. (1993). *Wettability*. New York: M. Dekker.

CaGBC (2009). What is LEED? Obtained: July 6, 2009 from http://www.cagbc.org/.

CSA A23.1, (2000). Concrete Materials and Methods of Concrete Construction/Methods of Test for Concrete. *Canadian Standards Association*: Mississauga.

CSA A165.1, (2004). CSA Standards on Concrete Masonry Units. *Canadian Standards Association*: Mississauga.

CSA A179, (2004). Mortar and Grout for Unit Masonry. *Canadian Standards Association*: Mississauga.

CSA S304.1, (2004). Design of masonry structures. *Canadian Standards Association*: Mississauga.

Chen, C. H., Huang, R., Wu, J. K., & Yang, C. C. (2006). Waste E-glass particles used in cementitious mixtures. *Cement and Concrete Research, 36*(3), 449-456.

Corinaldesi, V., Gnappi, G., Moriconi, G., & Montenero, A. (2005). Reuse of ground waste glass as aggregate for mortars. *Waste Management, 25*(2), 197-201.

Drysdale, R. G., & Hamid, A. A., (2005). *Masonry structures behaviour and design* (Canadian ed.). Mississauga: Canadian Masonry Design Centre.

Dweik, H. S., Ziara, M. M., & Hadidoun, M. S. (2008). Enhancing the concrete strength and thermal insulation using thermoset plastic waste. *International Journal of Polymeric Materials*, 57(7), 635-656.

Enviros RIS (2001). Plastic waste management strategy for Ontario. Obtained: July 10, 2008. Obtained from: http://www.cpia.ca/epic/media/default.php?ID=1759.

Federico, L. M., & Chidiac, S. E. (2009). Waste glass as a supplementary cementitious material in concrete –critical review of treatment methods. *Cement and Concrete Composites*, 31(8), 606-610.

Fournier, B. & Berube, M. (2000). Alkali-aggregate reaction in concrete: a review of basic concepts and engineering implications. *Canadian Journal of Civil Engineering*, 27(2), 167-191.

Frechet, J. M. J. (1994). Functional polymers and dendrimers: reactivity, molecular architecture, and interfacial energy. *Science*, 263(5154), 1710-1715.

Gavela, S., Karakosta, C., Nydriotis, C., Kaselouri-Rigopoulou, V., Kolias, S., Tarantili, P. A., Magoulas, C., Tassios. D., & Andreopoulos, A. (2004). *A study of concretes containing thermoplastic wastes as aggregates.* Paper presented at the International RILEM Conference on Use of Recycled Materials in Buildings and Structures, 9-11 Novemeber, 2004. Retrieved from: http://congress.cimne.upc.es/rilem04/frontal/Papers.htm.

Ghaly, A. M., & Gill, M. S. (2004). Compression and deformation performance of concrete containing postconsumer plastics. *Journal of Materials in Civil Engineering*, 16(4), 289-296.

Hoff, G. C. (1972). Porosity-strength considerations for cellular concrete. *Cement and Concrete Research, 2*(2), 91-100.

Ismail, I., Saim, A. A., & Saleh, A. L., (2003). Properties of hardened concrete bricks containing expanded polystyrene beads. *Proceedings of the 5th Asia-Pacific Structural Engineering and Construction Conference*, 171-179.

Ismail, Z. Z., & Al-Hashmi, E. A. (2008). Use of waste plastic in concrete mixture as aggregate replacement. *Waste Management, 28*(11), 2041-2047.

Ismail, Z. Z. & Al-Hashmi, E. A. (2009). Recyclying of waste glass as a partial replacement for fine aggregate in concrete. *Waste Management.* 29 (2), 655-659.

Jin, W., Meyer, C., & Baxter, S., (2000). "Glascrete" – Concrete with glass aggregate. *ACI Materials Journal.* 97(2), 208-213.

Kearsley, E. P., & Wainwright, P. J. (2002). The effect of porosity on the strength of foamed concrete. *Cement and Concrete Composites*, 32(2), 233-239.

Kosmatka, S. H., Kerkhoff, B., Panarese, W. C., MacLeod, N. F., & McGrath, R. J., (2002). Design and control of concrete mixtures. Ottawa: *Cement Association of Canada.*

Kozlova, S., Millrath, K., Meyer, C., & Shimanovich, S., (2004). A suggested screening test for ASR in cement-bound composites containing glass aggregate based on autoclaving. *Cement and Concrete Composites.* 26(7), 827-835.

Kumar, R., & Bhattacharjee, B. (2003). Porosity, pore size distribution and in situ strength of concrete. *Cement and Concrete Research, 33*(1), 155-164.

Kurtis, K. E., & Monteiro, P. J. M. (2003). Chemical additives to control expansion of alkali-silica reactive gel: proposed mechanisms of control. *Journal of Materials Science,* 38(9), 2027-2036.

Lam, C. S., Poon, C. S., & Chan, D. (2007). Enhancing the performance of pre-cast concrete blocks by incorporating waste glass – ASR consideration. *Cement and Concrete Composites, 29*(8), 616-625.

Marzouk, O. Y., Dheilly, R. M., & Queneudec, M. (2007). Valorization of post-consumer waste plastic in cementitious concrete composites. *Waste Management, 27*(2), 310-318.

Meyer, C. (2004). Concrete Materials and Sustainable Development in the USA. *Structural Engineering International.* Obtained: December 5, 2008 from http://www.civil.columbia.edu/meyer/publications/publ.html.

Mihaljevic, S. N., & Chidiac, S. E. (2009). Use of post-consumer waste in concrete and concrete block – literature review. *In the proceedings of the 11th Canadian Masonry Symposium, 31 May - 3 June 2009* (pp. 929-940). Toronto, Canada: Canada Masonry Centre.

Montgomery, D. C., & Runger, G. C., (2003). *Applied statistics and probability for engineers* (3rd ed.). New York: John Wiley & Sons, Inc.

Panyakapo, P., & Panyakapo, M. (2008). Reuse of thermosetting plastic waste for lightweight concrete. *Waste Management, 28*(9), 1581-1588.

Park, S. B., Lee, B. C., & Kim, J. H. (2004). Studies on mechanical properties of concrete containing waste glass aggregate. *Cement and Concrete Research, 34*(12), 2181-2189.

Polley, C., Cramer, S. M., & de la Cruz, R. V. (1998). Potential for using waste glass in Portland cement concrete. *Journal of Materials in Civil Engineering*, 10(4), 210-219.

Rößler, M., & Odler, I. (1985). Investigation on the relationship between porosity, structure and strength of hydrated Portland cement pastes I. effect of porosity. *Cement and Concrete Research,* 15(2), 320-330.

Sangha, C. M., Alani, A. M., & Walden, P. J. (2004). Relative strength of green glass cullet concrete. *Magazine of Concrete Research*, 56(5), 293-297.

Schwarz, N., Cam, H., & Neithalath, N. (2008). Influence of a fine glass powder on the durability characteristics of concrete and its comparison to fly ash. *Cement and Concrete Composites, 30*(6), 486-496.

Schwarz, N., & Neithalath, N. (2008). Influence of a fine glass powder on cement hydration: Comparison to fly ash and modeling the degree of hydration. *Cement and Concrete Research, 38*(4), 429-436.

Shao, Y., Lefort, T., Moras, S., & Rodriguez, D. (2000). Studies on concrete containing ground waste glass. *Cement and Concrete Research, 30*(1), 91-100.

Shayan, A., & Xu, A. (2004). Value-added utilisation of waste glass in concrete. *Cement and Concrete Research, 34*(1), 81-89.

Shayan, A., & Xu, A. (2006). Performance of glass powder as a pozzolanic material in concrete: A field trial on concrete slabs. *Cement and Concrete Research, 36*(3), 457-468.

Shi, C., & Zheng, K. (2007). A review on the use of waste glasses in the production of cement and concrete. *Resources, Conservation and Recycling, 52*(2), 234-247.

Siddique, R. (2008). Waste Materials and By-Products in Concrete. *Springer*, 147-175.

Taha, B., & Nounu, G. (2008). Properties of concrete contains mixed colour waste recycled glass as sand and cement replacement. *Construction and Building Materials, 22*(5), 713-720.

Terro, M. J. (2006). Properties of concrete made with recycled crushed glass at elevated temperatures. *Building and Environment, 41*(5), 633-639.

Topçu, İ B., Boğa, A. R., & Bilir, T. (2008). Alkali–silica reactions of mortars produced by using waste glass as fine aggregate and admixtures such as fly ash and Li_2CO_3. *Waste Management, 28*(5), 878-884.

APPENDIX A STRESS-STRAIN CURVES FOR BLOCKS

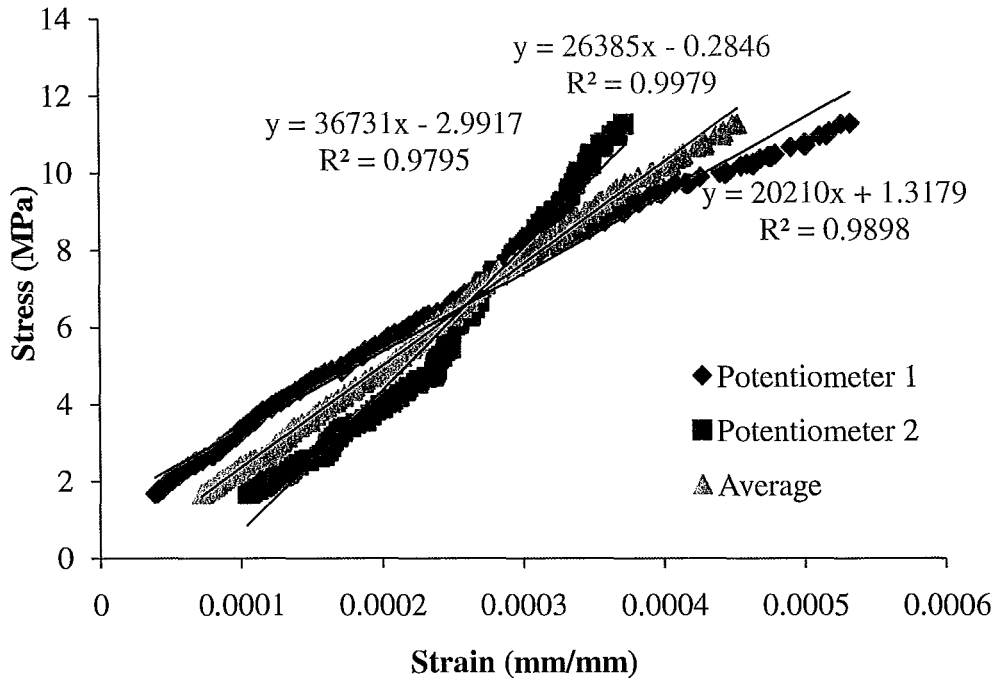

Figure A.1 Stress-strain curve for control block

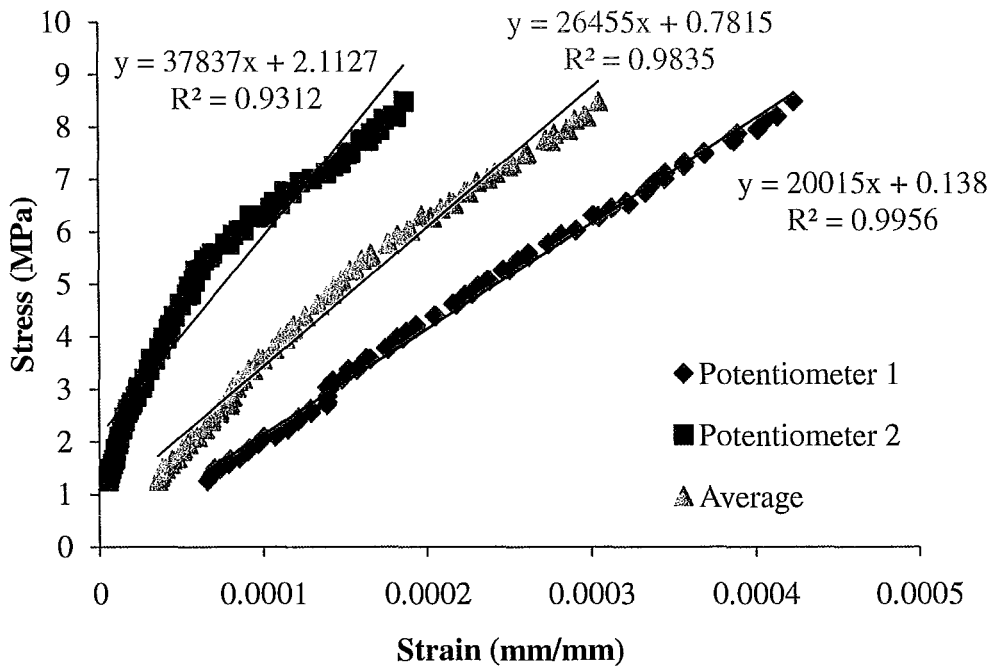

Figure A.2 Stress-strain curve for 3% LDPE block

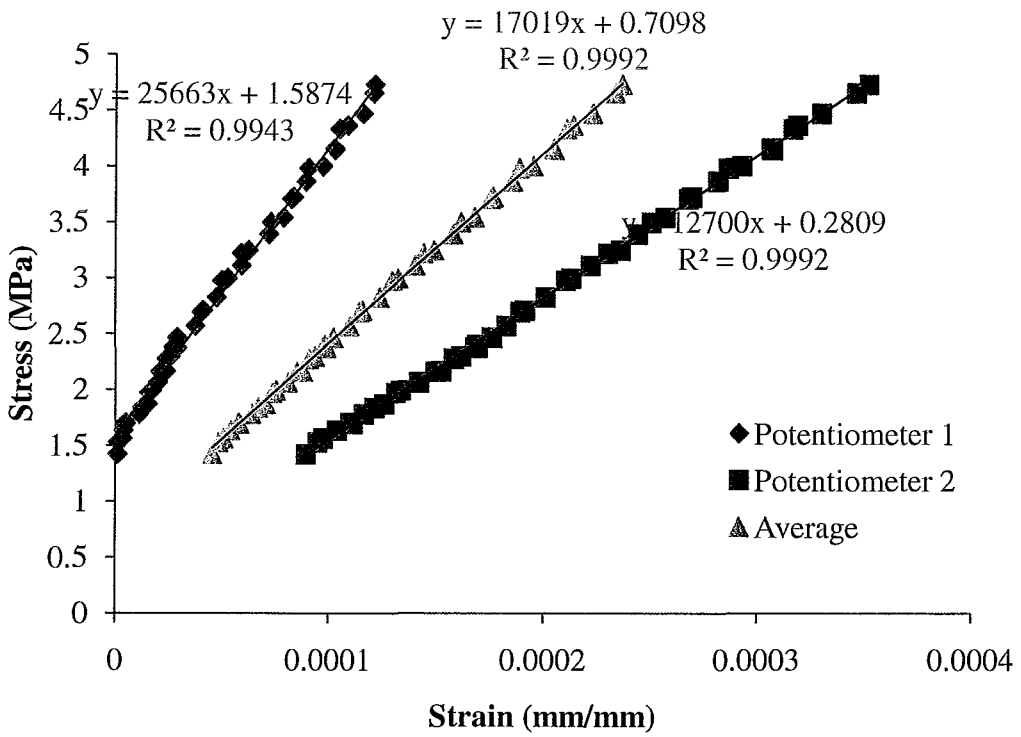

Figure A.3 Stress-strain curve for 6% LDPE block

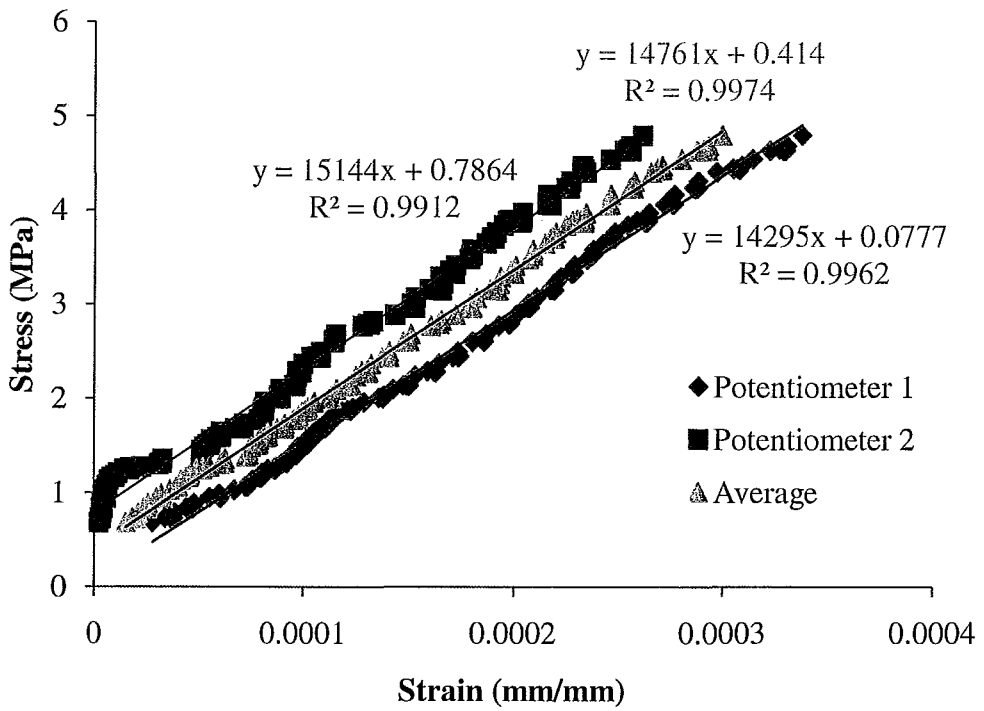

Figure A.4 Stress-strain curve for 9% LDPE block

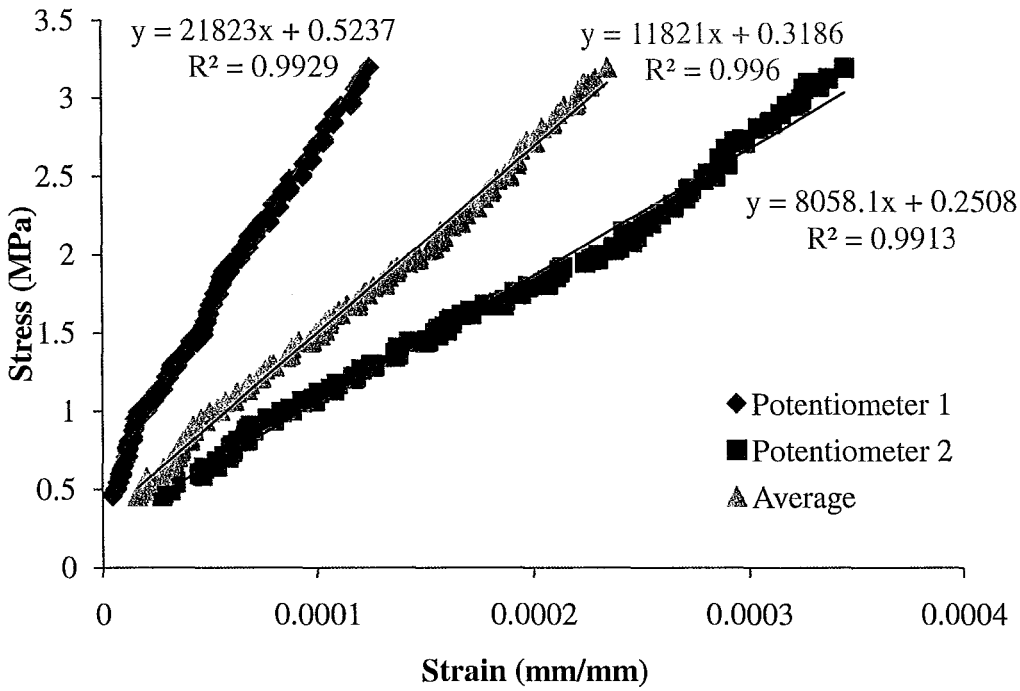

Figure A.5 Stress-strain curve for 15% LDPE block

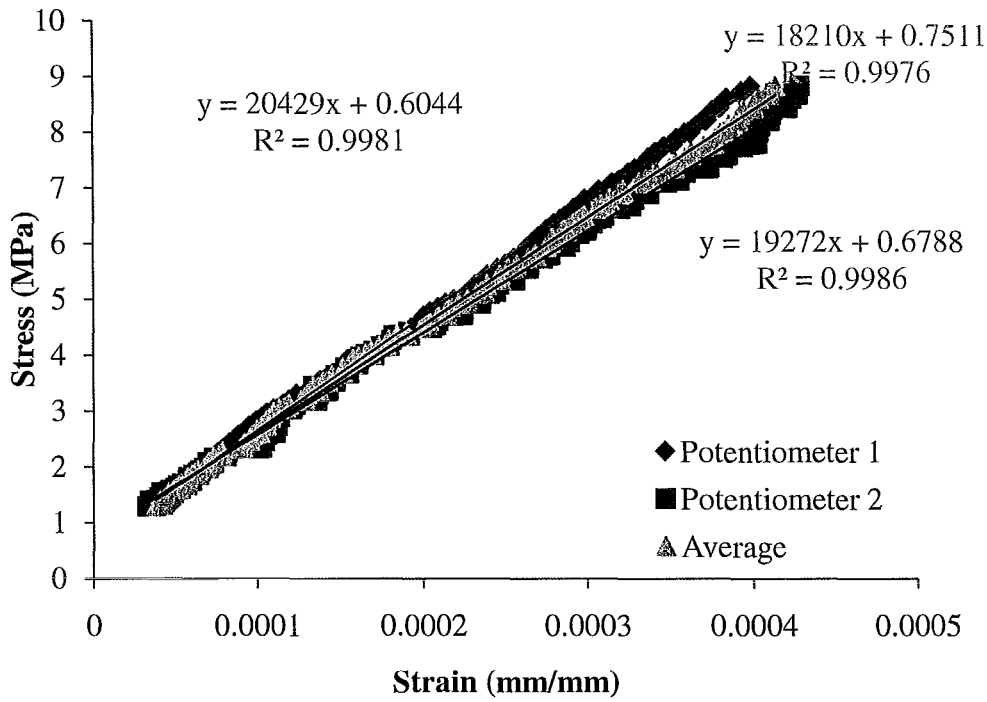

Figure A.6 Stress-strain curve for 3% HDPE block

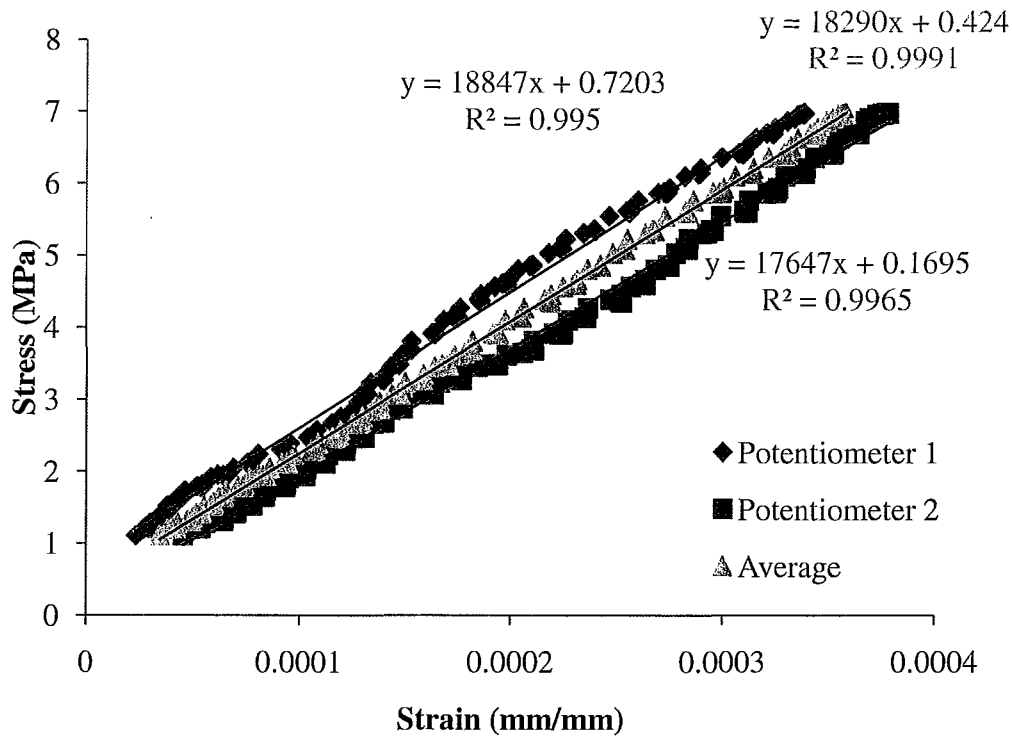

Figure A.7 Stress-strain curve for 6% HDPE block

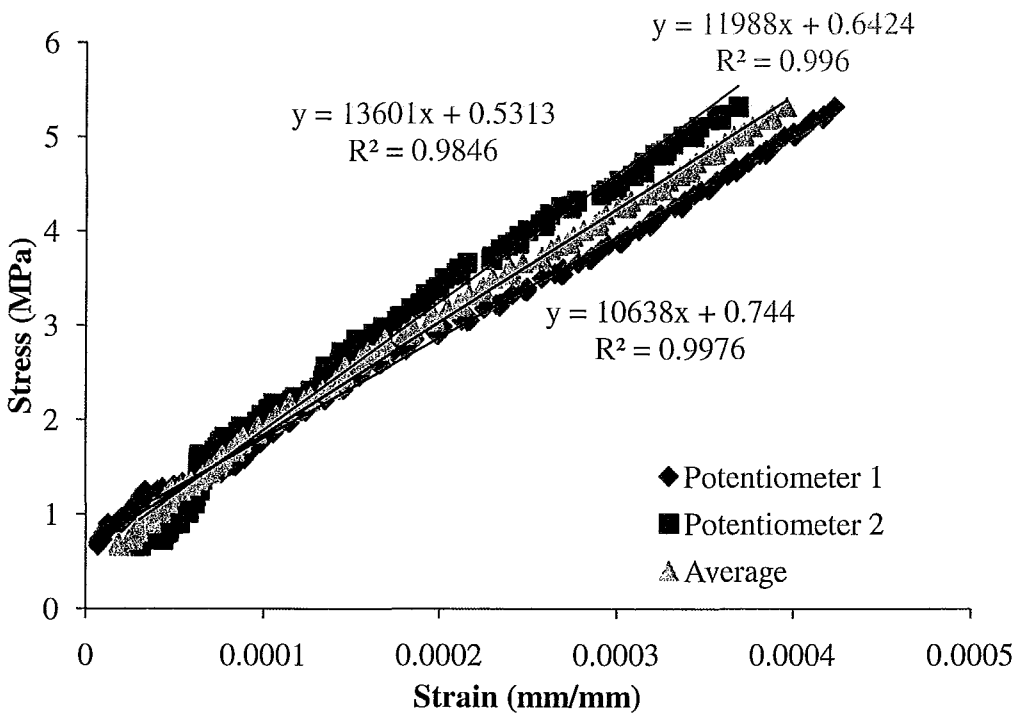

Figure A.8 Stress-strain curve for 9% HDPE block

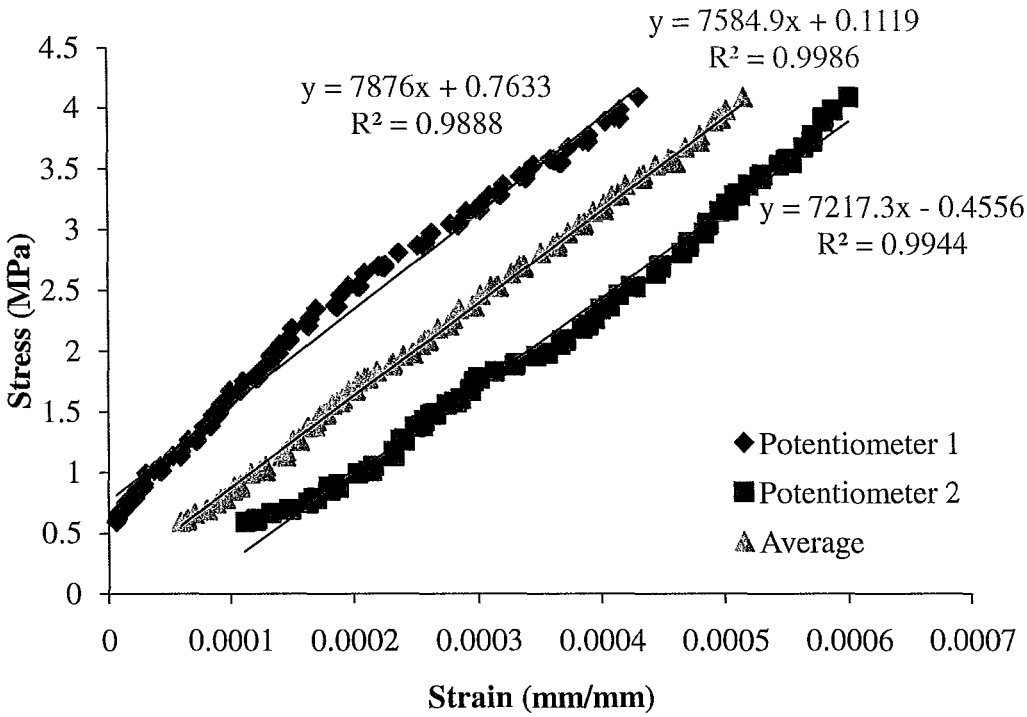

Figure A.9 Stress-strain curve for 15% HDPE block

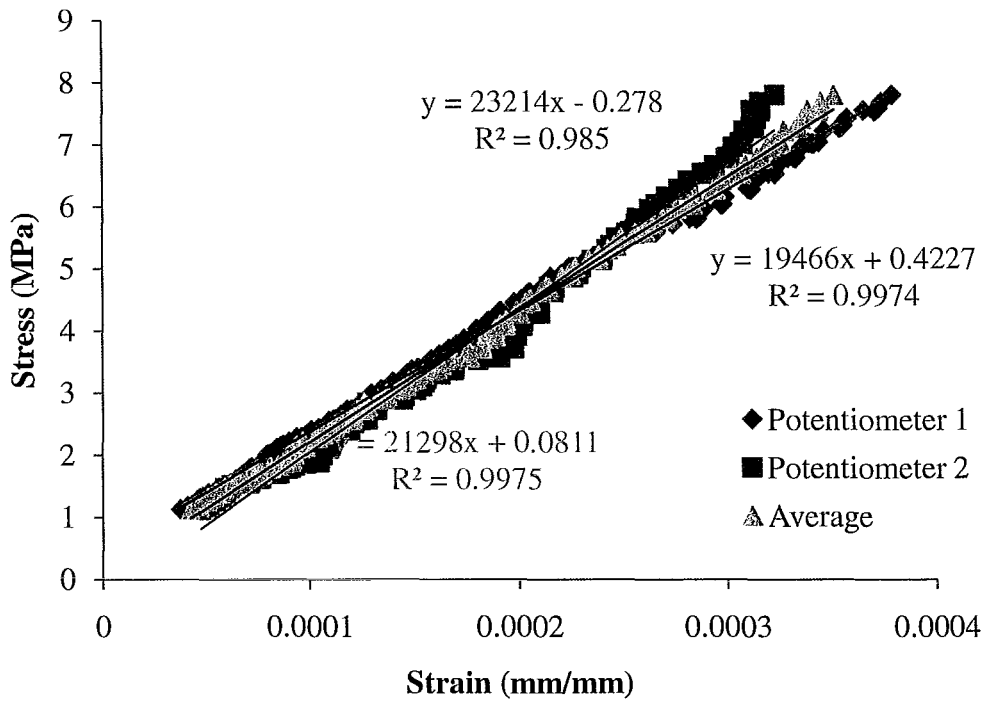

Figure A.10 Stress-strain curve for 3% grafted HDPE block

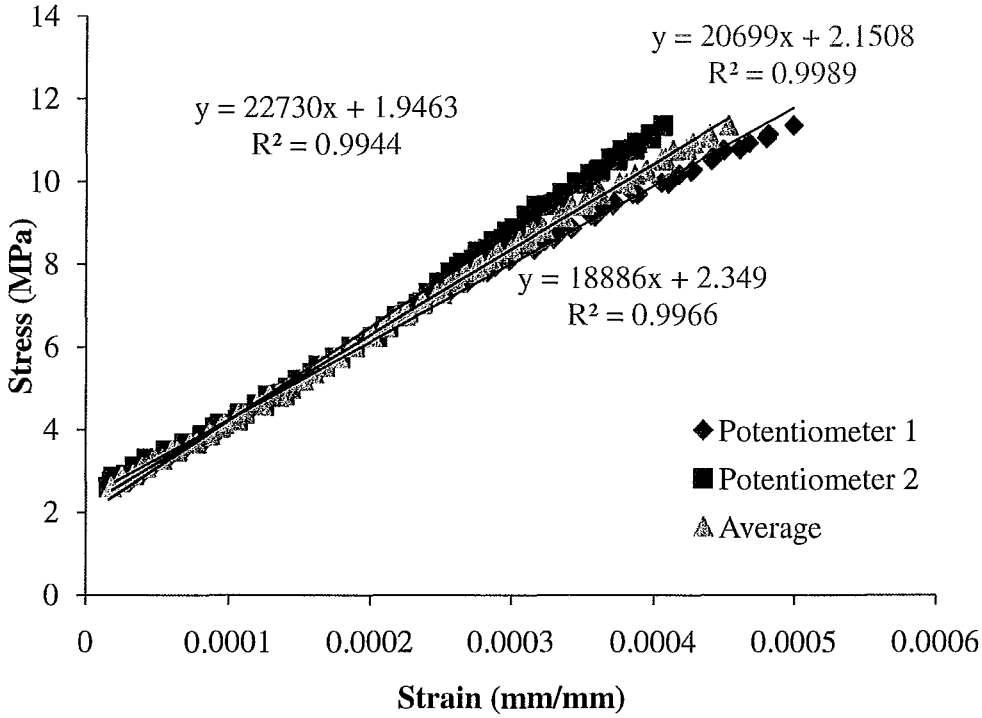

Figure A.11 Stress-strain curve for 10% WGP block

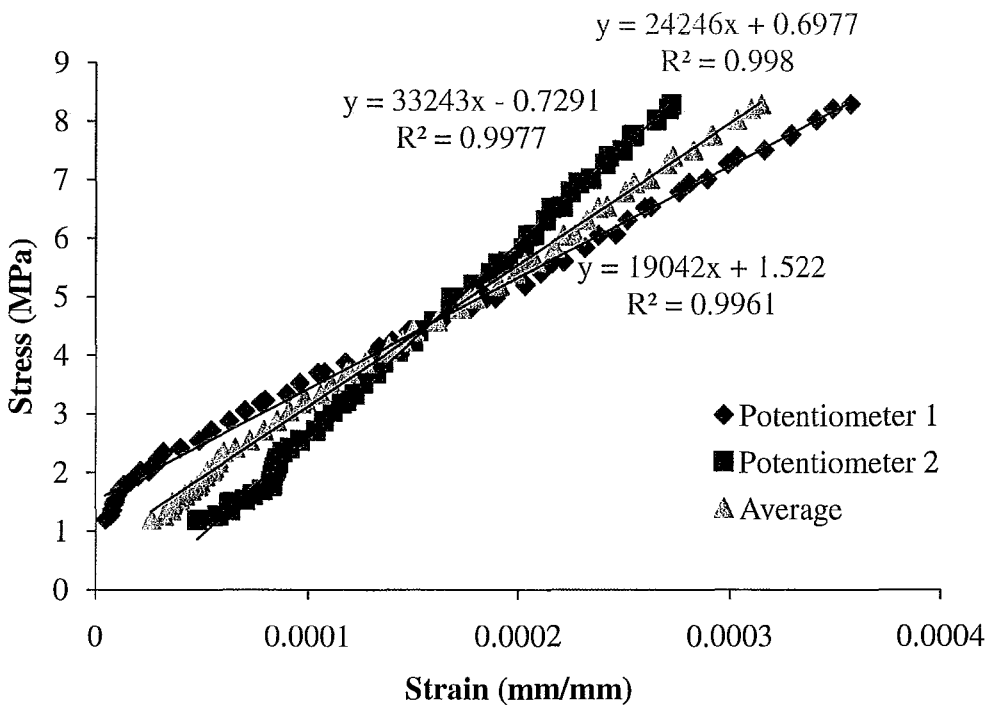

Figure A.12 Stress-strain curve for 25% WGP block

APPENDIX B STRESS-STRAIN CURVES FOR PRISMS

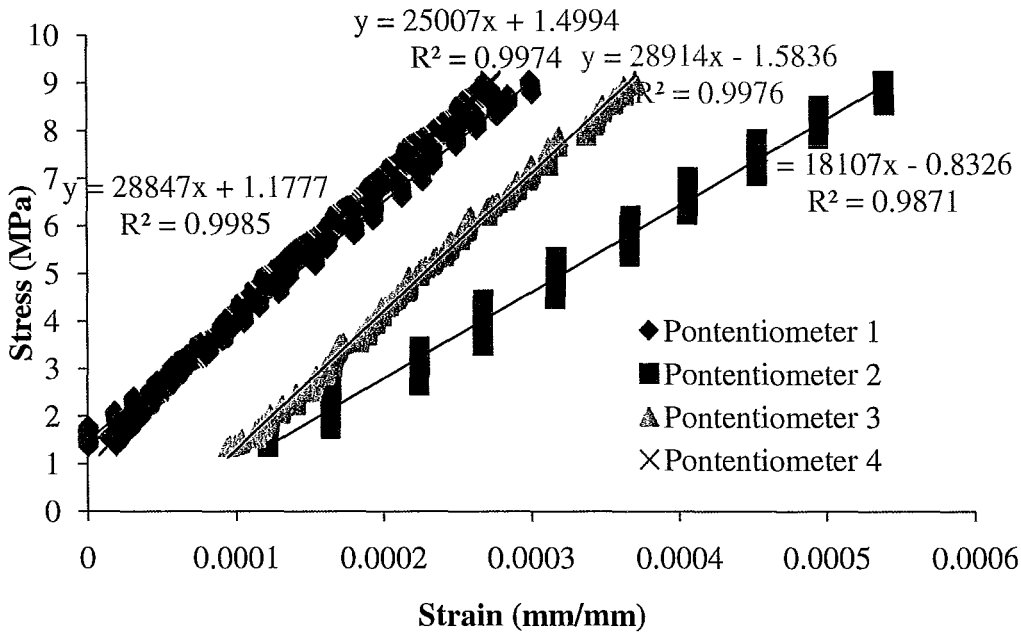

Figure B.1 Stress-strain curve for control prism

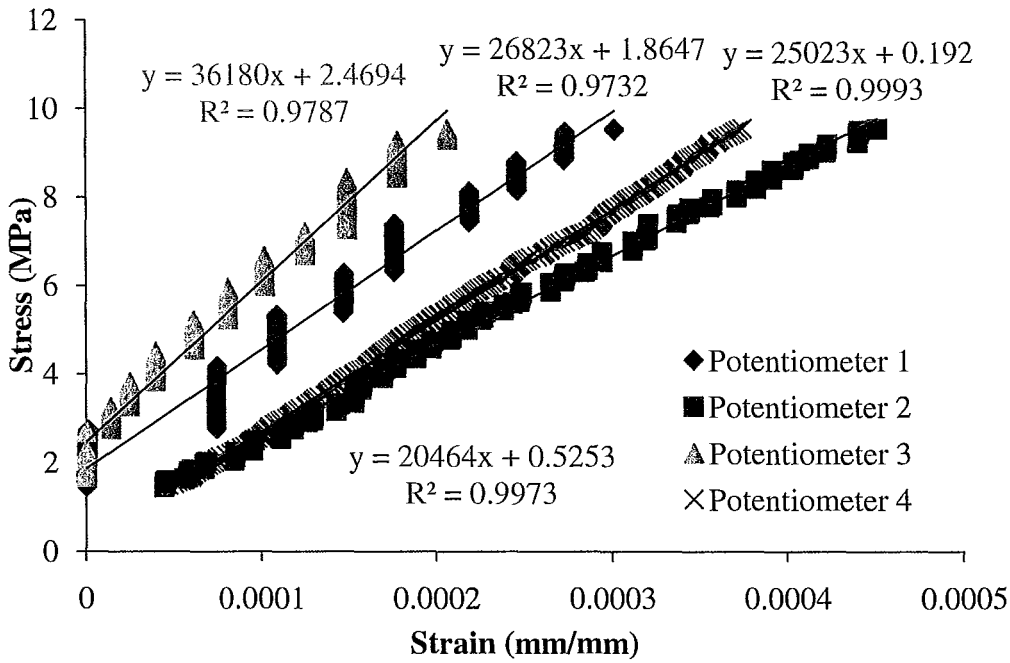

Figure B.2 Stress-strain curve for 3% LDPE prism

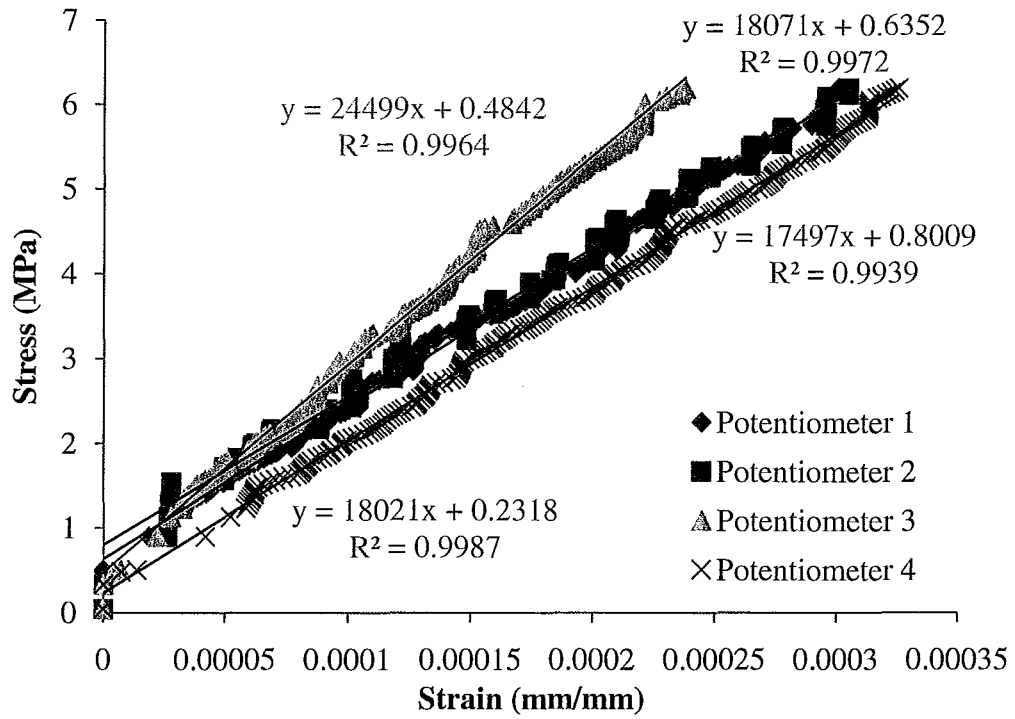

Figure B.3 Stress-strain curve for 6% LDPE prism

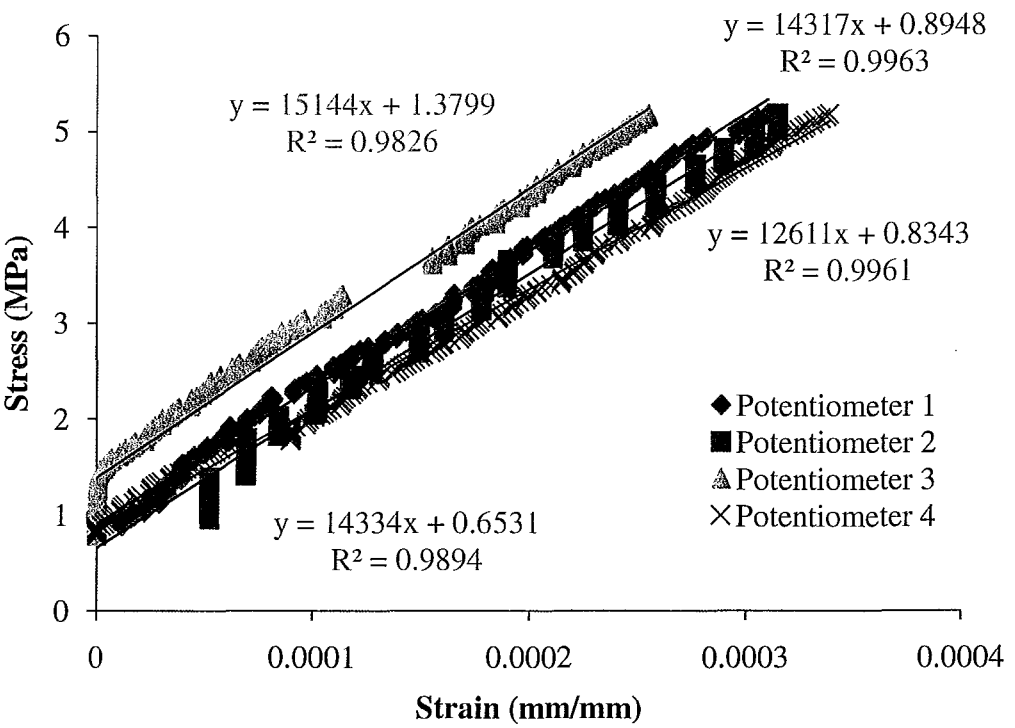

Figure B.4 Stress-strain curve for 9% LDPE prism

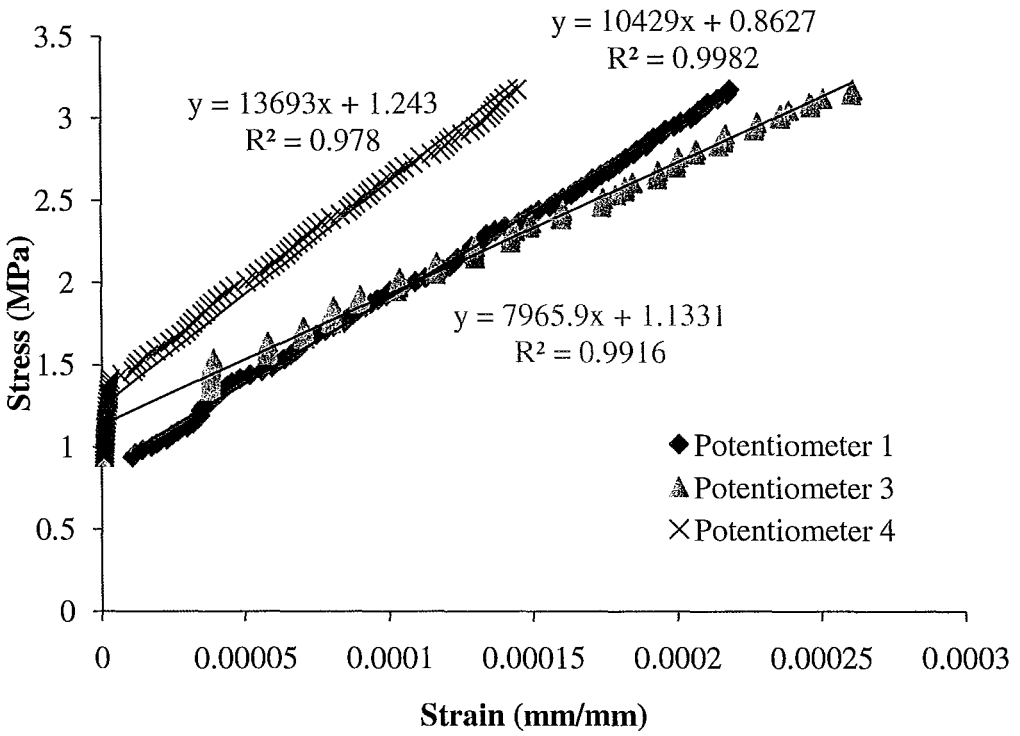

Figure B.5 Stress-strain curve for 15% LDPE prism

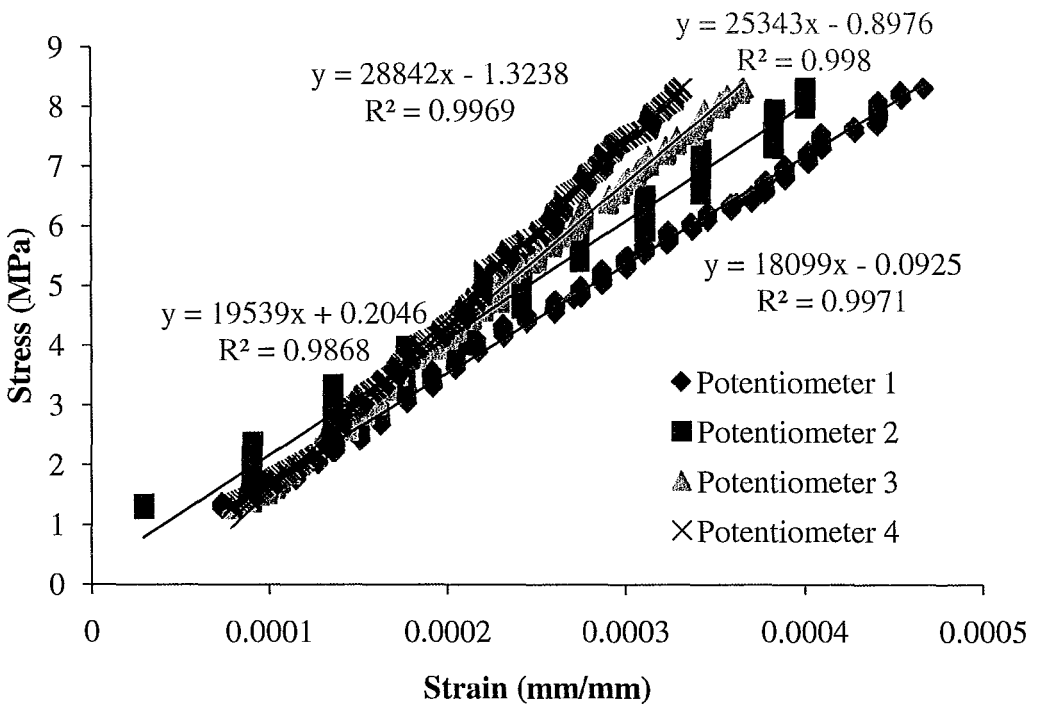

Figure B.6 Stress-strain curve for 3% HDPE prism

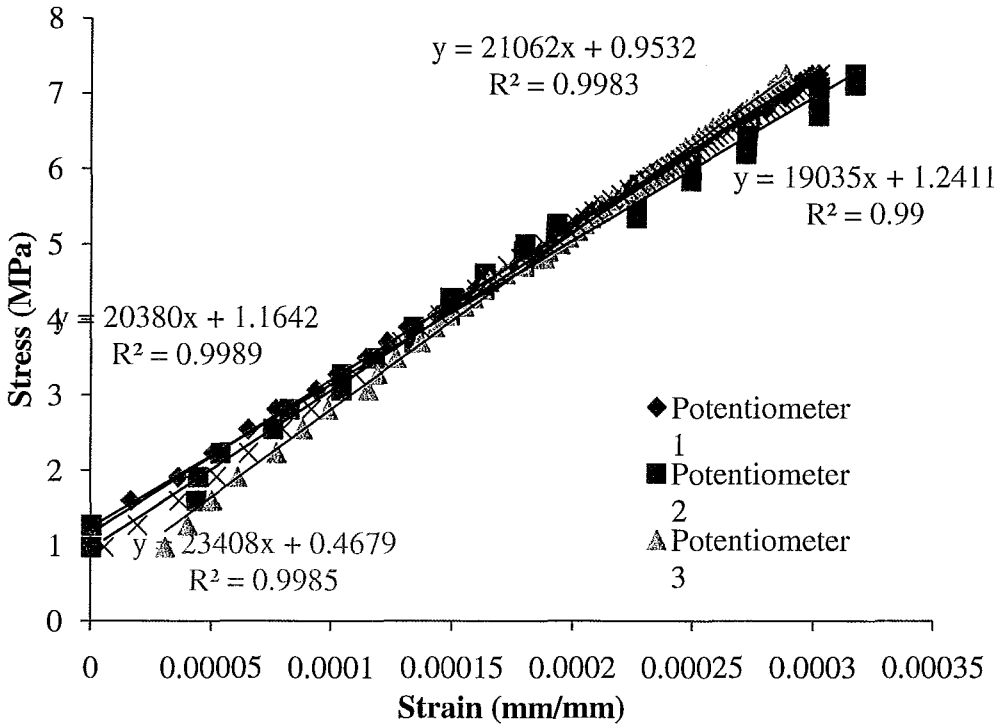

Figure B.7 Stress-strain curve for 6% HDPE prism

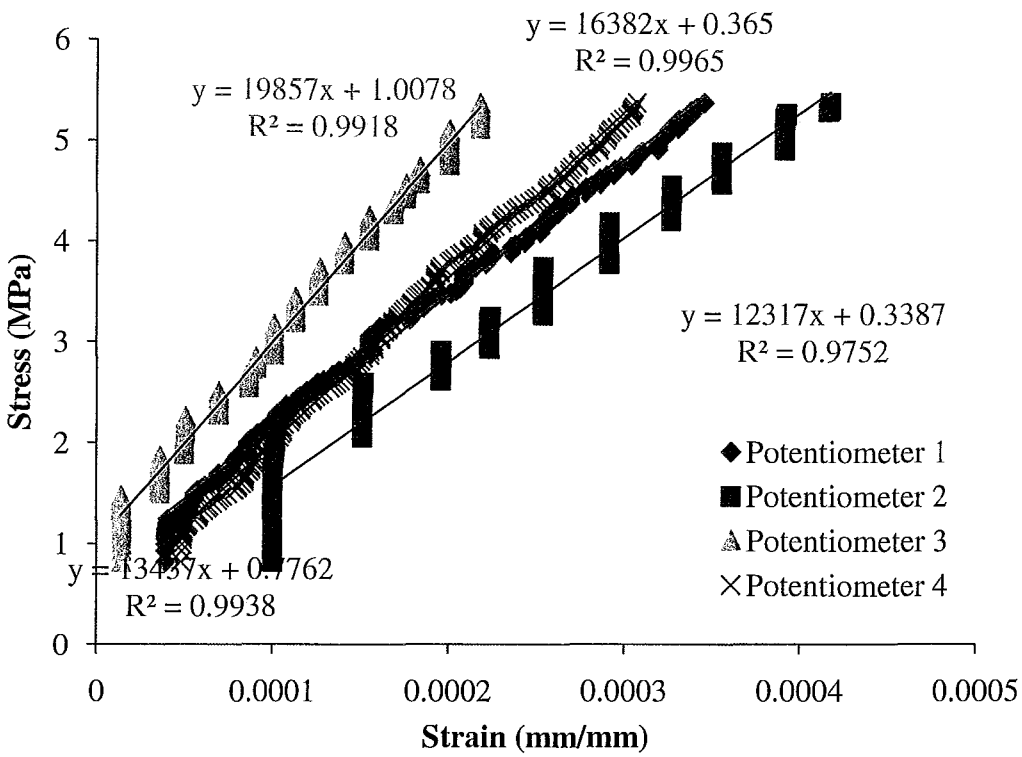

Figure B.8 Stress-strain curve for 9% HDPE prism

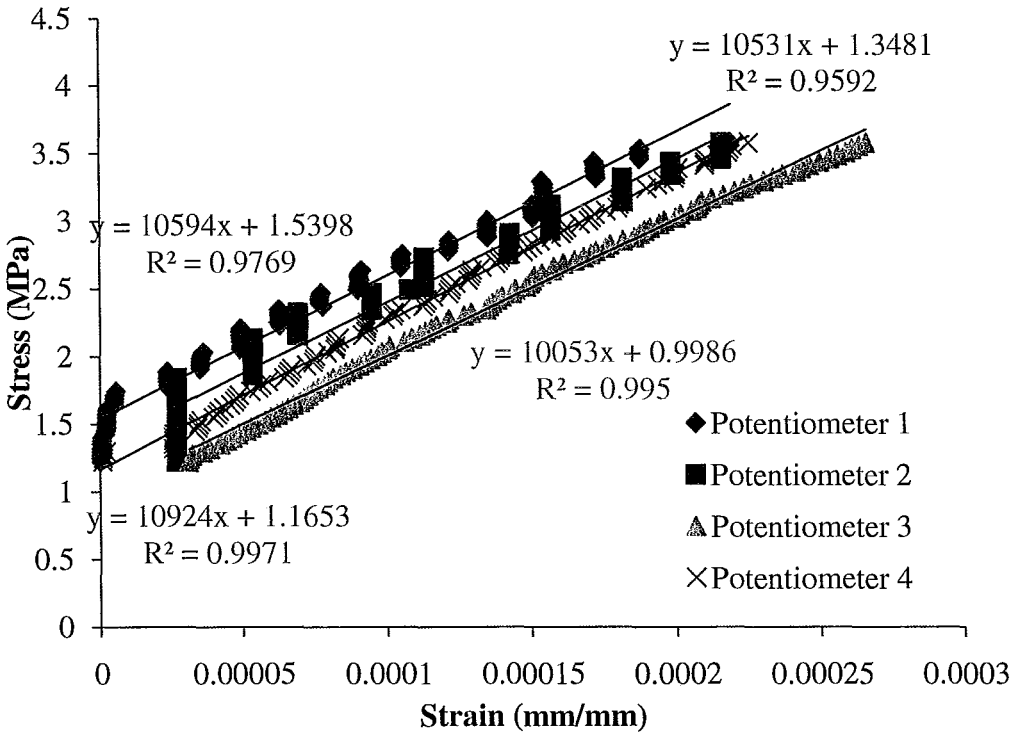

Figure B.9 Stress-strain curve for 15% HDPE prism

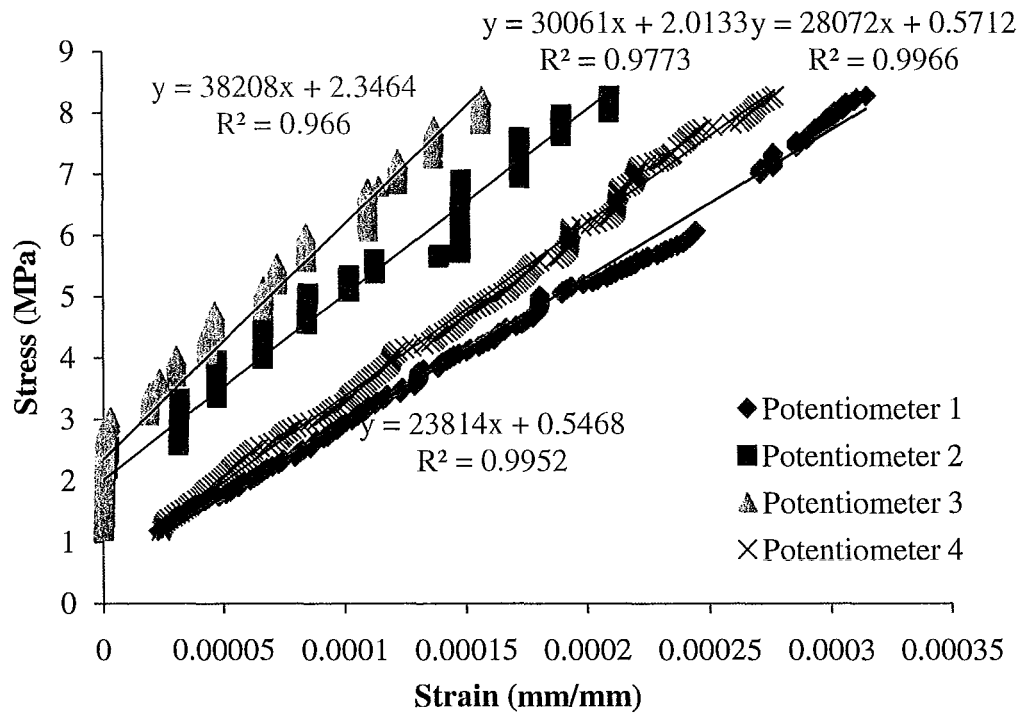

Figure B.10 Stress-strain curve for 3% grafted HDPE prism

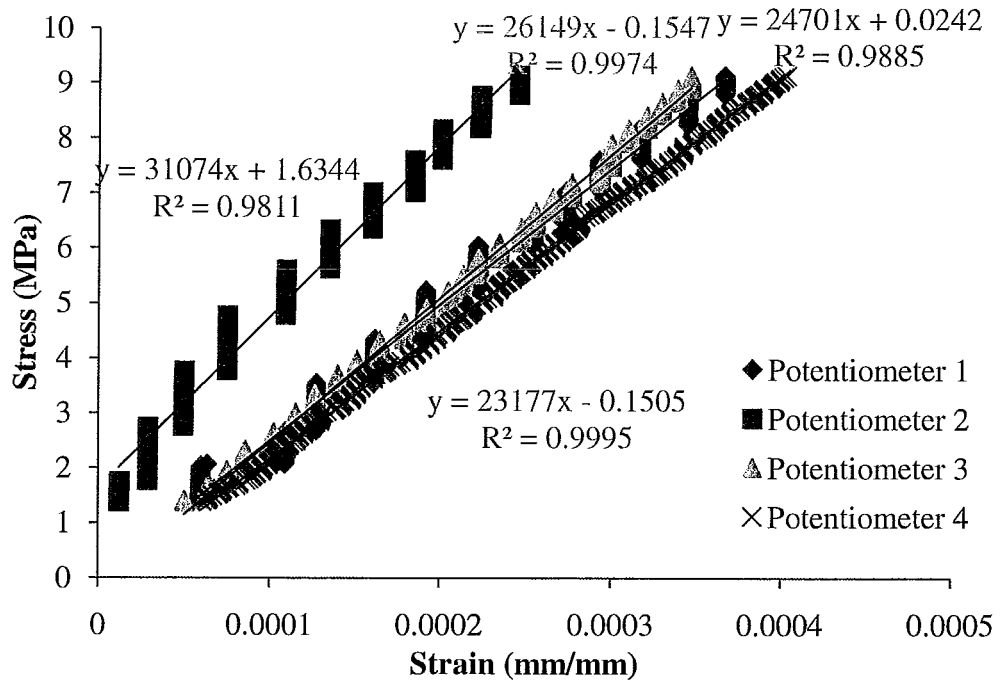

Figure B.11 Stress-strain curve for 10% WGP prism

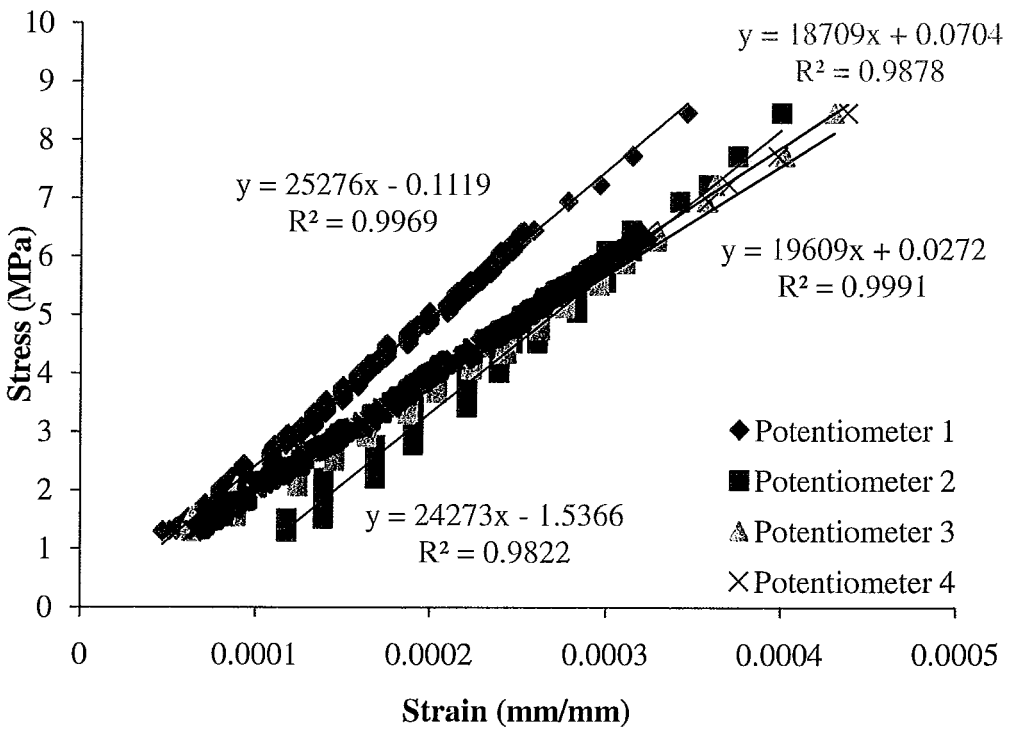

Figure B.12 Stress-strain curve for 25% WGP prism